MONITORING EARLY AGE SETTING OF FLYASH MODIFIED CONCRETE USING NDT TECHNIQUES

A Dissertation Submitted
In Partial Fulfilment of the Requirements
For the degree of

MASTERS OF ENGINEERING
IN
STRUCTURAL ENGINEERING

Submitted by:
JAPNEET SIDHU

(ROLL NO. 801422016)

UNDER THE SUPERVISION OF

Dr. SHRUTI SHARMA
Associate Professor
Civil Engineering
Thapar University, Patiala

Dr. SANDEEP SHARMA
Assistant Professor,
Mechanical Engineering
Thapar University, Patiala

DEPARTMENT OF CIVIL ENGINEERING
THAPAR UNIVERSITY
PATIALA-147004
JULY 2016

DECLARATION

I, Japneet Sidhu, hereby declare that this thesis entitled **"MONITORING EARLY AGE SETTING OF FLYASH MODIFIED CONCRETE USING NDT TECHNIQUES"** in fulfilment of the requirement for the award of the Degree of **Master of Engineering** in **Civil Structures Engineering** and submitted in Civil Engineering Department, Thapar University, Patiala is an authentic record of my work carried out during a period from July 2015 to July 2016 under the supervision of **Dr. Shruti Sharma, Associate Professor,** Department of Civil Engineering and **Dr. Sandeep Sharma, Assistant Professor**, Department of Mechanical Engineering , Thapar University, Patiala.

This matter presented in this thesis has not been submitted by me for the award of any other degree of this or any other university.

JSidhu

Date: 15/07/2016

Japneet Sidhu
Roll No. : 801422016

CERTIFICATE

This is to certify that the above statement made by the student concerned is correct and true to the best of my knowledge and belief.

Shruti Sharma 26/7/16

Dr. Shruti Sharma
Associate Professor
Department of Civil Engineering
Thapar University,Patiala

Dr. Sandeep Sharma
Assistant Professor
Department of Mechanical Engineering
Thapar University,Patiala

Countersigned by

Dr.Naveen Kwatra,
Professor and Head,
Department of Civil Engineering
Thapar University,Patiala-147004

Dr. S.S.Bhatia,
Dean of Academic Affairs,
Thapar University,Patiala-147004

ACKNOWLEDGEMENT

A dissertation cannot be completed without the help of many people who contribute through their constructive criticism in the evolution and preparation of this work. The satisfaction that accompanies the successful completion of any task would be incomplete without the mentioning of various people who directly or indirectly contributed to it and made it possible. Many are responsible for the knowledge and experience gained during the course of this work.

Foremost, I would like to express my sincere gratitude to my advisor Dr. Shruti Sharma for her continuous support during my thesis work, for her patience, motivation, enthusiasm, and immense knowledge. Her guidance helped me in the entire time of research and writing of this thesis. I could not have imagined having a better advisor and mentor for my thesis work.

I also like to offer my sincere thanks to all the faculty members, teaching and non - teaching staff of Civil Engineering Department (CED), and staff of central library, TU, Patiala for their assistance. I am extremely thankful to Mr. Ram Simran, and all other manpower for helping me carry out the experimental work. The constant support of my friends Nikita Bhalla, Ashutosh Sharma, Vishal Dhiman, Varun Garg and Devender Sharma is sincerely appreciated for helping me out whenever needed.

I would also like to thank to my parents, grandparents and my brother for their encouraging words and constant support during the entire duration of my thesis work.

July, 2016

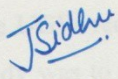

Japneet Sidhu

(801422016)

ABSTRACT

Strength monitoring is important in concrete structures to determine the structure's readiness for service. In this study suitability of non destructive testing (NDT) techniques of acoustic emission and ultrasonic guided waves methods for monitoring early age setting properties of flyash modified concrete is explored. In ultrasonic guided waves method, guided wave is transmitted and received through a waveguide that is embedded in early age concrete. As the cementitious material sets and hardens, the strength of the received waves changes, indicating the transition from semi-fluid to solid state. This approach monitors the attenuation of the fundamental guided longitudinal wave mode, resulting from the leakage of energy from the cylindrical steel rod to the surrounding flyash modified concrete. The evolution of the material's properties is related to the energy leakage or attenuation of the guided wave. Whereas in Acoustic Emission, waves arising out of the solidification of the concrete are recorded using Acoustic Emission (AE) sensors mounted at different locations. Both the techniques are different in their nature of application, i.e., Ultrasonic Guided Wave (UGW) is active in nature and Acoustic Emission Technique (AET) is passive in nature. Ultrasonic Guided Wave depends on the transmitted signal whereas the Acoustic Emission Techniques depends on the stress changes occurring inside the system.

Experiments were performed on concrete mixtures with varying flyash contents in concrete i.e. 0%, 5%, 10%, 15%, 20% and 30%. For AET and ultrasonic guided waves, cube specimens of size (150mmx150mmx150mm) with embedded mild steel rods were used to monitor early setting and hardening. For AET, the system was paused while UGW reading was taken to in order to prevent the recording of noise. The focus of the study was to track every aspect of the setting and hardening process of flyash concrete immediately after pouring of fresh concrete using these newly developed NDT Techniques of AE and UGW.

CONTENTS

LIST OF FIGURES

LIST OF TABLES

CHAPTER 1

INTRODUCTION

1.1General

The main attributes of cement mortar and concrete that are most vital are rheology and setting and hardening. Rheology ascertains workability and compaction ability whereas setting ascertains the end of workability whereas hardening is responsible for the strength gain and stiffness development of the mortar/concrete. Setting time determination is an important parameter required for determining formwork removal and surface finishing during the construction of concrete structures and pavements. Setting time is further divided into initial and final setting times and these are the times when concrete changes from the fluid to solid state and starts to gain strength, respectively.

1.2Setting and Hardening of concrete

Setting

Setting time is characterized as the transition from a fluid state to a plastic state i.e. the solidifying and stiffening of the concrete after it has been placed .A solid can be "set" in terms that it is no more a fluid, however it might even now be extremely weak; you may not be able to walk on it, for instance. Setting is because of early-stage calcium silicate hydrate development and because of ettringite formation.

The terms 'initial set' and 'final set' are arbitrary definitions of early and later set; there are laboratory procedures for determining these using weighted needles penetrating into the cement paste. It has been found that this transition can occur in less than one hour or could take up to 24 hours. Initial setting time is that time period between the time water is added to cement and time at which 1 mm square section needle fails to penetrate the cement paste, placed in the Vicat's mould 5 mm to 7 mm from the bottom of the mould. It is the time when the paste has gained enough rigidity to no longer be in a fluid state. Initial setting time test is important for transportation, placing and compaction of cement concrete.

Final setting time is that time period between the time water is added to cement and the time at which 1 mm needle makes an impression on the paste in the mould but 5 mm attachment does not make any impression. It is the time when rigidity has increased to a point that the paste becomes a solid of very low strength. Determination of final setting time period facilitates safe removal of scaffolding or form. In general, cement exhibit initial set in 1 to 4

hours and final set in 5 to 8 hours. Final set is then followed by substantial increases in strength, referred to as the hardening stage. As per Indian Standards, initial setting time should not be less than 30 minutes and final setting time should not be more than 600 minutes.

Setting time is reduced if the weather is hot as heat speeds the chemical reaction. As the concrete sets, the workability reduces and the concrete steadily becomes more difficult to compact and mould, however it is still inherently weak and can be easily damaged. It is essential that cement sets neither too rapidly nor too slowly. In the first case there might be insufficient time to transport and place the concrete before it becomes too rigid. In the second case too long a setting period tends to slow up the work unduly, also it might postpone the actual use of the structure because of inadequate strength at the desired age. Setting should not be confused with hardening, which refers to the gain in mechanical strength after certain degree of resistance to the penetration of a special attachment pressed into it.

Two abnormal setting behaviours that may occur are

1) False set
   It refers to rapid setting that occurs without the liberation of much heat. Plasticity can be regained by further mixing without the need to add more water, and thus is not a problem where concrete is mixed for long periods (ready mixed concrete). Increasing mixing time when possible helps reducing the false set problem.

2) Flash set or quick set
   This behaviour is accompanied by the liberation of considerable heat. The plasticity of the mixture cannot be regained with additional mixing or water. To avoid flash set, a small amount of gypsum ($CaSO_4.2H_2O$) inter grounded with the cement clinker retards the hydration reaction of tricalcium aluminate so that calcium silicates can set first.

   The hydration reactions the cement undergoes when mixed with water are shown in the schematic diagram below

Basic Elements of cement

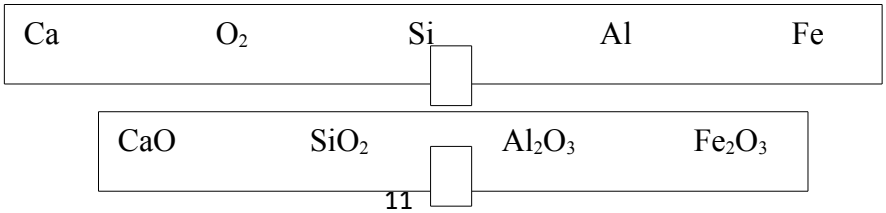

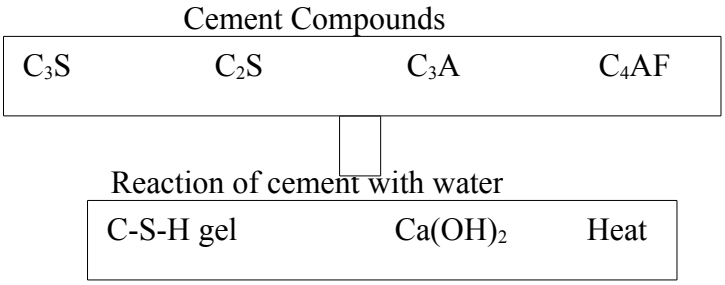

Fig.1.1: Schematic diagram of hydration of cement

For C_3S hydration

$$2C_3S + 6H \rightarrow C_3S_2H_3 + 3\ Ca(OH)_2 \quad \text{.....(1.1)}$$

For C_2S hydration

$$2\ C_2S + 4H \rightarrow C_3S_2H_3 + Ca(OH)_2 \quad \text{.....(1.2)}$$

For C_3A hydration

$$C_3A + 6H \rightarrow C_3AH_6 \quad \text{..... (1.3)}$$

C4AF hydrates to tricalcium aluminate hydrate and calcium ferrite $CaO.Fe_2O_3$.

Influence of the Compound Composition on Properties of Cement

C_3S and C_2S - are the most important compounds - responsible for strength.

C_3S - contributes most to the strength development during the first four weeks.

C_2S - influences the gain in strength from 4 weeks onwards. At the age of about one year, the two compounds, contribute approximately equally to ultimate strength.

C3A contributes to the strength of the cement paste at one to three days, and possibly longer, but causes retrogression at an advanced age, particularly increments with a high C_3A or (C_3A+C_4AF) content. The role of C_4AF in the development of strength of cement is not clear till now, but there certainly is no appreciable positive contribution.

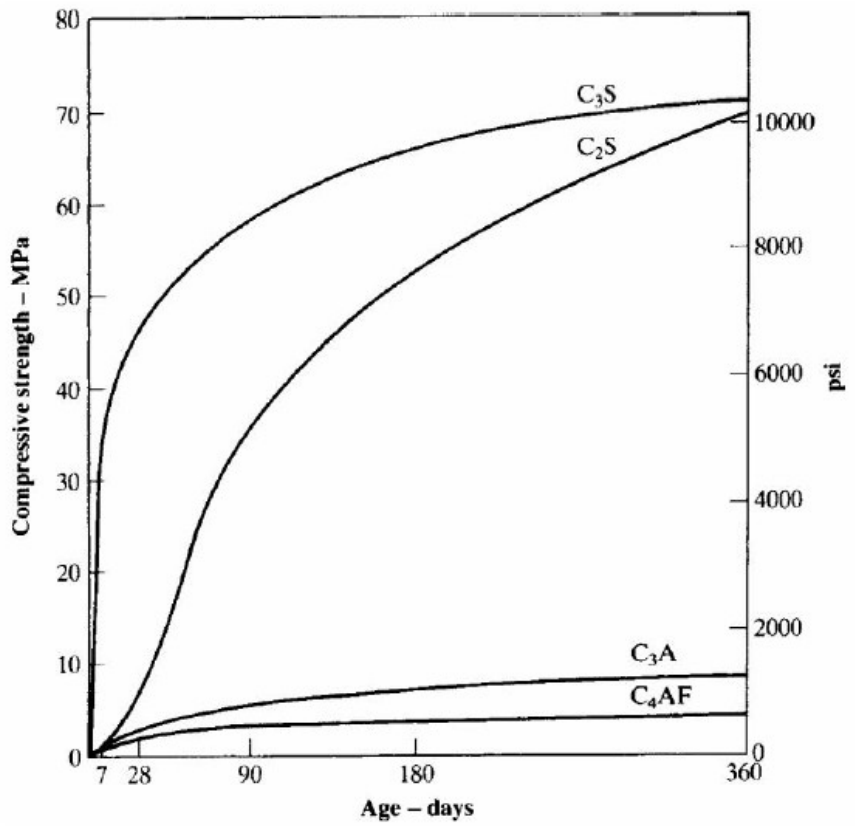

Fig.1.2: Influence of compound composition on compressive strength of cement (http://www.uomisan.edu.iq)

Hardening

The process of strength growth may continue for weeks or months after the concrete has been mixed and placed. Hardening is due to largely the formation of calcium silicate hydrate as the cement hydrates. Hardening time is when concrete has a sufficient bearing capacity to support construction loads. This hardening of concrete may occur in a few hours, or could take up to 2-3 weeks.

Generally speaking, concrete will reach a useful strength in about 3 days although this does depend on the mix design and constituent materials. The majority of strength is gained within a month. It is important to remember that concrete will reach its maximum strength only if moisture is present during the hardening process.

The hardening process is therefore not dependant on the concrete 'drying out', and it is normally important that the concrete is properly 'cured' to maintain the moisture in the

concrete (especially at vulnerable surfaces) while the cement water reaction is active. Early loss of moisture will cause a reduction in strength and lead to poorer durability.

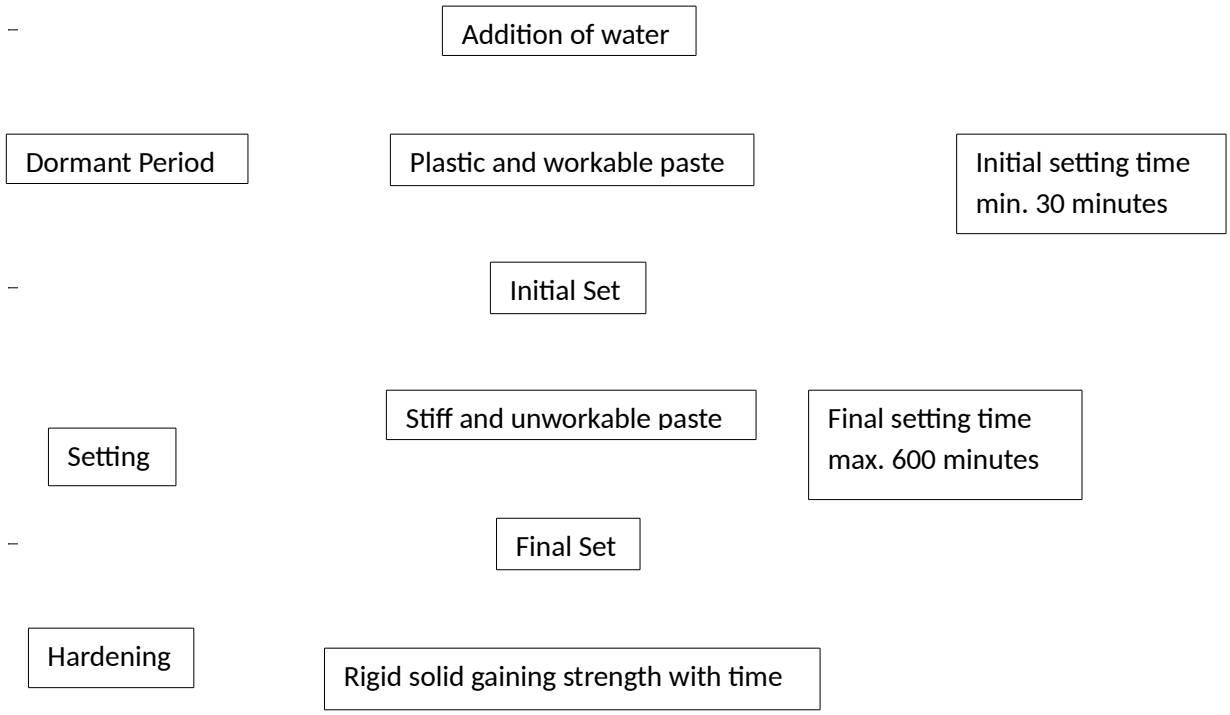

Fig.1.3: Schematic diagram for setting and hardening of cement paste(Randhawa, 2011)

- The difference between setting and hardening can be understood as follows

C_3A reacts first with water forming hydrated calcium alumina silicates. These compounds contribute very little to mechanical strength of concrete, but the cement starts losing its plasticity because of loss of water due to reaction and formation of gel. This loss of plasticity without development of strength is called setting action.

Cement is said to harden when cement paste further reacts with water bringing C_2S and C_3S into action. These compounds contribute to mechanical strength. Hardening therefore is associated with development of strength.

- Factors that affect the setting and hardening time include, but are not limited to
- Type and amount of cementitious material (cement and fly ash);

- Type and amount of aggregate
- Fineness of cement
- Water content;
- Presence of admixtures(accelerators, air entrainers, and water reducers);
- Properties of surrounding soil(permeability and degree of saturation);
- Relative Humidity
- Ambient temperature; and
- Curing conditions

➢ Importance of studying setting and hardening of concrete

Nowadays, more attention is given to the knowledge of the early age concrete behaviour. This period is extremelyimportant for the construction process. It determines the construction speed, the age at formwork removal and the workability period of the concrete. Moreover, a better understanding of the setting age is also important for the study of the influence of the type of cement on the development of the concrete properties at early-age. The most usual method to monitor the setting and hardening of cementitious systems is the penetration test, such as the Vicat needle on cement pastes and the pin-penetration on mortars. However, the interpretation of its results is relatively arbitrary. Moreover, this method is not applicable to concrete. But techniques for monitoring the evolution of early-age properties of cementitious materials have recently been developed. Several techniques are now available, the most common out of which is Ultrasonic Pulse Velocity (UPV) method. The following sections discuss the penetration tests and the UPV test methods performed on concrete to determine the setting and hardening properties of concrete.

1.3 Penetration tests

The penetration resistance in fresh concrete was traditionally considered as a way to know the initial and final setting times by mechanical means depending on the force applied and the geometry of the system.

1.3.1 Vicat's Apparatus

This apparatus is used for consistency tests and for setting time tests. The cement paste of normal consistency is formed and is filled in the mould. A needle of 1 mm diameter is made to just touch the top surface of the cement paste and freely fall in it. Initial setting time is the time from the mixing of the cement and the water to the time

when the penetration of the needle is just above 5 mm from the bottom of the base plate or mould. For the final setting time we have to use another needle which has a enlarged 5 mm hollow cylindrical base. The final setting time is the time from the mixing of the water to the time when this needle just makes the impression on the surface of the cement but does not penetrate into it.

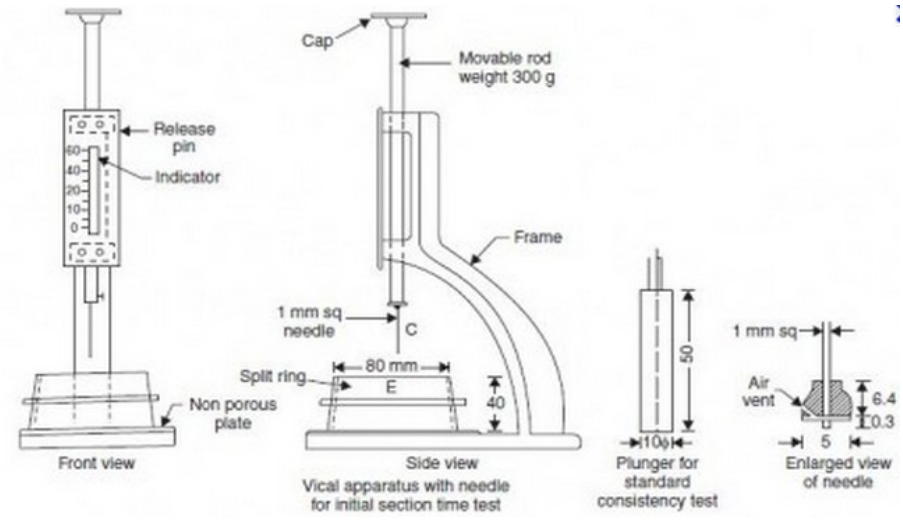

Fig.1.4: Vicat's Apparatus (http://civilengineeringmaterials2012.blogspot.in)

1.3.2 Penetrometer

Penetration plunger has a 1/20 sq. in. tip area. Plunger is steadily pushed into the mortar to a 1 in. depth, as indicated on the shaft, at periodic time intervals. Penetrometer's calibrated range is 0-700psi. Resistance in psi is indicated on the scale. The point of initial set is reached when the penetration value is 500psi (3,448 kPa) as per ASTM C780.

1.3.3 Proctometer

In protometer, force is applied at much higher velocities. This method consists of a needle mounted on a spring which is manually pushed into the sample and the digital display gives the value of force applied.

1.4 Ultrasonic Pulse Velocity

Fig.1.5: Ultrasonic pulse velocity test apparatus (http://www.controls-group.com)

The UPV method involves measuring the speed of travel of an ultrasonic pulse through concrete. This speed is influenced by the density and elastic modulus of the concrete. It is often used for relative strength assessments. The technique is most effective and economic for comparative assessments of quality (density) and detection of voids, delaminations, and under compacted and honey combed areas because the pulse takes longer to travel around defective areas. Low frequency ultrasonic pulses (about 30 kHz) are sent by the transmitting transducer and received by the second transducer with the time taken for the ultrasonic pulse to travel recorded by a timer. The pulse velocity is determined by dividing the path length between the two transducers by the pulse travel time.

Pulse velocity= (Path length/Travel time)

$$V = \frac{L}{t} \quad \text{..... (1.4)}$$

Generally higher pulse velocity is associated with higher strength of concrete. The pulse velocity can be affected by concrete mix composition, concrete density and compaction, moisture condition and age of concrete.

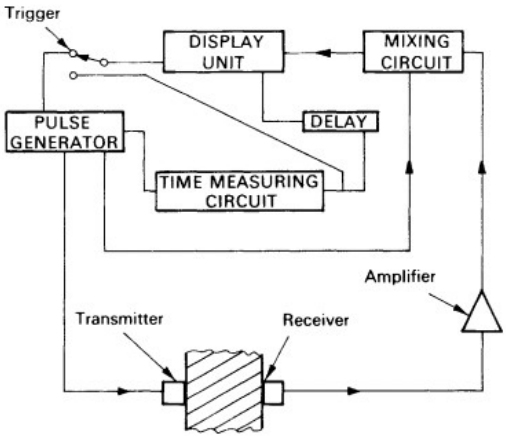

Fig.1.6: Typical UPV testing equipment (https://www.researchgate.net)

Arrangement of transducers in UPV

• Following are three basic ways in which the transducers may be arranged:

– Transducers coupled on opposite faces (direct transmission)

– Transducers coupled on adjacent faces (semi-direct transmission)

– Transducers coupled on same faces (indirect transmission)

The above mentioned arrangements of transducers are shown below:

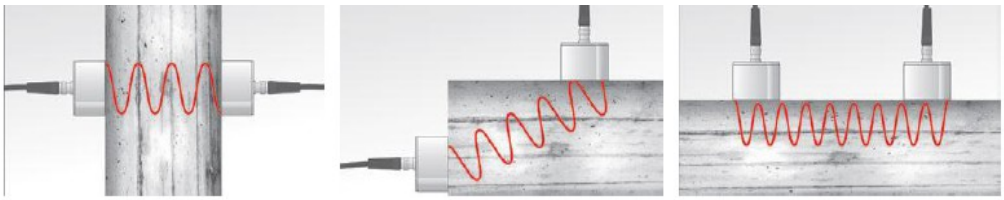

Fig. 1.7: Ultrasonic pulse velocity testing transmission methods (Randhawa, 2011)

- The direct method is the most reliable from the point of view of transit time measurement as well as path length measurement
- The semi-direct method is less reliable than the direct method and should only be used if the angle between the transducers is not too great, and if the path length is not too large.
- The indirect method is the least accurate because received signal is subject to errors due to scattering of pulse by discontinuities.

Advantages

• UPV test is truly non-destructive and can be performed both in lab as well as in-situ

• UPV measurement has been found to be a valuable and reliable method of examining interior of a body of concrete

• Modern UPV test equipment is robust, reasonably cheap and easy to operate, and reliable even under site conditions.

Limitations

• Operators must be well trained and aware of the factors affecting the readings.

• It is essential that the test results are properly evaluated and interpreted by experienced engineers who are familiar with the technique.

• The UPV method only gives an estimate of the extent of cracking within concrete; however, the use for detection of flaws within the concrete is not reliable when the concrete is wet.

• The UPV test is least reliable for estimation of strength of concrete because of the many factors affecting calibrations.

• Application of the UPV test for determining depth of fire damage is limited to only the portions which are free from cracking due to very high temperature.

1.5Various Non Destructive Testing (NDT) Techniques

Apart from the above mentioned techniques to determine the setting and hardening of concrete, there are several other NDT techniques that have come up for the same. A few other NDT Techniques are mentioned below.

- **Visual and Optical Testing:** Visual inspection involves using an inspector's eyes to look for defects. The inspector may also use special tools such as magnifying glasses or mirrors to gain access and inspect the subject area more closely. Visual scanning, inspection or testing can successfully detect these unacceptable surface discontinuities without applying expensive test methods.
- **Penetrant Testing:** After surface cleaning, coloured penetrants are applied to the surface by brushing or spraying, and the excess penetrant is cleaned after enough time for the liquid to penetrate into cracks by capillary action. Then an absorbent developer, (e.g. white dry powder), is applied to the cleaned surface which draws the coloured penetrant liquid out by reverse capillary action. The stain that remains on the developer due to the coloured penetrant is visually inspected as an indication of cracks.

- **Magnetic Particle Testing (MT):** This technique is based on using magnetic fields and fine magnetic particles, such as iron filings to detect flaws in components. The material to be tested is magnetized using an external magnetic field. When there is a crack close to the surface, magnetic poles are created at the edges of the crack. The air gap due to the crack cannot support as much magnetic field as the material, and therefore, the magnetic field spreads out (flux leakage). After magnetization, magnetic particles are sprinkled on the surface, the excess particles are cleaned and the ones attracted at the flux leakage fields are used as the indications of flaws. The above process and how cracks cause flux leakage is illustrated in **Fig 1.8.**

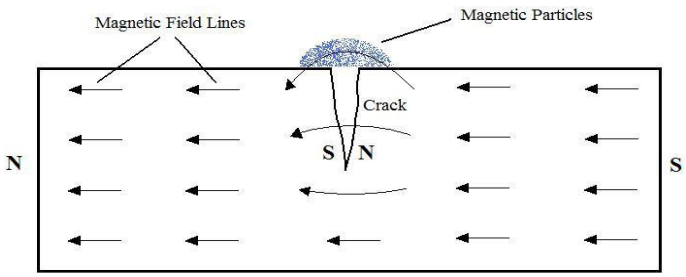

Fig. 1.8: Flux leakage in magnetic particle testing (http://www.googleimages.com)

- **Ultrasonic Testing (UT):** ultrasonic testing uses transmission of high-frequency sound waves into a material to detect imperfections or to locate changes in material properties. The most commonly used ultrasonic testing technique is pulse echo, wherein sound is introduced into a test object and reflections (echoes) are returned to a receiver from internal imperfections or from the part's geometrical surfaces.
- **Acoustic Emission Testing (AE):** when a solid material is stressed, imperfections within the material emit short bursts of acoustic energy called "emissions." as in ultrasonic testing; acoustic emissions can be detected by special receivers. Emission sources can be evaluated through the study of their intensity, rate, and location.

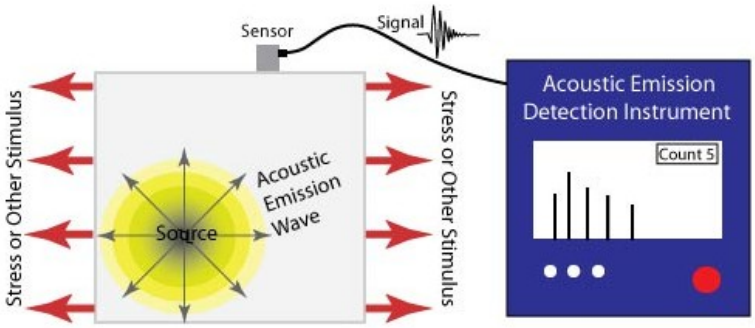

Fig. 1.9: Acoustic emission (https://www.nde-ed.org)

- **Infrared Thermography:** The presence of flaws within the concrete affects the heat conduction properties. The presence and location of hidden defects like delaminations or voids is indicated by the differences in surface temperature between sound and unsound concrete. This technique can provide a fair indication of the location of reinforcing bars, cables and cable ducts and concrete surface cracking.

- **Radiographic methods:** Radiographic methods for concrete inspection include gamma-ray radiography, X-ray radiography, and X-ray radioscopy. A radiographic image is taken through a concrete component to reveal a picture of the interior. Radiography is a reliable method to "see through" a concrete component, and can detect interior flaws such as voids in post tensioning ducts and locating cables and cable ducts, reinforcing bars and cover thickness.

- **Impact Echo Method:** The Impact-Echo method is a stress wave method for flaw detection in structural components which is based on monitoring the surface motion resulting from a short-duration mechanical impact (Carino, 2001). The basic principle of impact-echo technique is introducing a stress pulse into the structure using an impact source such as a hammer or a ball drop. The impact generated stress waves travel between the surface and the defects that may exist in the structure and the reflected waves are monitored by transducers to detect the delaminations **(Fig 1.10)**.

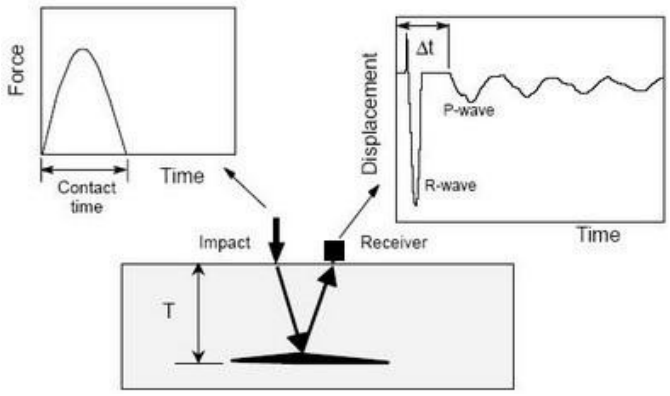

Fig. 1.10: Impact echo method (Carino, 2001).

- **Rebound Hammer Testing:** The rebound hammer (such as the Schmidt Hammer) is a simple device that is used to measure the hardness and predict the strength of the

concrete. This is a spring-loaded impacting device that incorporates a scale to measure the energy of the rebound following the impact. The extent of rebound gives an indication of the strength of the concrete at the surface position tested. The average of about 10 to 20 impacts would give an approximate indication as to the compressive strength of concrete at that location.

1.6 Purpose of NDT Techniques

The non-destructive evaluation techniques are being increasingly adopted in concrete structures for the following purposes:

(i) Estimating the in-situ compressive strength

(ii) Estimating the uniformity and homogeneity

(iii) Estimating the quality in relation to standard requirement

(iv) Identifying areas of lower integrity in comparison to other parts

(v) Detection of presence of cracks, voids and other imperfections

(vi) Monitoring changes in the structure of the concrete which may occur with time

(vii) Identification of reinforcement profile and measurement of cover, bar diameter, etc.

(viii) Condition of prestressing/reinforcement steel with respect to corrosion

(ix) Chloride, sulphate, alkali contents or degree of carbonation

(x) Measurement of Elastic Modulus

(xi) Condition of grouting in prestressing cable ducts

Out of the various available NDT Techniques, the objective of this research is to determine the efficacy of Acoustic Emission and Ultrasonic Guided Waves Technique for monitoring early age properties of flyash modified concrete

1.7 Conventional Vs NDT Techniques

Conventionally, the penetration test according to ASTM C403 is used to determine setting times by measuring penetration resistance of mortar mixtures or mortar sieved from concrete. However, this method is not suitable for in-situ field testing and continuous monitoring of the early age properties of concrete. During the past two decades, many studies have shown the possibility of using ultrasonic waves to monitor setting times and to characterize early age properties of cementitious materials. Nowadays the characterization of cement-based materials during the stiffening process by ultrasound measurement techniques and acoustic emissions are well established. Methods based on ultrasound and acoustics are better suited for the characterization of the setting and hardening of cement based materials than traditional test methods like the vicat-needle test, the penetrometer test or the flow test, because the travel time, the attenuation and the frequency content of ultrasound waves sent through the material are closely correlated with the elastic properties of concrete or mortar. These parameters can be continuously monitored during the stiffening giving a comprehensive picture. Acoustic emission method can monitor changes in materials behaviour over a long time and without moving one of its components i.e. sensors. This makes the technique quite unique along with the ability to detect crack propagations occurring not only on the surface but also deep inside the material.

1.8 Objectives of research

The purpose of this research is to investigate the feasibility of using ultrasonic guided waves and Acoustic emission technique for monitoring the setting and hardening processes of flyash concrete. The objective of using new NDT methods like Ultrasonic Guided Wave and Acoustic Emission Technique are summarized as follows:

- To determine the efficacy of Acoustic Emission and Ultrasonic Guided Waves Technique for monitoring early age properties of flyash modified concrete
- To check the credibility of acoustic emissions and ultrasonic guided waves in monitoring setting and monitoring of concrete containing flyash in varying proportions.

1.9 Literature review for monitoring setting and hardening of concrete

The following presents the review of works done in setting and hardening of concrete. The works done so far are mainly using penetration resistance tests and UPV tests which are discussed below.

Reinhardt and Grosse (2003) studied the two main properties of cementitious mortar and concrete, i.e. rheology and setting and hardening. A testing device was developed which utilizes the velocity of ultrasound (US)-waves in order to continuously monitor the setting and hardening of cementitious materials. Two development steps were emphasised, i.e. the design of the container and the exact determination of the transmitted Ultrasonic-pulse. The results showed that the beginning of setting can be determined from the velocity vs. age of mortar curve by a mathematical procedure while the final setting is still due to empirical experience. It was concluded the method is adjustable to concrete and can also be used for other materials like gypsum, lime, starch and other stiffening materials.

Lee et al. (2004) found that the present standard test available for the setting times of concrete is the penetration resistance test specified by ASTM C403. This test is good for standard concrete mixtures but is not appropriate for high-performance concrete (HPC) because of the high viscosity of the mortar. For this issue, the ultrasonic pulse velocities (UPV) were measured using an ultrasonic monitoring system during the first 24 hrs for mortar and concrete specimens having various water-to-cementitious materials (w/cm) ratios, with and without fly ash (FA). Various characteristics observed from the UPV test agreed with the previous theory of cement hydration, which describes the mixture as viscous suspension transforming into saturated porous solid phase. Also, it was found that the development of UPV in concretes, particularly without FA, was faster than that of mortars with the same w/cm. The values of concrete UPV corresponding to the initial and final setting (ASTM C403) did not show a consistent trend with those of mortar UPV. Hence, it was concluded that the methods and monitoring device used in this research were useful for the in-situ monitoring of the setting of concrete, particularly in HPC.

Kamada et al. (2005) studied setting /hardening properties and for this, the experiments were divided in two phases. In first phase, physical properties were evaluated using viscometer and in second phase chemical propertied were studied using SEM and XRD to investigate hydration product was carried out. It was observed that in first phase initially velocity was that of in air(340 m/s) and inflexion occurred when velocity reached that of in water

(1500m/s), this was stage one in which with the increase in hydration products velocity increased. Stage two is marked by region between two inflexion points and from second inflexion point to the end of measurement was stage three. With addition of retarder dosages the stage durations delayed. Hence with velocity of wave, velocity gradient and time of inflexion point setting states of cement paste can be determined. In the second phase, the velocities attained were larger than that in just phase; at start they were in range of 1100-1600m/s and increased to 1800m/s. This was because of higher w/c ratio in first phase. Further final velocity of 4000m/s was recorded with short duration stage 2.

Robeyst et al. (2007) studied the setting of fresh mortar and concrete samples, made with Portland cement and four types of blast-furnace slag cement. The early age properties of mortar and concrete samples were continuously monitored with the ultrasonic wave transmission method. A revised measurement setup with new sensors and a preamplifier improved the quality of the acquired signal at very early age. The evolution of the velocity and frequency spectrum of the ultrasonic wave was investigated and compared with the results of traditional methods, such as penetrometer tests. The results lead to the conclusion that characteristic points in the graphs of penetration resistance and the ultrasonic velocity curves are correlated.

Chang and Lien (2008) utilized the impact pulse velocity non-destructive method to estimate the compressive strength of the concrete at early age. The results concerning the correlation between the compressive strength at early ages of concrete and that hardened under standard conditions. The relationship of pulse velocity and strength were established for concrete but they were controlled under various water-cement ratio. The result highlighted that Pulse velocity correlates well with strength at early ages but was insensitive to increases in compressive strength after concrete curing. This paper also discusses the influence of the curing time in concrete and water-cement ratio on the coefficients of variation of the compressive strength deduced both in a destructive and non destructive methods. Lastly, it was concluded that accuracy of compressive strength estimation can be predicted by the impact method.

Darquennes et al. (2009) conducted three different techniques to study the evolution of the setting and the hardening of concrete which were later compared: (1) ultrasonic monitoring

using the FreshCon system, (2) a resistivity method and (3) the mechanical Kelly-Bryant method. The experimental tests were carried out on two slag cement concretes in order to compare these methods and to evaluate their ability to monitor continuously the setting and hardening process of concretes with different slag content in the cement. Globally, the initial setting age values given by the three methods was in good agreement, but only the two non-destructive methods (ultrasonic and electric) allow determining the final setting. However, it was concluded that the three methods were complementary and the non destructive methods give additional information (like chemical reactions, stiffness evolution) about the hydration process of cementitious materials. They were also able to tackle the differences in the setting behaviour due to the slag content in the cement.

Nicolas and Nele (2009) noted that research on ultrasonic methods to monitor the setting of concrete has mainly focused on the wave velocity as a useful quantity. So in order to investigated the application of wave energy as a parameter, the ultrasonic wave transmission technique was performed on several concrete and mortar samples in which increasing amounts of the Portland cement was replaced by blast-furnace slag or fly ash. The transmitted ultrasonic wave energy was calculated as the sum of the squared amplitudes of the received signal, divided by the reference energy (E/Eref). The increase of the energy during setting was retarded if ordinary Portland cement was replaced by blast-furnace slag or fly ash. The final setting determined by the standard penetration resistance test occurred shortly after the peak in the derivative curve of the ultrasonic energy. In addition, the values E/Eref = 0.02 and 0.15 were proposed to easily calculate respectively initial and final setting based on the ultrasonic energy measurements. Due to the sensitivity of the energy measurement to the quality of the sensor contact, it was suggested that care should be taken to limit drying shrinkage of the cementitious samples.

Sleiman et al. (2010) examined the possibility of using alternative tests to the Vicat needle method to monitor setting time of cement pastes, and tried to relate the penetration length to the cement paste yield stress. Initially a slow steady increase of the yield stress with time was observed followed by dramatic increase of the yield stress, indicating the change of the cement paste from fluid to solid state. The test results obtained by deformation measurements for normalized consistency cement paste depicted that the deformation increased quickly; while the yield stress was almost constant. The end of this stage corresponded to the beginning of the setting period. After that the deformation increased slowly. Yield stress

increased quickly indicating the transition of the cement paste from fluid to solid state, end of this stage corresponded to the end of the normalized setting period. It clearly appeared that the cement paste's rapid deformation allows measuring the cement paste yield stress. As a result, the static vicat needle was found to be sufficient to monitor the yield stress evolution and was able to monitor the evolution of a cement-based paste during thixotropic reversible period and during setting period.

Zhu and Kee (2010) noted that conventional ultrasonic setups typically measure longitudinal (P) waves in fresh cement pastes and need access two sides of the specimen. This type of setup was not suitable for in-situ field testing. In this study, embedded piezoelectric bender elements were used to generate and measure both P and shear (S) waves in fresh cement pastes. The shear waves were observed at very early age of the cement hydration. The velocities of P and S waves are obtained from B-scan images of a collection of recorded signals over time. Experimental results indicate that the shear wave velocity was closely related to the setting time of cement pastes and less affected by air contents than the P wave velocity. Shear modulus and Poisson's ratios of the cement pates were derived from the measured P and S wave velocities.

Trtnik and Gams (2015) addressed a new ultrasonic approach for observing initial compressive strength development of different cement based materials with different compositions. Nine different mixtures were used which studied the effect of (1) water/cement (w/c) ratio, (2) cement type , (3) aggregate shape , and (4) maximum aggregate size on the development of early age compressive strength and Ultrasonic characteristics was analyzed. Tests were conducted on cubic specimens with the dimensions of 70 x 70 x 70 mm. It showed the strong influence of formation of ettringite on P-wave velocity which had small influence on stiffening and compressive strength.

Carette and Staquet (2016) studied the influence of eco –binders by ultrasonic P and S wave transmission on setting time in mortar and concrete. Limestone, Blast furnace slag and gypsum were used; five composition concrete were made; Reference Mix (C1 contains only Portland cement), C2 (Blast furnace slag) and C3(Limestone filler). C4 combined LF and BFS. With high w/b ratio from C1 (w/b=0.4)to C5 (0.57=w/b). P and S waves velocities decreased due to increase in particle spacing. Due to replacement of 30% LMF both initial and final setting time are accelerated. Due to 70% BFS replacement setting and hardening are

delayed. But when 30% of BFS was replaced by LMF the setting process shifted to an earlier age and duration of setting also decreased.

1.10 Closing remarks

This chapter gives a general introduction about the setting and hardening of concrete and the hydration reactions involved in the process. The most commonly used techniques for monitoring setting and hardening till date i.e. use of penetration tests and Ultrasonic Pulse Velocity have been presented. Various other NDT techniques for concrete monitoring have been briefly discussed. This chapter also discusses the works done so far on monitoring setting and hardening of concrete. In the next chapter use of flyash in concrete and its setting and hardening properties is discussed.

CHAPTER 2
FLYASH CONCRETE-ITS SETTING AND HARDENING

2.1 Introduction

Fly Ash is a by-product of the combustion of pulverized coal in electric power generation plants. When the pulverized coal is ignited in the combustion chamber, the carbon and volatile materials are burned off. However, some of the mineral impurities of clay, shale, feldspars, etc., are fused in suspension and carried out of the combustion chamber in the exhaust gases. As the exhaust gases cool, the fused materials solidify into spherical glassy

particles called Fly Ash. Due to the fusion-in-suspension these Fly Ash particles are mostly minute solid spheres and hollow cenospheres with some particles even being plerospheres, which are spheres containing smaller spheres. The size of the Fly Ash particles varies but tends to be similar to slightly larger than Type I Portland Cement. The Fly Ash is collected from the exhaust gases by electrostatic precipitators or bag filters. Chemical makeup of Fly Ash is primarily silicate glass containing silica, alumina, iron and calcium. Colour generally ranges from dark grey to yellowish tan for Fly Ash used for concrete.

ASTM C 618 Standard Specification for Coal Fly Ash and Raw or Calcined Natural Pozzolan for Use as Mineral Admixture in Concrete has two designations for Fly Ash used in concrete - Class F and Class C.

Class F Fly Ash is normally produced from burning anthracite or bituminous coal that meets the applicable requirements. This class of Fly Ash has pozzolanic properties and will have a minimum silica dioxide plus aluminium oxide plus iron oxide of 70%.

Class C Fly Ash is normally produced from sub bituminous coal that meets the applicable requirements. This class of Fly Ash, in addition to having pozzolanic properties, also has some cementitious properties and will have a minimum silica dioxide plus aluminium oxide plus iron oxide content of 50%.

Class C Fly Ash is used at dosages of 15 to 40% by mass of the cementitious materials in the concrete. Class F is generally used at dosages of 15 to 30%.

2.2 Quality of flyash as per BIS, ASTM

To utilize fly ash as a Pozzolana in Cement concrete and Cement Mortar, Bureau of Indian Standard (BIS) has formulated IS: 3812 Part - 1 2003. In this code quality requirement for siliceous fly ash (class F fly ash) and calcareous fly ash (class C fly ash) with respect its chemical and physical composition have been specified. These requirements are given in **Table 2.1** & **Table 2.2**:

Table 2.1: Chemical Requirements of flyash (http://www.ntpc.co.in)

Sl. No.	Characteristic	Requirements	
		Siliceous fly ash	Calcareous fly ash
i)	**Silicon dioxide** (SiO_2) + **Aluminium oxide** (Al_2O_3) + **Iron oxide** (Fe_2O_3), in percent by mass, Min..	70	50
ii)	**Silicon dioxide** in percent by mass, Min.	35	25
(iii)	**Reactive Silica** in percent by mass, Min (Optional Test)	20	20
iv)	**Magnesium Oxide** (MgO), in percent by mass, Max. .	5.0	5.0
v)	**Total sulphur as sulphur trioxide** (SO_3), in percent by mass, Max.	3.0	3.0
vi)	**Available alkalis** as Sodium oxide (Na_2O), percent by mass, Max.	1.5	1.5
vii)	**Total Chlorides** in percent by mass, Max	0.05	0.05
viii)	**Loss on Ignition**, in percent by mass, Max.	5.0	5.0

Table 2.2: Physical Requirements of flyash (http://www.ntpc.co.in)

Sl. No	Characteristics	Requirements for Siliceous fly ash and Calcareous fly ash
i)	**Fineness-** Specific surface in m^2/kg by Blaine's permeability method, Min.	320
ii)	**Particles** retained on 45 micron IS sieve (wet sieving) in percent, Max. (Optional Test)	34
iii)	**Lime reactivity** – Average compressive strength in N/mm^2, Min.	4.5
iv)	**Compressive strength** at 28 days in N/mm^2, Min.	Not less than 80 percent of the strength of corresponding plain cement mortar cubes
v)	**Soundness by autoclave test -** Expansion of specimen in percent, Max.	0.8

2.3 Chemistry of Flyash in Concrete- Pozzolanic Properties

Fly Ash is a pozzolanic material which is defined as siliceous or siliceous and aluminous material which in itself possesses little or no cementitious value chemically reacts with Calcium Hydroxide (lime) in presence of water at ordinary temperature and form soluble compound comprises cementitious property similar to cement.

Hydration reactions of cement (eq.1.1, 1.2 and 1.3) indicate that during the hydration process of cement, lime is released out and remains as surplus in the hydrated cement. This leached out surplus lime renders deleterious effect to concrete such as make the concrete porous, give chance to the development of micro- cracks and thus affect the durability of concrete. If fly ash is available in the mix, this surplus lime becomes the source for pozzolanic reaction with fly ash and forms additional C-S-H gel having similar binding properties in the concrete as those produced by hydration of cement paste. The reaction of fly ash with surplus lime continues as long as lime is present in the pores of liquid cement paste. Pozzolanic activity of fly ash is an indication of the lime fly ash reaction. The alumina in the pozzolana may also react in the flyash lime or fly ash cement system and produce calcium aluminate hydrate, ettringite, gehlenite and calcium monosulpho-aluminate hydrate. Thus the sum of reactive silica and alumina in the fly ash indicate the pozzolanic activity of the fly ash.

Cement Reaction: $C_3S + H \rightarrow C\text{-}S\text{-}H + CaOH$ (hydration) .....(2.1)

Pozzolanic Reaction: CaOH + S(silica from ash constituents) → C-S-H .....(2.2)

2.4 Benefits of flyash to concrete

Generally, fly ash benefits fresh concrete by reducing the mixing water requirement and improving the paste flow behaviour. The resulting benefits are as follows:

2.4.1Benefits to fresh concrete:

- **Improved workability.** The spherical shaped particles of fly ash act as miniature ball bearings within the concrete mix, thus providing a lubricant effect. This improves concrete pumpability by reducing frictional losses and flat work finishability.

- **Decreased water demand.** The replacement of cement by fly ash reduces the water demand for a given slump. When fly ash is used at about 20 percent of the total cementitious, water demand is reduced by approximately 10 percent. Higher fly ash contents will yield higher water reductions. The decreased water demand has little or no effect on drying shrinkage/cracking. Some fly ash is known to reduce drying shrinkage in certain situations.

- **Reduced heat of hydration.** Replacing cement with the same amount of fly ash can reduce the heat of hydration of concrete. This reduction in the heat of hydration does not sacrifice long-term strength gain or durability. The reduced heat of hydration lessens heat rise problems in mass concrete placements.

2.4.2 Benefits to Hardened Concrete.

One of the primary benefits of fly ash is its reaction with available lime and alkali in concrete, producing additional cementitious compounds.

- **Increased ultimate strength.** The additional binder produced by the fly ash reaction with available lime allows fly ash concrete to continue to gain strength over time. Mixtures designed to produce equivalent strength at early ages (less than 90 days) will ultimately exceed the strength of straight cement concrete mixes (**Fig 2.1**).

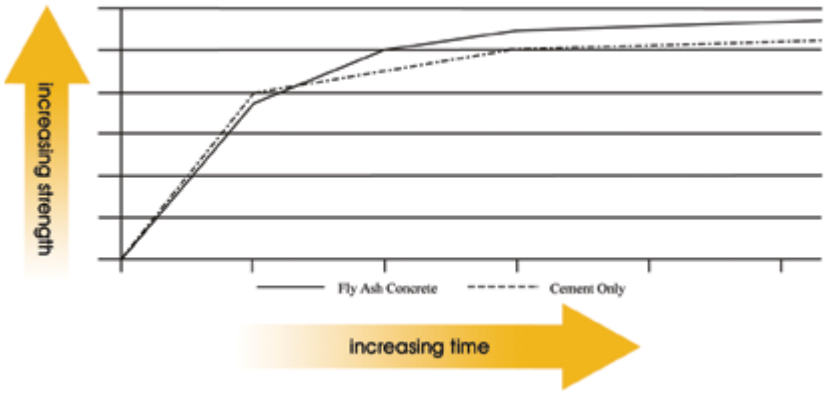

Fig.2.1: Typical strength gain of fly ash concrete (https://www.fhwa.dot.gov)

- **Reduced permeability.** The decrease in water content combined with the production of additional cementitious compounds reduces the pore interconnectivity of concrete, thus decreasing permeability. The reduced permeability results in improved long-term durability and resistance to various forms of deterioration (**Fig. 2.2**)

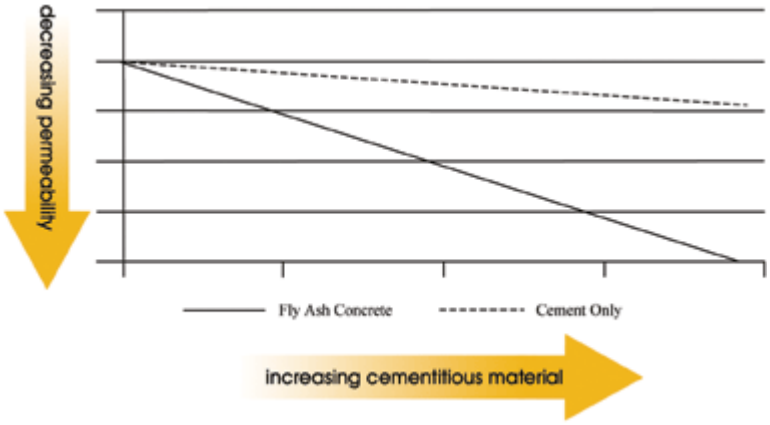

Fig.2.2: Permeability of fly ash concrete (https://www.fhwa.dot.gov)

- **Improved durability.** The decrease in free lime and the resulting increase in cementitious compounds, combined with the reduction in permeability enhance concrete durability. This affords several benefits:

    - Improved resistance to ASR. Fly ash reacts with available alkali in the concrete, which makes them less available to react with certain silica minerals contained in the aggregates.

    - Improved resistance to sulphate attack. Fly ash induces three phenomena that improve sulphate resistance:

- Fly ash consumes the free lime making it unavailable to react with sulphate
- The reduced permeability prevents sulphate penetration into the concrete
- Replacement of cement reduces the amount of reactive aluminates available

- Improved resistance to corrosion. The reduction in permeability increases the resistance to corrosion.

Figure 2.3: Fly ash concrete used in severe exposure applications (https://www.fhwa.dot.gov)

- Fly Ash is economical. The cost of Fly Ash is generally less than Portland Cement depending on transportation. Significant quantities may be substituted for Portland Cement in concrete mixtures and yet increase the long term strength and durability. Thus, the use of Fly Ash may impart considerable benefits to the concrete mixture over a plain concrete for less cost.

2.4.3 Environmental benefits of fly ash use in concrete

Use of fly ash in concrete imparts several environmental benefits and thus it is eco friendly. It saves the cement requirement for the same strength thus saving of raw materials such as limestone, coal etc required for manufacture of cement. Manufacture of cement is high-

energy intensive industry. In the manufacturing of one tonne of cement, about 1 tonne of CO is emitted and goes to atmosphere. Less requirement of cement means less emission of result in reduction in green house gas emission. Due to low calorific value and high ash content in Indian Coal, thermal power plants in India, are producing huge quantity of flyash. This huge quantity is being stored / disposed off in ash pond areas. The ash ponds acquire large areas of agricultural land. Use of fly ash reduces area requirement for pond, thus saving of good agricultural land.

2.5Various applications of flyash

Pulverized Fuel Ash is versatile resource material and can be utilized in variety of applications. The pozzolanic property of fly ash makes it a resource for making cement and other ash based products. The Geo-technical properties of bottom ash, pond ash & coarse fly ash allow it to use in construction of embankments, structural fills, reinforced fills low lying area development etc. The physico chemical properties of pond ash is similar to soil and it contains P, K, Ca, Mg, Cu, Zn, Mo, and Fe, etc. which are essential nutrients for plant growth. These properties enable it to be used as a soil amender & source of micronutrients in Agriculture/ Soil Amendment.

The major utilization areas of PFA are as under: -

(1)Manufacture of Portland Pozzolana Cement & Performance improver in Ordinary Portland Cement (OPC).

(2) Part replacement of OPC in cement concrete.

(3) High volume flyash concrete.

(4) Roller Compacted Concrete used for dam & pavement construction.

(5) Manufacture of ash bricks and other building products

(6) Construction of road embankments, structural fills, low lying area development.

(7) As a soil amender in agriculture and wasteland development

2.6Literature Review of flyash in concrete

The following section presents the review of works done in flyash concrete related to optimum dosages, workability and setting and hardening of flyash concrete.

Naik and Singh (1997) studied the effect of flyash obtained from various sources on the setting and hardening characteristics of concrete systems. In general, the initial and final setting times of concretes were greatly affected by both the source and flyash content. In general it was found that the times of setting of concrete were retarded upto a certain level of cement replacement. The amount of delay varied with flyash source and beyond this level (60%) a reverse trend was observed.

Siddique (2003) carried out an experimental investigation dealing with concrete incorporating high volumes of Class F fly ash. Portland cement was replaced with three percentages (40%, 45%, and 50%) of Class F fly ash. Tests were performed for fresh concrete properties: slump, air content, unit weight, and temperature. Compressive, splitting tensile, and flexural strengths, modulus of elasticity, and abrasion resistance were determined up to 365 days of testing. Test results indicated that the use of high volumes of Class F fly ash as a partial replacement of cement in concrete decreased its 28-daycompressive, splitting tensile, and flexural strengths, modulus of elasticity, and abrasion resistance of the concrete. However, all these strength properties and abrasion resistance showed continuous and significant improvement at the ages of 91 and 365 days, which was most probably due to the pozzolanic reaction of fly ash. Based on the test results, it was concluded that Class F fly ash can be suitably used up to50% level of cement replacement in concrete for use in precast elements and reinforced cement concrete construction.

Siddique (2010) studied wear resistance of high-volume fly ash concrete (HVFA) intended for pavement applications. In order to increase the percentage utilization of flyash, an investigation was carried out for its large scale utilization. Concrete mixtures were prepared by replacing cement with 40, 50, and 60% of fly ash. Experiments were conducted for fresh concrete properties, compressive strength and wear resistance. Test results indicated that wear resistance of concrete having cement replacement up to 40% was comparable to the normal concrete. Beyond 40% fly ash content, concretes exhibited slightly lower resistance to wear in relation non-fly ash concretes. There is very good correlation between wear resistance and compressive strength (R_2 value between 0.8482 and 0.9787) depending upon age.

Patil et. al. (2012) carried out an investigation to study the utilization of fly ash in cement concrete as a partial replacement of cement as well as an additive so as to provide an environmentally consistent way of its disposal and reuse. The cement in concrete matrix is

replaced from 5% to 25% by step in steps of 5%. It is observed that replacement of cement in any proportion lowers the compressive strength of concrete as well as delays its hardening. This provides an environmental friendly method of fly ash disposal. However the rate of strength development is less, Due to lesser rate of strength development flyash finds specific application in mass concreting e. g.dam construction.

Mukherjee et al (2013) reported that that the zero slump concrete showed higher compressive compared to workable concrete with super plasticizer up to 60% replacement with flyash .The strength gain with time is higher compared to the OPC concrete at all replacement level of cement by flyash and the optimum strength gain was noted at 70%replacement at 28 days.

Jatale et.al. (2013) studied the effect of partial replacement of cement by fly-ash. Studies have been conducted on concrete mixes with 300 to 500 kg/cum cementious materials at 20%, 40%, 60% replacement levels. In this paper the effect of fly-ash on workability, setting time, density, air content, compressive strength, modulus of elasticity were studied. It was found that use of fly ash improves the workability of concrete; density and air content of concrete mix are generally unaffected with the use of fly ash. Use of fly ash slightly retards the setting time of concrete, but it is compensated by reduction in the admixture dosage to maintain the same workability. Bleeding in fly ash concrete is significantly reduced and other properties like cohesiveness, pumping characteristics and surface finish are improved. . As the fly ash content increases there is reduction in the strength of concrete. This reduction is more at earlier ages as compared to later ages.

Upadhyaya (2014) studied the compressive strength of concrete with different dosage of flyash as partial replacement of cement. From the experimental investigations, it was observed that the optimum replacement of flyash to cement without changing much compressive strength is 10%. It was also observed that blocks containing flyash were lighter in weight than concrete blocks with no flyash. At 30% replacement, flyash blocks show very low compressive strength in comparison to concrete containing no flyash.

Harrison et. al. (2014) In this study, cement was replaced by fly ash accordingly in the range of 0% (without fly ash), 10%, 20%, 30%, 40%,50% and 60% by weight of cement for M-25 mix with 0.46 water cement ratio. Concrete mixtures were produced, tested and compared in

terms of compressive strength. It was observed that 20% replacement Portland Pozzolana Cement (PPC) by fly ash strength increased marginally (1.9% to 3.2%) at 28 and56 d respectively. It was also observed that up to 30% replacement of PPC by fly ash strength is almost equal to referral concrete after 56 d. PPC gained strength after the 56 d curing because of slow hydration process.

2.7Closing Remarks

Flyash concrete is widely used nowadays due to its very many advantages amongst which increase in strength and improvement in durability are the most important .Flyash concrete has various environmental benefits also as flyash disposal otherwise creates a problem .Also flyash inclusion in concrete results in a decrease in the cost. As flyash inclusion in concrete is common nowadays, it becomes necessary to investigate its early age properties of curing using non-destructive tools. The focus of research is that the Non – Destructive Techniques of UGW and AE pick up the initial setting and hardening of flyash modified concrete effectively.

CHAPTER-3

ULTRASONIC GUIDED WAVES TECHNIQUE

3.1Fundamentals of Ultrasonic Waves in Media

It is known that frequency range of sound audible to humans is approximately 20 to 20,000 Hz (cycles per second). Ultrasound is simply sound that are above the frequency range of human hearing. When a disturbance occurs at a portion in an elastic medium, it propagates through the medium in a finite time as a mechanical sound wave by the vibrations of molecules, atoms or any particles present. Such mechanical waves are also called elastic waves. A simple illustration of the ultrasonic waves produced in a solid is shown in **Fig. 3.1**, where distortion caused depending on whether a force is applied normal or parallel to the surface at one end of the solid can result in producing compression or shear vibrations, respectively, so that two types of ultrasonic waves, i.e. longitudinal waves or transverse waves, propagate through the solid. The energy of the wave is also carried with it.

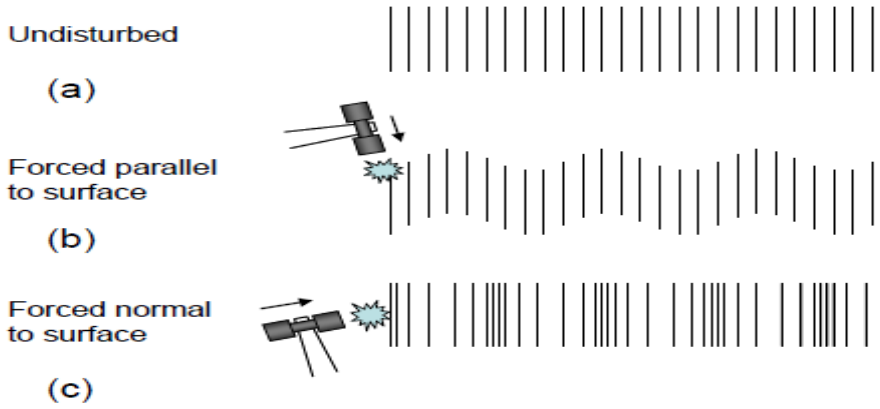

Fig. 3.1: Schematics of ultrasonic waves in a bulk specimen: (a)equilibrium state

(b) transverse vibrations (c)longitudinal vibrations(http://www.googleimages.com)

An ultrasonic wave moves at a velocity (the wave velocity) that is determined by the material properties and shape of the medium, and occasionally the frequency. The ultrasonic wave imparts motion to the material when it propagates. This is referred to as particle motion, to distinguish it from the wave motion. This particle motion is usually specified as a particle velocity *v*. It is noted in ultrasonic measurements that the particle velocity is much smaller than wave velocity. Also, one can understand that no ultrasonic wave propagates in vacuum because there are no particles that can vibrate in vacuum.

3.2Basic Concepts of Wave Propagation

3.2.1 Some Common Terms Used:

•**Sound Waves: -**Sound waves are simply organized mechanical vibrations travelling through a medium, which may be a solid, a liquid, or a gas. These waves will travel through a given medium at a specific speed or velocity, in a predictable direction, and when they encounter a boundary with a different medium they will be reflected or transmitted according to simple rules. This is the principle of physics that underlies ultrasonic flaw detection.

• **Frequency: -**All sound waves oscillate at a specific frequency, or number of vibrations or cycles per second, which we experience as pitch in the familiar range of audible sound. Human hearing extends to a maximum frequency of about20,000 cycles per second (20 KHz), while the majority of ultrasonic flaw detection applications utilize frequencies between 500 KHz to 10 MHz.

• **Wave Speed:** The speed of a sound wave varies depending on the medium through which it is travelling, affected by the medium's density and elastic properties.

• **Wavelength (λ)**: It is the distance between any two corresponding points in the wave cycle as it travels through a medium. Wavelength is related to frequency and velocity by the simple equation

$$\lambda = c/ \upsilon \qquad \text{.....(3.1)}$$

where, λ = wavelength, c = sound velocity, υ = frequency

In ultrasonic flaw detection, the generally accepted lower limit of detection for a small flaw is one-half wavelength, and anything smaller than that will be invisible. In ultrasonic thickness gauging, the theoretical minimum measurable thickness is one wavelength.

•**Attenuation**

When an ultrasonic wave propagates through a medium, ultrasonic attenuation is caused by a loss of energy in the ultrasonic wave and other reasons. The attenuation can be seen as a reduction of amplitude of the wave. There are some factors affecting the amplitude and waveform of the ultrasonic wave, such as ultrasonic beam spreading, energy absorption, dispersion, nonlinearity, transmission at interfaces, scattering by inclusions and defects, Doppler effect and so on.

• **Acoustic impedance (Z):** Sound travels through materials under the influence of sound pressure. Because molecules or atoms of a solid are bound elastically to one another, the excess pressure results in a wave propagating through the solid. The Acoustic impedance (Z)of a material is defined as the product of its density (ρ) and acoustic speed in medium

$$Z = \rho V \qquad \text{.....(3.2)}$$

Acoustic impedance is important in determining acoustic transmission and reflection at the boundary of two materials having different acoustic impedances.

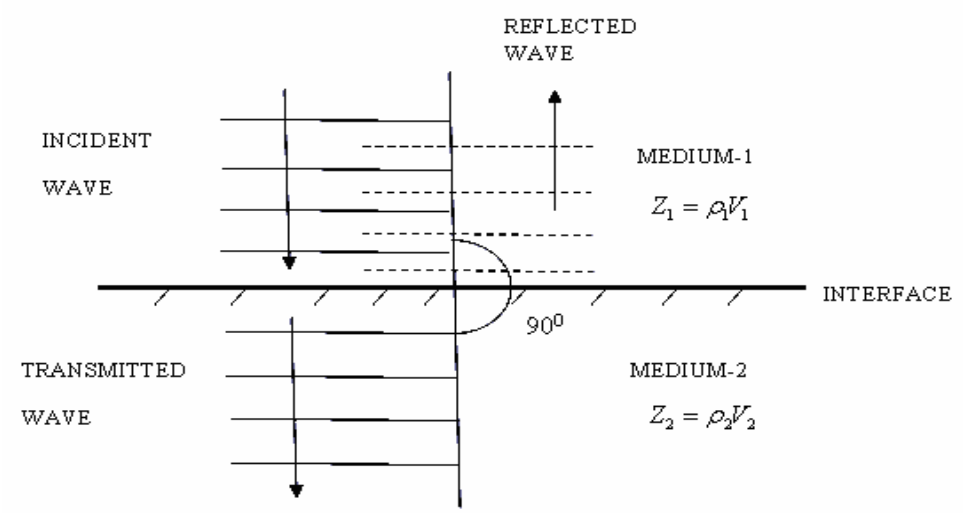

Fig. 3.2: Reflection and Transmission of sound wave at normal incidence(Bindal, 1999)

• **Reflection and Transmission Coefficients:** Ultrasonic waves are reflected at boundaries where there is a difference in acoustic impedances (Z) of the materials on each side of the boundary as shown in the **Fig. 3.2**. This difference in Z is commonly referred to as the impedance mismatch. The greater the impedance mismatch, the greater the percentage of energy that will be reflected at the interface or boundary between one medium and another. When the acoustic impedances of the materials on both sides of the boundary are known, the fraction of the incident wave intensity that is reflected can be calculated with the equation below. The value produced is known as the reflection coefficient.

$$\text{Reflection coefficient }, R = \frac{Z_2 - Z_1}{Z_2 + Z_1} = \frac{\rho_2 V_2 - \rho_1 V_1}{\rho_2 V_2 + \rho_1 V_1} \qquad \text{.....(3.3)}$$

Transmission coefficient, $T = \frac{2Z_2}{Z_2 + Z_1} = \frac{2\rho_2 V_2}{\rho_2 V_2 + \rho_1 V_1}$. .....(3.4)

3.2.2 Reflection, Refraction and Mode Conversion of Waves

When sound travels in a solid material, one form of wave energy can be transformed into another form. Mode conversion occurs when a wave encounters an interface between materials of different acoustic impedances and the incident angle is not normal to the interface.

When sound waves pass through an interface between materials having different acoustic velocities, refraction takes place at the interface. The larger the difference in acoustic velocities between the two materials, the more the sound is refracted.. Snell's Law holds true for shear waves as well as longitudinal waves and can be written as

$$\frac{\sin\theta_1}{V L_1} = \frac{\sin\theta_2}{V L_2} = \frac{\sin\theta_3}{V S_3} = \frac{\sin\theta_4}{V S_4} \quad \text{.....}$$

….(3.5)

3.2.3 Modes of Wave Propagation:

The ultrasonic waves propagate in a number of ways in a medium. On the basis of the mode of particle displacement, these waves can be classified as given in Table 3.1

a) Longitudinal or Compressional waves (L-waves)

b) Transverse or Shear waves (S-waves)

c) Surface or Rayleigh waves

d) Lamb or Plate waves

e) Creeping or Head waves

Out of these longitudinal and transverse wave propagations are most important and are extensively used in ultrasonic NDT applications for Civil structures. Surface waves and lamb waves are used for monitoring of thin plate geometries to locate surface defects.

Table 3.1: Types of Waves Propagation (http://www.ndt-ed.org)

Sr. no	Type of wave	Direction of motion of particles
1	Longitudinal or Compression waves (L-waves)	Parallel to wave direction
2	Transverse or Shear waves (S-waves)	Perpendicular to wave direction
3	Surface or Rayleigh waves	Elliptical orbit – symmetrical mode
4	Plate waves- Lamb	Component perpendicular to surface (extensional wave)
5	Plate waves- Love	Parallel to plane layer, perpendicular to wave direction
6	Stoneley (Leaky Rayleigh Waves)	Wave guided along interface
7	Sezawa	Anti symmetric mode

- **Longitudinal or Compressional waves**:

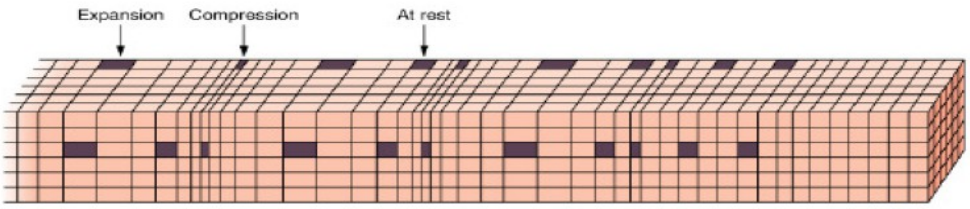

Fig 3.3: Propagation of Longitudinal waves (http://www.googleimages.com)

In longitudinal waves, the oscillations occur in the longitudinal direction or the direction of wave propagation. Since compressional and dilatational forces are active in these waves, they are also called pressure or compressional waves.

- **Transverse or Shear waves:**

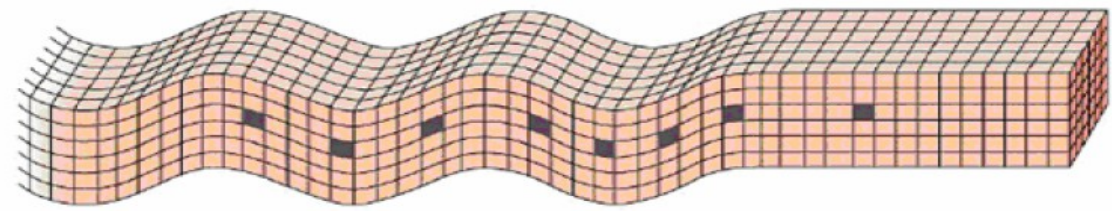

Fig 3.4: Propagation of Transverse or Shear waves (http://www.googleimages.com)

In the transverse or shear wave, the particles oscillate at a right angle or transverse to the direction of propagation. Shear waves require an acoustically solid material for effective propagation, and therefore, are not effectively propagated in materials such as liquids or gasses. Shear waves are relatively weak when compared to longitudinal waves.

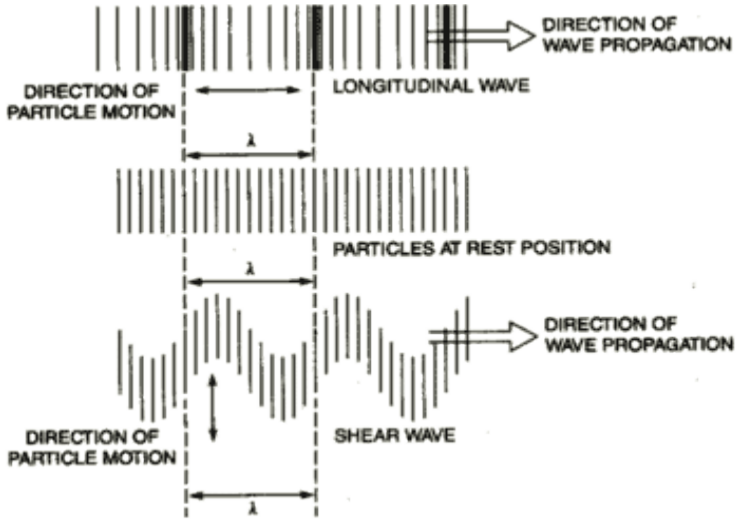

Fig 3.5: Particle Movement Showing the Propagation of Longitudinal and Shear Waves (http://www.ndt-ed.org)

- **Surface (or Rayleigh) waves:**

Surface (or Rayleigh) waves travel the surface of a relatively thick solid material penetrating to a depth of one wavelength. The particle movement has an elliptical orbit as shown in the image below. Rayleigh waves are useful because they are very sensitive to surface defects and they follow the surface around curves. Because of this, Rayleigh waves can be used to inspect areas that other waves might have difficulty reaching.

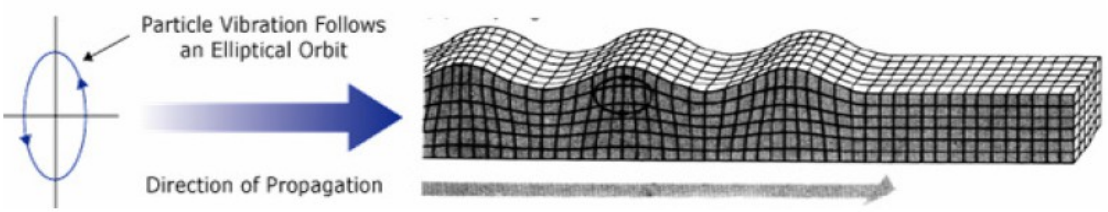

Fig 3.6: Propagation of Surface or Rayleigh Waves (http://www.googleimages.com)

- **Lamb waves or Plate waves:**

Plate waves can be propagated only in very thin metals. Lamb waves are the most commonly used plate waves in NDT. With lamb waves, a number of modes of particle vibration are possible, but the two most common are symmetrical and asymmetrical.. Symmetrical lamb waves move in a symmetrical fashion about the median plane of the plate. Wave motion in the symmetrical mode is most efficiently produced when the exciting force is parallel to the plate. The asymmetrical lamb wave mode is often called the "flexural mode" because a large portion of the motion moves in a normal direction to the plate, and a little motion occurs in the direction parallel to the plate. In this mode, the body of the plate bends as the two surfaces move in the same direction.

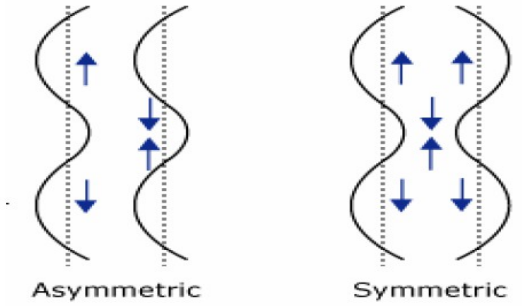

Fig 3.7: Lamb Waves Propagation (a) Symmetrical (Dilatational) and

(b) Asymmetrical (Bending) waves (http://www.googleimages.com)

- **Creeping or Head waves:**

These waves are also called head waves. The behaviour of creeping waves is similar to that of longitudinal waves. They travel as fast as longitudinal. These are generated parallel to scanning surface, enabling detection of surface breaking defects. These have limited range

and as these travel just below the surface and not on the surface, so the couplant has no influence.

3.3Ultrasonic Testing

3.3.1 Basic Principles of Ultrasonic Testing

Ultrasonic Testing (UT) uses high frequency sound energy to conduct examinations and make measurements. Ultrasonic inspection can be used for flaw detection/evaluation, dimensional measurements, material characterization, and more. To illustrate the general inspection principle, a typical pulse/echo inspection configuration as illustrated below will be used.

A typical UT inspection system consists of several functional units, such as the pulser/receiver, transducer, and display devices. A pulser/receiver is an electronic device that can produce high voltage electrical pulses. Driven by the pulser, the transducer generates high frequency ultrasonic energy. The sound energy is introduced and propagates through the materials in the form of waves. When there is a discontinuity (such as a crack) in the wave path, part of the energy will be reflected back from the flaw surface. The reflected wave signal is transformed into an electrical signal by the transducer and is displayed on a screen. In the applet below, the reflected signal strength is displayed versus the time from signal generation to when a echo was received. Signal travel time can be directly related to the distance that the signal travelled. From the signal, information about the reflector location, size, orientation and other features can sometimes be gained.

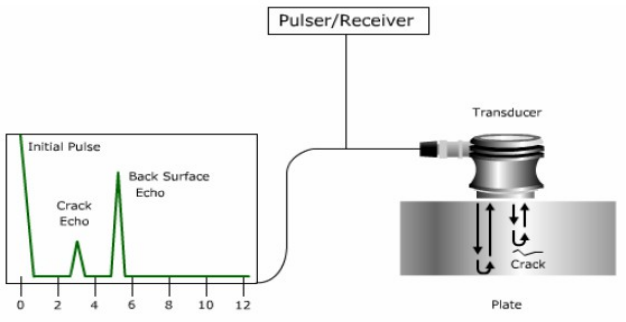

Fig. 3.8: Pulse echo method ultrasonic inspection principle (http://www.ndt-ed.org)

Ultrasonic Inspection is a very useful and versatile NDT method. Some of the **advantages** of ultrasonic inspection that are often cited include:

- It is sensitive to both surface and subsurface discontinuities.

- The depth of penetration for flaw detection or measurement is superior to other NDT methods.
- Only single-sided access is needed when the pulse-echo technique is used.
- It is highly accurate in determining reflector position and estimating size and shape.
- Minimal part preparation is required.
- Electronic equipment provides instantaneous results.
- Detailed images can be produced with automated systems.
- It has other uses, such as thickness measurement, in addition to flaw detection.

As with all NDT methods, ultrasonic inspection also has its **limitations**, which include:

- Surface must be accessible to transmit ultrasound.
- Skill and training is more extensive than with some other methods.
- It normally requires a coupling medium to promote the transfer of sound energy into the test specimen.
- Materials that are rough, irregular in shape, very small, exceptionally thin or not homogeneous are difficult to inspect.
- Cast iron and other coarse grained materials are difficult to inspect due to low sound transmission and high signal noise.
- Linear defects oriented parallel to the sound beam may go undetected.
- Reference standards are required for both equipment calibration and the characterization of flaws.

3.3.2Methods of Ultrasonic Testing

1.Pulse echo method

In the pulse-echo method, a piezoelectric transducer with its longitudinal axis located perpendicular to and mounted on or near the surface of the test material is used to transmit and receive ultrasonic energy as shown in **Fig 3.9**. The ultrasonic waves are reflected by the opposite face of the material or by discontinuities, layers, voids, or inclusions in the material,

and received by the same transducer where the reflected energy is converted into an electrical signal. The electrical signal is computer processed for display on a video monitor or TV screen. The display can show the relative thickness of the material, depth into the material and where the flaws are located in the X-Y plane.

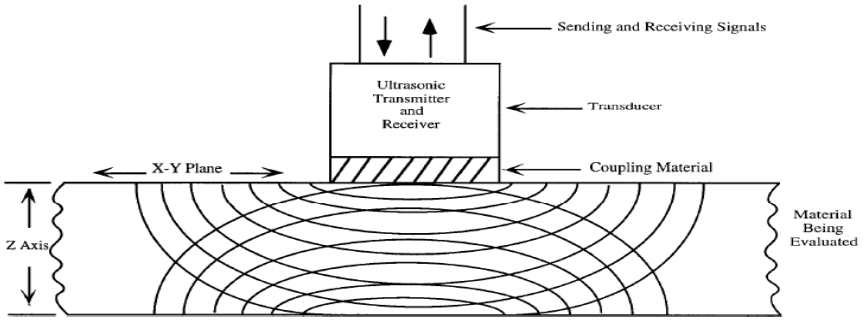

Fig. 3.9: Principle of pulse echo method of inspection (Vermani, 2008)

2.Pulse-Transmission Method

In the pulse-transmission method, an ultrasonic transmitter is used on one side of the material while a detector is placed on the opposite side. One unit acts as transmitter and the other unit as receiver. The beam from the transmitter T travels through the material to its opposite surface where the receiving transducer R is placed as shown in **Fig 3.10**. Scanning of the material using this method will result in the location of defects, flaws, and inclusions in the X-Y plane.

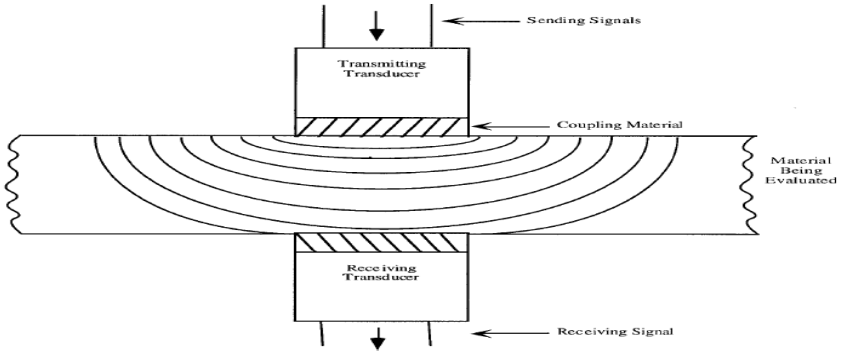

Fig 3.10 Principle of through transmission of ultrasonic testing (Vermani, 2008)

3. Two Transducer Method

The pulse echo method can be used with either single or double crystal unit in single transducer unit the probe acts as both transmitter and receiver .In two transducer arrangement, one transmits and other receives the ultrasonic waves .These are placed on same

side of specimen and pulse wave is send in to the specimen by the transducer T (Transmitter) and the echoes reflected from the back surface or any defect are received by the transducer R (Receiver) and displayed on the flaw detector screen. For specific applications like wall thickness measurement special type of transducers in which the transmitting and the receiving crystals are housed in a single unit are also used .These transducers are popularly known as 'twin' or T-R probes. For example, **Fig 3.11** in which two transducers are placed on the same side of the plate at certain angle to detect the damage.

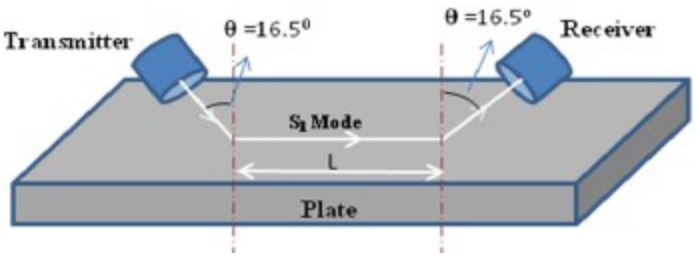

Fig. 3.11: Transducers arranged at an angle to the Plate(http://www.googleimages.com)

3.4 Classification of Ultrasonic Waves for NDT Applications

Ultrasonic waves can be classified in two types depending upon the NDT applications;

• Body waves or bulk waves

• Surface waves or guided waves.

Body waves propagate through a bulk material, hence attenuate, while the surface waves propagate along the surface of a body as shown in **Fig 3.12**.The inspection of large structures using conventional ultrasonic bulk wave (*longitudinal and shear waves)* techniques is slow because scanning is required if the whole structure is to be tested.

Surface waves are often called guided waves because the geometry of the body guides them .Ultrasonic guided waves (*Rayleigh and Lamb waves, bar, plate and cylindrical guided waves)*potentially provide an attractive solution to this problem because they can be excited at one location on the structure and will propagate many meters (Cawley, 2002).

Guided waves refer to mechanical (or elastic) waves in ultrasonic and sonic frequencies that propagate in a bounded medium (such as pipe, plate, rod, etc.) parallel to the plane of its boundary.

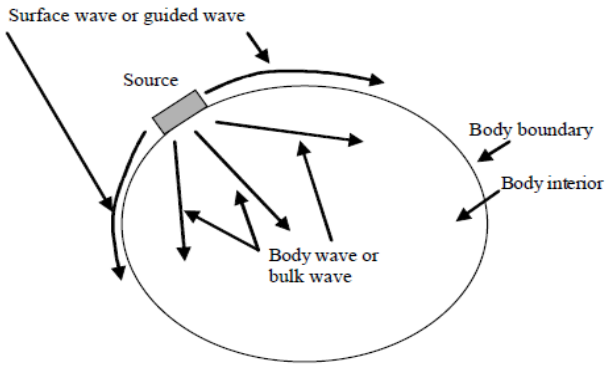

Fig.3.12: Body waves and surface waves generated by an ultrasonic source (Kundu, 2007)

Guided waves can further be classified into following types, as shown in **Fig 3.13**:

• Bar waves

• Cylindrical wave

• Rayleigh waves

• Lamb waves

• Rayleigh-Lamb waves

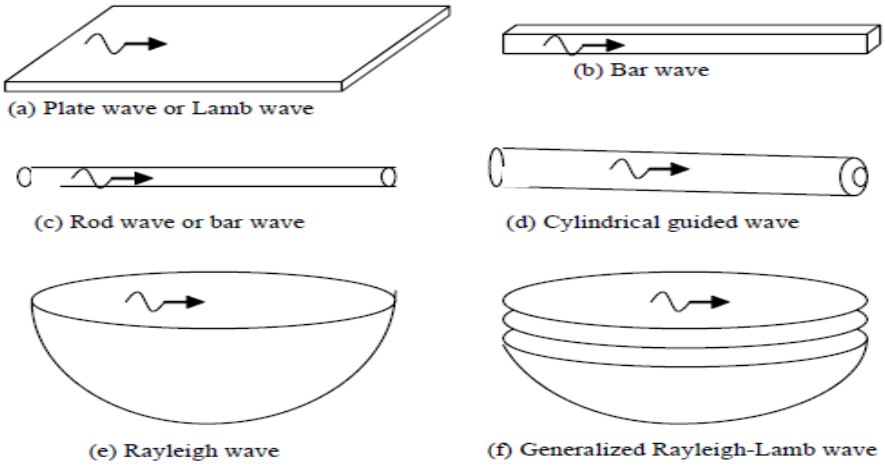

Fig. 3.13: Different types of guided waves in various problem geometries (Kundu, 2007)

Cylindrical Guided Waves: Elastic waves propagating through a hollow cylinder or pipe are called cylindrical guided waves (**Fig 3.13(d)**). Since for a cylinder the two stress-free surfaces- inner and outer surfaces – are parallel to each other as in a plate, sometimes the cylindrical guided waves are also called Lamb waves.

Bar waves: When guided waves propagate through a rod or bar they are known as bar waves (**Fig 3.13(c)**).

Rayleigh wave: If the structure is a homogenous half-space then the guided wave propagating along the surface of the half-space is called Rayleigh wave (**Fig 3.13(e)**).

Lamb waves: Waves propagating through a plate type structure with two parallel stress-free boundaries are known as Lamb waves, again named after its inventor. Lamb waves are also known as plate waves because they propagate through plates (**Fig 3.13(a)**).

Rayleigh-Lamb waves: Waves propagating parallel to the free surface of a multilayered solid half-space are known as generalized Rayleigh-Lamb waves or simply Rayleigh waves (**Fig 3.13(f)**).

3.5 Ultrasonic Guided Waves

In an infinite isotropic solid medium only two types of independent wave propagation exist, i.e., compressional and shear waves. Both waves propagate with constant velocities and are non-dispersive. When geometry constraints are introduced and the dimensions are close to the wavelength, the wave becomes dispersive and is called a guided wave (Reis et al., 2005). In an infinite bulk of a perfectly elastic material, ultrasonic waves travel as bulk waves, decaying in amplitude because of the spread of the wave front. However, in a finite perfectly elastic medium, the sound wave is reflected from the structure boundaries, and the energy is contained within the elastic medium as a guided wave, which propagates with constant amplitude.

Ultrasonic Guided Wave inspection and structural health monitoring is being considered today in such natural wave guide structures as plates, multi-layer structures, rods, rails, piping and tubing, an interface, and curved or flat layers on a half space. An increased understanding of the basic physics and wave mechanics associated with guided wave inspection has led to an increase in practical non destructive evaluation and inspection problems. Computing power today is also making dreams come true, where only a vision was possible decades ago. A principal advantage of guided waves is inspection over long distances with excellent sensitivity from a single probe position. There is also an ability to inspect hidden structures and structures under water, coatings, insulations, and concrete.

To think of the utilization of ultrasonic guided waves we can consider a variety of different natural wave guides as outlined in **Table 3.2**. Guided wave inspection is a natural for any of these structures so when you really think about it guided waves can be applied to many, many structures very quickly and efficiently.

Table 3.2: Natural Waveguides (Rose, 2004)

Plates (aircraft skin)
Rods (cylindrical, square, rail, etc.)
Hollow cylinder (pipes, tubing)
Multi-layer structures
Curved or flat surfaces on a half-space
Layer or multiple layers on a half-space
An interface

Table 3.3: Benefits of Guided Waves over Bulk waves (Rose, 2004)

Inspection over long distances from a single probe position
By mode and frequency tuning, to establish wave resonances and excellent overall defect detection and sizing potential.
Often greater sensitivity than that obtained in standard normal beam ultrasonic inspection or other NDT techniques. (Beam focusing is on the horizon for even improved sensitivity.)
Ability to inspect hidden structures and structures under water, coatings, insulations, and concrete with excellent sensitivity.
Cost effectiveness because of inspection simplicity and speed.

An understanding of the basic wave mechanics and wave propagation principles for various sensors and mode types is essential, though, if one is to carry out some reliable tests. The benefits of guided waves are illustrated in **Table 3.3**. The most interesting one of course is to be able to inspect over long distances from a single probe position.

The wave is termed “guided” because it travels along the medium guided by the geometric boundaries of the medium. Since the wave is guided by the geometric boundaries of the medium, the geometry has a strong influence on the behaviour of the wave (Achenbach, 1975).In contrast to ultrasonic waves used in conventional ultrasonic inspections that propagate with a constant velocity, the velocity of the guided waves varies significantly with

the wave frequency and the geometry of the medium. In addition, at a given wave frequency, the guided waves can propagate in different wave modes and orders (Sang-Young Kim et al., 2001). Guided waves travel either at boundaries (Surface Waves) or between the boundaries (Lamb Waves) as shown in **Fig 3.14**. Guided waves are the result of the intersection occurring at the interface between the two different materials. This interaction produces reflection, refraction and mode conversion between longitudinal and shear waves which can be predicted using appropriate boundary conditions. Guided waves are highly dependent on wavelength and frequency, and propagating guided waves can only exist at specific combinations of frequency, wave number and attenuation.

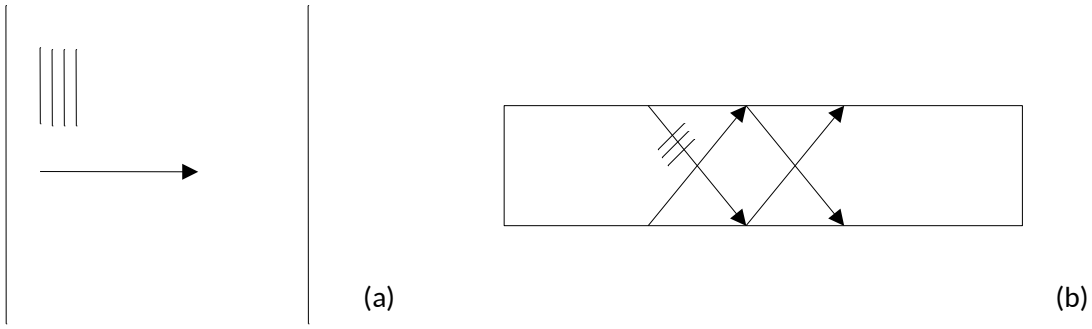

Fig. 3.14: Schematic of (a) bulk wave and (b) Guided wave propagation (Demma, 2003)

The complex effect of the boundaries results in dispersion of the wave and generates different modes that have predictable frequency-dependent properties. The velocity-frequency relationships of guided waves can be displayed as dispersion curves (Pavalakovic et al., 2000). Every natural wave guided has associated with it a set of dispersion curves that presents to us the wave propagation possibilities in that structure. At each point of a dispersion curve there is a different wave structure. When studying the dispersion curve it is easy to understand that there is a corresponding frequency bandwidth associated with the abscissa value, but there is also a phase velocity bandwidth associated with the ordinate value on the phase velocity dispersion curve. This means that we are actually exciting a fairly large zone and multiple modes could propagate in a structure at the same time.

Adding further finite layers around the material, such as concrete around steel bar as in case of RC structures further complicates the waveguide, as energy can now be passed between the layers. In this case, a guided wave will still propagate in the structure as a whole, but with properties that depend on the elastic and damping properties of all the layers. Stress and displacement boundary conditions must be satisfied at the boundaries between layers.

Attenuation through leakage can occur if the outermost layer may be considered infinite in extent. Hence, steel bar in concrete is modelled as a solid cylinder embedded in an infinite concrete medium, considering both the materials as isotropic, homogenous and elastic. A global matrix method is employed for solution of wave propagation equation using optimization techniques (Ervin et al., 2009) which was then developed into a standard software Disperse (Pavalakovic et al., 2000).

For a layered system, the solution includes phase velocity, frequency and attenuation. Attenuation is due to material absorption and energy leakage into the surrounding concrete. The waves propagate in longitudinal, flexural and torsional modes due to complex effect of boundaries and they have frequency dependant properties. In such cases specific modes can be excited selectively by choosing a frequency bound. Longitudinal waveforms have axial and radial displacements, torsional waveforms have angular displacements and flexural waveforms have all three displacements. They are represented by L (m, n); T (m, n) and F(m, n) respectively where 'm' and 'n' represent the circumferential displacements and sequential order of mode respectively.

3.6 Literature Review

In the following, the use of Ultrasonic Guided Waves till date for monitoring RC or concrete structures is being reviewed.

Kim et al. (2001) studied that long-range guided wave inspection is a new emerging technology for rapidly and globally inspecting a large area of a structure from a single test location. Also, a general overview of the guided wave properties and its application for long range inspection of structures, the principle and instrument system for a guided wave inspection technology called "magnetostrictive sensor (MsS)" that generates and detects guided waves electromagnetically in the material under testing, and examples of long-range guided wave inspection of structures that can be accomplished using the MsS.

Kundu et al. (2002 a) studied the feasibility of detecting and quantifying delamination at the interface between steel bar and concrete using ultrasonic guided waves was investigated in this paper. These waves can propagate a long distance along the reinforcing steel bar or concrete beam as guided waves are sensitive to interface bonding condition between the steel

bar and concrete. The traditional ultrasonic methods are good for detecting large voids in concrete but are not efficient for detecting delamination at the interface between concrete and steel bar since they use reflection, transmission and scattering of longitudinal waves by internal discontinuities. In this study, special solid couplers between the steel bars (or concrete beam) and ultrasonic transducers have been used to launch flexural cylindrical guided waves (or lamb waves) in steel bar (or concrete). This investigation showed that the guided wave testing technique was an efficient and effective tool for health monitoring of reinforced concrete structures.

Kundu et al. (2002 b) applied the ultrasonic guided wave technique to concrete beams reinforced by glass fiber reinforced polymer bars to investigate the effect of high attenuation. This study showed that ultrasonic guided wave testing technique has potential for both glass fiber reinforced polymer/concrete and steel/concrete interface testing.

Kundu et al. (2003) investigated the feasibility of detecting interface degradation and separation of steel bars in concrete beams using Lamb waves. In this study, a special coupler between the steel bar and ultrasonic transducers was used to launch non-axisymmetric guided waves in the steel bar. This investigation showed that the Lamb wave inspection technique was an efficient and effective tool for health monitoring of reinforced concrete structures.

Reis et al. (2005) studied the development of a wireless embedded sensor system to monitor and assess corrosion damage in reinforced concrete, reinforced mortar specimens were manufactured with seeded defects to simulate corrosion damage. Taking advantage of waveguide effects of the reinforcing bars, these specimens were then tested using an ultrasonic approach. Using the same ultrasonic approach, specimens without seeded defects were also monitored during accelerated corrosion tests. Both the ultrasonic sending and the receiving transducers were mounted on the steel rebar. Advantage was taken of the lower frequency (<250 kHz) fundamental flexural propagation mode because of its relatively large displacements at the interface between the reinforcing steel and the surrounding mortar. Waveform energy (indicative of attenuation) was presented and discussed in terms of corrosion damage. Current results indicated that the loss of bond strength between there reinforcing steel and the surrounding concrete can be detected and evaluated.

Rizzo et al. (2007) studied the method based on outlier analysis and the wavelet transform for structural damage detection based on guided ultrasonic waves. The basic idea is to denoise and compress the ultrasonic signals by the discrete wavelet transform and use the relevant wavelet coefficients to construct a one-dimensional or multidimensional damage index. The damage index was then fed to an outlier analysis to detect anomalies that were representative of structural defects. By extracting the essential information from the ultrasonic signals, the dimension of the damage index was kept at a minimum, as desirable for continuous structural monitoring. The general framework was applied to the detection of notch-like defects in a seven-wire strand by using built-in magnetostrictive devices for ultrasound transduction. Random noise was digitally added to the raw ultrasonic measurements to create statistical populations of the baseline (undamaged) conditions and the damaged conditions. This application demonstrates the effectiveness of the multidimensional analysis compared to the uni dimensional analysis, while keeping the number of features as low as four.

Ervin et al. (2008) invoked the Guided longitudinal modes in both low (<200 kHz) and high(2–8 MHz) frequency ranges to monitor damage in reinforced mortar specimens undergoing accelerated uniform corrosion. The fundamental longitudinal mode, i.e. $L(0, 1)$, and the $L(0,9)$ mode were invoked for low- and high-frequency testing, respectively. Because of the significant amount of axial displacement at the steel/mortar interface, the L(0, 1) mode was so appreciably attenuated for the particular specimen size used that it is was not detected until after corrosion had initiated and corrosion product accumulation caused mortar cracking. Once detected, the L(0, 1) mode was sensitive to the combined effects of bond deterioration and mortar stiffness reduction. The L(0, 9) mode had negligible radial and axial displacement at the steel/mortar interface. As a result, the L(0, 9) mode is relatively insensitive to the surrounding interface conditions at high frequencies. This allows for changes in the steel cross-sectional area and bar topography to be isolated and monitored from the onset of corrosion up to severe pitting.

Ervin et al. (2009) studied the creation of an embeddable ultrasonic sensing network for assessment of reinforcement deterioration. Towards this effort, guided ultrasonic waves were used to monitor reinforced mortar specimens undergoing accelerated uniform and localized corrosion. Longitudinal waves were invoked at higher frequencies (2- 9MHz), where the attenuation is a local minimum. Using a through transmission configuration, waveforms were

sensitive to both forms of corrosion damage. Scattering, mode conversions and reflections from irregularities at the bar surface from uniform corrosion and the severely tapered crosssection from localized corrosion are thought to cause the increase in attenuation. Because localized corrosion did not yield a discontinuity that was nearly perpendicular to the bar axis, incident waves were severely scattered, mode converted and rapidly attenuated. As evidence, this was the inability of pulse-echo testing to detect reflected waveforms for the localized corrosion.

Sharma et al. (2010) used high frequency ultrasonic guided waves to develop a damage detection methodology for steel bars embedded in concrete with simulated notch and debond defects. Both pulse transmission and pulse echo techniques were adopted and the time off light and signal attenuation was observed to locate and quantify damages accurately. The method is then successfully applied to reinforced concrete beam specimens undergoing accelerated chloride corrosion. The simulated and actual corrosion results were compared. The ultrasonic signals effectively relate to the state of reinforcing bar undergoing actual corrosion.

Sachu, (2010) studied the use of high frequency ultrasonic guided waves to develop a damage detection methodology for tendons embedded in concrete corrosion of simulated notch and debond defects. Conventional techniques of pulse transmission and pulse echo techniques were used for testing. The time of flight in P/E and signal attenuation in both P/E and P/T was observed to locate and quantify damages accurately. The method was then successfully applied to reinforced concrete beam specimens with embedded tendons undergoing accelerated chloride corrosion. Suitable surface and core seeking ultrasonic guided wave modes were identified which were sensitive to delamination and pitting effects of corrosion respectively. These modes were used to ultrasonically monitor reinforced concrete beams undergoing accelerated impressed current corrosion in chloride environment. The simulated and actual corrosion results were compared to show suitability of simulated techniques. Tendon in concrete results in pitting of tendons and debonding from surrounding grout. It was concluded that ultrasonic guided waves can be utilized for onsite inspection of embedded tendons for any breaks/cracks in tendons and corrosion related damages.

Sharma and Mukherjee (2010) investigated the type of corrosion mechanism in chloride and oxide environments in RC beams. Ultrasonic guided waves with specific core and surface

seeking modes were used for monitoring rebar corrosion in beams. It was observed that in case of chloride corrosion in beams, when core-seeking mode was propagated, the signal was highly attenuated, thus indicating pitting and non-uniform area loss. When surface seeking mode was propagated, there was an initial rise in signal strength and then a fall, thus indicating delamination followed by local loss of material. In case of Oxide corrosion in beams, it was observed that when core-seeking mode was propagated, there was a slow fall in signal strength, indicating the absence of pitting. When the surface seeking mode was propagated, there was an initial drop in the signal due to pressure built up by the formation of corrosion products, indicating a slow corrosion rate and localized corrosion and eventually, a gradual rise in signal strength was observed, indicating slow bond deterioration. The ultrasonic voltage trends of the received signal in both chloride and oxide corrosion specimens using surface-seeking and core-seeking mode were obtained. The mechanism and rate of rebar corrosion was successfully monitored in chloride and oxide environments through appropriate selection of modes. Simultaneous destructive tests were also carried out on RC beams, and it was found, that non-destructive Ultrasonic technique correlate well with the destructive technique.

Sharma and Mukherjee (2012) studied non-destructive evaluation of reinforcing bars that are corroding in the presence and absence of chlorides utilizing ultrasonic guided waves is reported. Calibration of the ultrasonic data with the physical condition of the bar in the two environments has been attempted which is done by conducting destructive tests of mass loss, tensile strength, and pull out strength at different stages of corrosion. Ultrasonic guided wave monitoring utilizing specific core and surface seeking modes successfully identifies the type, rate, and mechanism of corrosion in a reinforcing bar in concrete subjected to different exposure conditions. In general, huge pitting and non-uniform area loss highlighted by severe signal attenuation marks chloride corrosion is well picked up by core seeking mode. It begins with delamination shown by signal rise with surface seeking mode. In oxide corrosion, the rate of corrosion is slow, localized, and marked by slow bond deterioration as depicted by signal strength rise in surface seeking mode. Pitting is insignificant as shown by very slow signal fall in core seeking mode in OC. Thus, through a judicious selection of ultrasonic modes different types of corrosion in RC structures can be successfully identified.

Sharma and Mukherjee (2014) carried out a study on ultrasonic guided wave technique for monitoring the setting behaviour of freshly poured concrete of different workabilities. The

two mixes were control concrete(CC) and self-compacting concrete (SCC) for which slab specimens of dimensions 100 mm x 300 mm x 300 mm were used such that one 25 mm diameter bar was embedded at the centre of the specimen of 500 mm length with 100 mm projecting on both the sides . For the two mixes of varying workabilities the results using L(0,l) mode depicted fall in the signal strength with time due to better bond development between the bar and concrete . After the initial setting as the concrete hardens leakage from steel bar to concrete enhanced which lead to a fall in R value. Further on completion of hardening i.e. final setting the slope of curve reduced to zero. The fall was sharp in case of CC as compared to SCC where there was gradual reduction in R value till 26 hours and then it gathered speed.

Sharma and Mukherjee (2015) conducted a study on ultrasonic monitoring technique for freshly poured concrete with composition as 1:1.5:2.9 (cement, sand and aggregates) with 0.45 as the water-cement ratio. Specimen dimension of 150mm x 150mm x 300 mm with 25 diameter mild steel bar at the centre of it having 600mm length, 150 mm projected on both sides. It was observed that with 1 MHz frequency no drastic change was noticed whereas with 0.1 MHz as the concrete hardened, bond developed between bar and concrete and signal leaked and attenuated with fall in peak to peak voltage amplitude. Thus with increasing age of concrete the signal drops continuously. Hence L (0,1) mode with 0.1 MHz is called Surface Seeking Mode as it detects the interfacial changes . The R value fell from 1 to 0.9 in first 1½–2 h indicating the voltage amplitudes remain steady , further value dropped from 0.9 to 0.1 indicating phase change of concrete from fluid to solid in 2 to 18 hours , after that it fell from 0.1 to 0 marking the solidification of concrete .

3.7 Closing Remarks

This chapter highlights the various details of ultrasonic waves and discusses in detail the classifications of ultrasonic waves. Here the use of ultrasonic guided waves in structural health monitoring is discussed and the literature supporting the same is also reviewed. The next chapter highlights the various details of using Acoustic Emissions technique for concrete monitoring.

CHAPTER-4

ACOUSTIC EMISSIONS TECHNIQUE

4.1 Introduction to Acoustic Emission Testing

Acoustic Emission (AE) refers to the generation of transient elastic waves produced by a sudden redistribution of stress in a material. When a structure is subjected to an external stimulus (change in pressure, load, or temperature), localized sources trigger the release of energy, in the form of stress waves, which propagate to the surface and are recorded by sensors. With the right equipment and setup, motions on the order of picometers (10 -12 m) can be identified. Sources of AE vary from natural events like earthquakes and rock bursts to the initiation and growth of cracks, slip and dislocation movements, melting, twinning, and phase transformations in metals. In composites, matrix cracking and fiber breakage and debonding contribute to acoustic emissions. AE's have also been measured and recorded in polymers, wood, and concrete, among other materials.

Detection and analysis of AE signals can supply valuable information regarding the origin and importance of a discontinuity in a material. Because of the versatility of Acoustic Emission Testing (AET), it has many industrial applications (e.g. assessing structural integrity, detecting flaws, testing for leaks, or monitoring weld quality) and is used extensively as a research tool.

Acoustic Emission is unlike most other non destructive testing (NDT) techniques in two regards. The first difference pertains to the origin of the signal. Instead of supplying energy to the object under examination, AET simply listens for the energy released by the object. AE tests are often performed on structures while in operation, as this provides adequate loading for propagating defects and triggering acoustic emissions.

The second difference is that AET deals with dynamic processes, or changes, in a material. This is particularly meaningful because only active features (e.g. crack growth) are highlighted. The ability to discern between developing and stagnant defects is significant. However, it is possible for flaws to go undetected altogether if the loading is not high enough to cause an acoustic event. Furthermore, AE testing usually provides an immediate indication relating to the strength or risk of failure of a component. Other advantages of AET include

fast and complete volumetric inspection using multiple sensors, permanent sensor mounting for process control, and no need to disassemble and clean a specimen.

Unfortunately, AE systems can only qualitatively gauge how much damage is contained in a structure. In order to obtain quantitative results about size, depth, and overall acceptability of a part, other NDT methods (often ultrasonic testing) are necessary. Another drawback of AE stems from loud service environments which contribute extraneous noise to the signals. For successful applications, signal discrimination and noise reduction are crucial.

Acoustic emission method can monitor changes in materials behaviour over a long time and without moving one of its components i.e. sensors. This makes the technique quite unique along with the ability to detect crack propagations occurring not only on the surface but also deep inside the material. The acoustic emission method is considered to be a “passive” non-destructive technique, because usually identifies defects while they develop during the test. The acoustic emission method is often used to detect a failure at a very early stage of damage long before a structure completely fails.

4.2AE-Sources

As mentioned in the Introduction, acoustic emissions can result from the initiation and growth of cracks, slip and dislocation movements, twinning, or phase transformations in metals. In any case, AE’s originate with stress. When a stress is exerted on a material, a strain is induced in the material as well. Depending on the magnitude of the stress and the properties of the material, an object may return to its original dimensions or be permanently deformed after the stress is removed. These two conditions are known as elastic and plastic deformation, respectively.

The most detectible acoustic emissions take place when a loaded material undergoes plastic deformation or when a material is loaded at or near its yield stress. On the microscopic level, as plastic deformation occurs, atomic planes slip past each other through the movement of dislocations. These atomic-scale deformations release energy in the form of elastic waves which “can be thought of as naturally generated ultrasound” travelling through the object. When cracks exist in a metal, the stress levels present in front of the crack tip can be several times higher than the surrounding area. Therefore, AE activity will also be observed when the material ahead of the crack tip undergoes plastic deformation (micro-yielding).

Two sources of fatigue cracks also cause AE's. The first source is emissive particles (e.g. non metallic inclusions) at the origin of the crack tip. Since these particles are less ductile than the surrounding material, they tend to break more easily when the metal is strained, resulting in an AE signal. The second source is the propagation of the crack tip that occurs through the movement of dislocations and small-scale cleavage produced by triaxial stresses.

The amount of energy released by an acoustic emission and the amplitude of the waveform are related to the magnitude and velocity of the source event. The amplitude of the emission is proportional to the velocity of crack propagation and the amount of surface area created. Large, discrete crack jumps will produce larger AE signals than cracks that propagate slowly over the same distance. Detection and conversion of these elastic waves to electrical signals is the basis of AE testing. Analysis of these signals yield valuable information regarding the origin and importance of a discontinuity in a material. As discussed in the following section, specialized equipment is necessary to detect the wave energy and decipher which signals are meaningful.

4.3AE Signal Features

With the equipment configured and setup complete, AE testing may begin. The sensor is coupled to the test surface and held in place with tape or adhesive. An operator then monitors the signals which are excited by the induced stresses in the object. When a useful transient, or burst signal is correctly obtained parameters like amplitude, counts, measured area under the rectified signal envelope (MARSE), duration, and rise time can be gathered. Each of the AE signal feature shown in the image is described below.

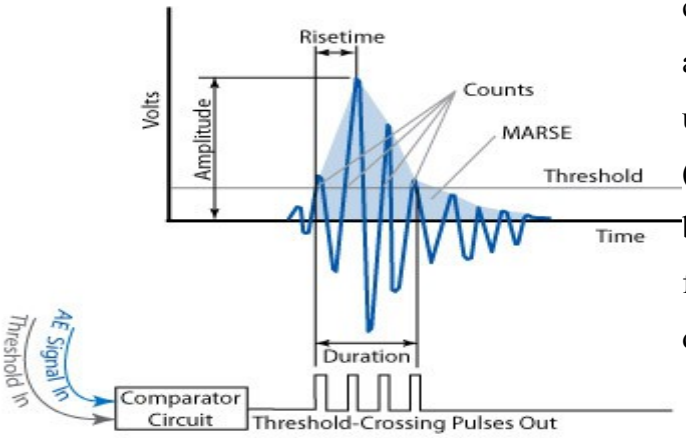

,

Fig 4.1: AE Signal Features (https://www.nde-ed.org)

Amplitude, A, is the greatest measured voltage in a waveform and is measured in decibels (dB). This is an important parameter in acoustic emission inspection because it determines the detectability of the signal. Signals with amplitudes below the operator-defined, minimum threshold will not be recorded.

Threshold: User defined value of amplitude in decibels (dB) . It is set based on background noise.

AE counts: Number of times an AE burst crosses the threshold.

AE energy: The area under amplitude – time curve above threshold value.

AE duration: Time between first and last threshold crossing.

AE hit: The detection and measurement of an AE signal on a channel

Rise – time: Time between first threshold crossing and maximum peak amplitude.

RA value: Rise time / maximum amplitude

Average Frequency = AE counts / duration

Data Display

Software-based AE systems are able to generate graphical displays for analysis of the signals recorded during AE inspection. These displays provide valuable information about the detected events and can be classified into four categories: location, activity, intensity, and data quality (cross plots).

Location displays identify the origin of the detected AE events. These can be graphed by X coordinates, X-Y coordinates, or by channel for linear computed-source location, planar computed-source location, and zone location techniques. Examples of each graph are shown to the right. Activity displays show AE activity as a function of time on an X-Y plot. Each bar on the graphs represents a specified amount of time. For example, a one-hour test could be divided into 100 time increments. All activity measured within a given 36 second interval would be displayed in a given histogram bar. Either axis may be displayed logarithmically in the event of high AE activity or long testing periods. In addition to showing measured activity over a single time period, cumulative activity displays (figure below right) can be created to show the total amount of activity detected during a test. This display is valuable for measuring the total emission quantity and the average rate of emission.

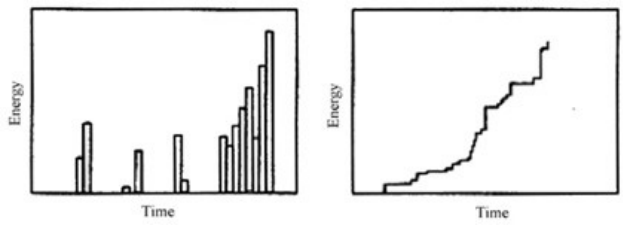

Fig 4.2: Data Display (https://www.nde-ed.org)

Intensity displays are used to give statistical information concerning the magnitude of the detected signals. As can be seen in the amplitude distribution graph to the near right, the number of hits is plotted at each amplitude increment (expressed in dB's) beyond the user-defined threshold. These graphs can be used to determine whether a few large signals or many small ones created the detected AE signal energy. In addition, if the Y-axis is plotted logarithmically, the shape of the amplitude distribution can be interpreted to determine the activity of a crack (e.g. a linear distribution indicates growth).

Abeele et al. (2009) studied microstructural changes occurring in freshly poured concrete during curing have been monitored on a laboratory scale using a combination of the Acoustic Emission (AE) Technique with linear and nonlinear ultrasonic/elastic wave spectroscopy. The evolution in the AE events, and in the linear and nonlinear ultrasonic behaviour of young concrete is analyzed as a function of the degree of hydration for various initial compositions during the first three days of the curing process. The results show a good correlation between the linear and nonlinear acoustic properties and the phase changes in the concrete due to chemical reactions and mechanical setting seen in the temperature profile.

Haneef (2013) studied the crack growth behaviour of plain and fly ash concretes with different curing periods during uniaxial compression testing using acoustic emission (AE) technique. Compressive strength of plain and fly ash concrete increase with curing periods and it becomes almost same order for 56 days curing. AE results have shown three distinct stages of AE activity in both concretes. The AE generated from the three stages has been attributed to crack closure/microcracking, steady crack propagation and unstable crack propagation. Fly ash concrete with proper curing produces evident filling effect for the pores and the occurrence of pozzolonic reaction leads to reduction of microcracking and corresponding decrease in amplitude of AE activity in the initial loading of fly ash concrete. The results showed that fly ash concrete specimen can withstand higher stress and strain without unstable crack propagation. An attempt has been made to compare types of cracking in both plain and fly ash concrete using AE parameters and it has been correlated with SEM images and final cracking pattern.

Shahidan (2014) investigated reinforced concrete beams by acoustic emission technique and classified damage. Beams had cross-section of 150 x 250 x1900mm and were subjected to 4-point loading. The load was increased from 2.5 KN until failure. Acoustic emission activities were found to be low at mid span and at certain distances from support. Acoustic emission activities were high but the cracks initiated and propagated from mid span. It was found that location of sensors was cause of it, it was suggested to place sensors near the mid span. Using RA value versus frequency for both low and high signal in acoustic emission wave form, high acoustic emission wave form occurred in case of fatigue test and in case of constant load acoustic emission waveforms reduced. Low waveforms were found to be dominant which lie in low RA region in RA versus frequency graph.

4.7 Closing Remarks

In this chapter acoustic emission as a NDT technique has been discussed. The literature review reveals that very few works have been reported to monitor freshly poured concrete using acoustic emission techniques. No work has been reported till date which investigates the early age properties of flyash concrete using NDT. In this study an attempt has been made to investigate early age setting of flyash concrete using latest NDT of ultrasonic guided waves and acoustic emission techniques.

CHAPTER-5

EXPERIMENTAL PROGRAM AND DETAILS

5.1 General

In this chapter different testing techniques i.e. compressive strength testing, SEM analysis, Ultrasonic guided waves technique and acoustic emissions, their equipment, setup details,

specimen details and methodology of conducting the tests is described. The materials used and their properties have been discussed. The idea behind conducting the destructive tests of compressive strength at different stages of concrete monitoring was to correlate and investigate the efficacy of NDT techniques with the destructive testing techniques.

5.2 Experimental Program and Test Matrix

The scope of work is to carry out destructive testing of compressive strength, Microstructural analysis using Scanning Electron Microscope (SEM) and non-destructive testing using Ultrasonic Guided Waves and Acoustic Emission techniques on the concrete mixes. Hence, the proposed experimental work has been divided as follows.

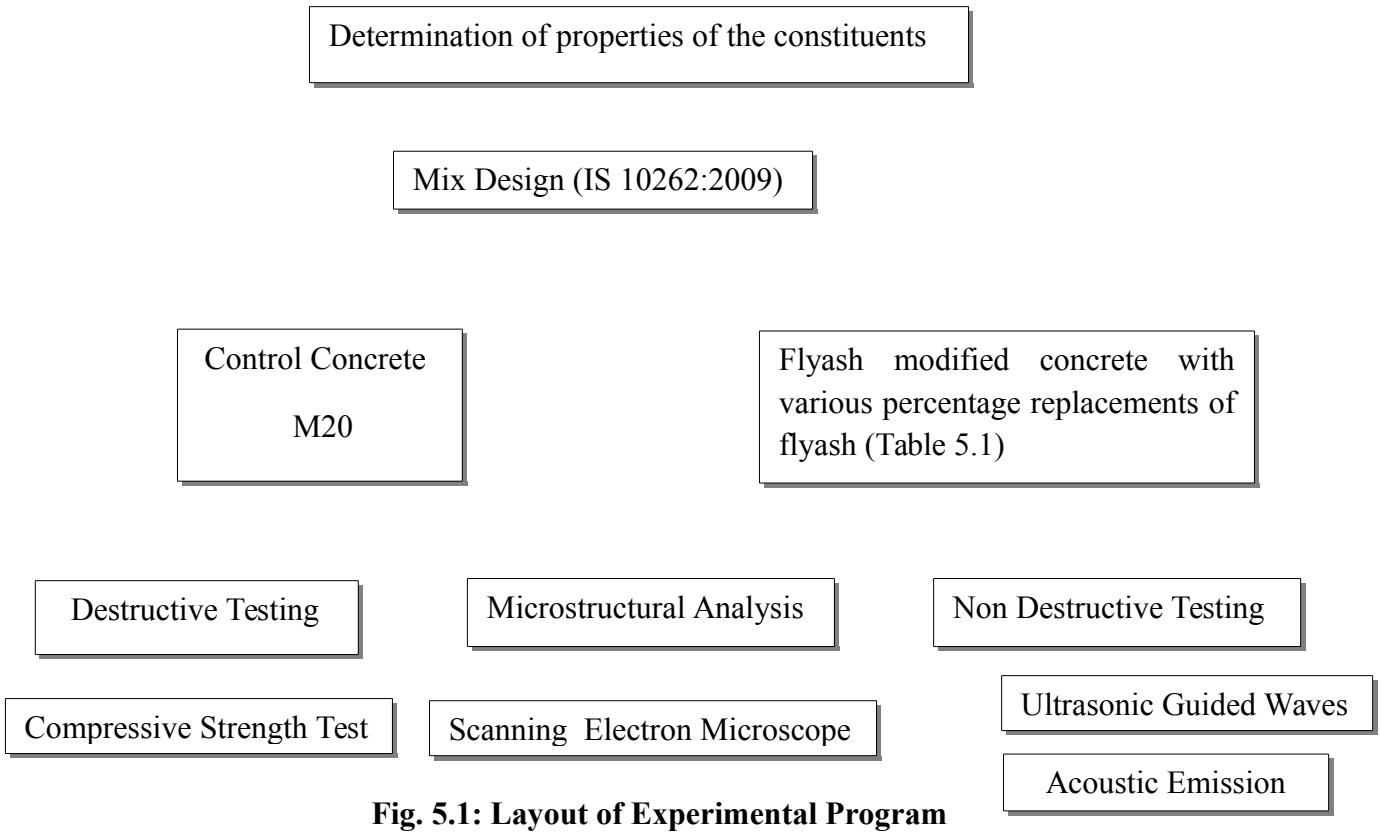

Fig. 5.1: Layout of Experimental Program

In this work, the setting properties of flyash modified concrete are studied and five replacement levels of flyash were chosen for modification. The percentage replacements were decided with the help of previous research carried out which show that up to 30%replacement level, the prepared mix were sticky. Beyond30% replacement level, workability and finishability of mix was decreased. It may be due to the fact that up to30% replacement level, fly ash particles also worked as filler material to fill the pores betweens fine aggregate particles, resulting in a dense sticky mix since, more water was available for lubrication.

However, beyond30% replacement level, more water was needed for lubrication due to more surface area. As such workability and finishability of mix was decreased beyond 30% replacement (Alvin et al., 2014).Hence the nomenclature for flyash modified concrete is detailed as below.

Table 5.1: Nomenclature for the concrete mixes prepared

Name	Description
CC	Control concrete
FA5	5% replacement of cement by flyash in concrete
FA10	10% replacement of cement by flyash in concrete
FA15	15% replacement of cement by flyash in concrete
FA20	20% replacement of cement by flyash in concrete
FA30	30% replacement of cement by flyash in concrete
CC(S)	CC on which steel sensors are used
FA30(S)	FA30 on which steel sensors are used

5.3 Materials used and their specifications

Cement, fine aggregates, coarse aggregates, flyash, water and MS bars are used in casting of cubes. The specifications and properties of these materials are as under:

5.3.1 Cement

43 Grade Ordinary Portland Cement (OPC) is used. Summary of various tests, carried out in accordance with procedure laid down in IS: 8112 -1989, conducted on cement is given in **Table 5.2**.

Table 5.2: Physical Properties of OPC

S.No	Characteristics	Experimental	Standard Values as per IS:8112

.		Values Obtained	-1989
1	Normal Consistency	33%	-
2	Initial Setting Time	50 min	Not less than 30 min
3	Final Setting Time	260 min	Not more than 600 min
4	Specific Gravity	3.05	-
5	Fineness	4.8%	-

5.3.2 Fine aggregates

The fine aggregates used are locally procured and conform to grading zone III, as per IS: 383-1870 .Sieve analysis and physical properties tests of the fine aggregates were carried out in accordance with IS: 383 -1870. The physical properties and sieve analysis results of fine aggregates are shown in **Table 5.3 and 5.4**.

Table 5.3: Sieve Analysis of Fine Aggregates

S. No.	IS Sieve Size	Weight Retained (in grams)	Percentage Weight Retained (in grams)	Cumulative Percentage of weight retained	Percentage passing
1	4.75 mm	14.5	1.45	1.45	98.55
2	2.36 mm	37	3.70	5.15	94.85
3	1.18 mm	246.5	24.65	29.80	70.20
4	600 micron	205.5	20.55	50.35	49.65
5	300 micron	287.5	28.75	79.10	20.90
6	150 micron	177	17.70	96.80	3.20
7	Pan	32	3.20		
	Total	1000.0		∑=262.65	
				FM=2.62	

Hence, Fineness Modulus (FM) of Fine Aggregates= 2.62

Table 5.4: Physical Properties of Fine Aggregates

S. No.	Characteristics	Values Obtained
1	Specific Gravity	2.6
2	Bulk Density	1.33g/cc
3	Water Absorption	0.89
4	Fineness Modulus	2.62

5.3.3 Coarse aggregates

Crushed stone aggregates (locally available) of nominal size 20 mm are used throughout the experimental study. The aggregates are tested as per IS: 383-1970 and the results of various tests conducted on coarse aggregates are given in **Table 5.5** and **Table 5.6**

Table 5.5: Physical Properties of Coarse Aggregates

S.No	Characteristics	Values Obtained
1	Type	Crushed
2	Water Absorption	1.1
3	Specific Gravity	2.74
4	Fineness Modulus	6.95

Table 5.6: Sieve Analysis of Coarse Aggregates

S.No.	Sieve size	Weight Retained (in grams)	Percentage weight retained	Cumulative percentage weight retained	Percentage passing
1	80 mm	0	0	0	100
2	40 mm	0	0	0	100
3	20 mm	68.5	2.28	2.28	97.72
4	10 mm	2776.5	92.55	94.83	5.17
5	4.75 mm	113.5	3.78	98.62	1.38
6	Pan	0	0		
	Total	3000			

Fineness Modulus of Coarse Aggregates=6.95

5.3.4 Flyash

Flyash used in the present work was obtained from Rajpura Thermal Power Plant, Rajpura, Punjab. The properties of flyash, obtained from the supplier are given in **Table 5.7**

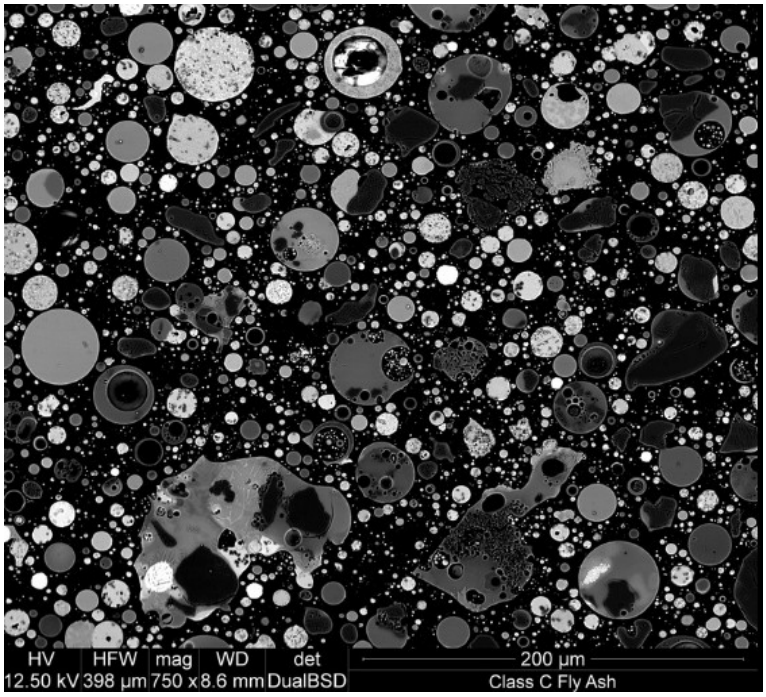

Fig 5.2: Photomicrograph made with a scanning electron microscope (SEM) and back-scatter detector (https://en.m.wikipedia.org/wiki/Fly_ash)

Table 5.7: Physical Properties of flyash used (Source: Rajpura Thermal Power Plant)

S. No.	Characteristics	Values
1	Colour	Pale grey
2	Specific Gravity	2.06
3	Class	F

Table 5.8: Chemical Properties of flyash used (Source: Rajpura Thermal Power Plant)

S.No.	Characteristics	Values
1	SiO_2	57.41
2	Al_2O_3	26.92
3	Fe_2O_3	5.21
4	CaO	2.05
5	MgO	0.71
6	SO_3	0.085
7	Loss on Ignition	1.18
8	Lime Reactivity	59.5

Table 5.9: Sieve Analysis of flyash used (Source: Rajpura Thermal Power Plant)

S.No.	Sieve No.	% weight retained
1	100	0.00
2	140	31.35
3	200	26.51
4	270	24.72
5	Pan	17.42

5.3.5 Water

Potable tap water from structures laboratory was used in the present study for casting.

5.4 Mix Design: M20 concrete (IS 10262: 2009)

Cement used: OPC

Specific Gravity of cement: 3.05

Specific Gravity of coarse Aggregate: 2.6

Specific Gravity of fine Aggregate:2.74

Grading of Fine : Zone III

A) Data for Mix Proportioning of a particular Grade of Concrete

a)	Grade Designation	M20
b)	Type of Cement	OPC
c)	Maximum nominal size of aggregate (mm)	20
d)	Minimum cement content (in kg/m^3)	300
e)	Maximum cement content (in kg/m^3)	450
f)	Maximum water cement ratio	0.45
g)	Workability desired slump of	75mm
h)	Exposure conditions (as per Table 5, 1S:456)	Moderate
i)	Type of aggregate	Angular
j)	Admixture used	None

B) Target Strength for Mix. Proportioning

ft` = ft + 1.65 s
Where
ft`= target mean compressive strength at 28 days in N/mm^2
ft= characteristic compressive strength at 28 days in N/mm^2=20 N/mm^2
s= standard deviation = 4 N/mm^2(Table: 3 IS 10262:2009)

ft` = 20+(1.65x4)
= 26.6

C) Selection of w/c

Adopted w/c Ratio – 0.45

Max. w/c ratio - 0.5 (Table 5 IS:456:2000)

D) Selection of Water Content

Maximum water content = 186kg/m^3 (Table 2 IS 10262:2009)
Water content after slump correction
Adopted = 186+0.03x186 = 191.58 kg/m^3 (Clause 4.2 IS 10262:2009)

E) Calculation of Cement Content

Cement content = $\frac{\text{Water content}}{\text{w/c}}$

$= \frac{191.58}{0.45}$

$= 425.73$ kg/m^3

F) Estimation proportions of coarse and fine aggregates

$\frac{\text{Volume of coarse aggregate}}{\text{Volume of total aggregate}} = 0.62$

$\frac{\text{Volume of fine aggregate}}{\text{Volume of total aggregate}} = 1 - 0.62 = 0.38$

G) Mix. Calculations (per unit volume of concrete)

Volume of Concrete = 1 m^3

Volume of cement = $\frac{\text{mass of cement}}{\text{Specific gravity}} \times \frac{1}{1000}$

$= \frac{425.73}{3.05} \times \frac{1}{1000}$

$= 0.1396$ m^3

Volume of water $= \frac{191.58}{1} \times \frac{1}{1000}$

$= 0.191.58$ m^3

Volume of aggregate = 1 (Volume of water + Volume of cement)

$= 1-(0.1396 + 019158) = 0.6688$ m^3

Mass of coarse aggregate = 0.6688 x 0.62x1000 x 2.6
= 1078.16 kg.
Mass of fine aggregate = 0.6688 x 0.38x1000 x 2.74
= 696.35 kg

H) Adopted mix. Proportions

Cement (kg/m^3) : 425.73
Coarse Aggregate : 1078.14
Fine : 696.35
Water : 191.38

Ratio of cement fine aggregate : coarse aggregate

= 1:1.63:2.53

5.5Experimental Setup Details

5.5.1Compressive Strength Test

Compression test was carried out in order to determine the strength developed by the concrete. Cubes of 150mm x 150mm x 150mm were cast and after 24 hours of casting, the specimens were put in water for curing. These specimens were then tested after 3, 7, 28, 56 days of curing on Universal Testing Machine(UTM). Rate of load application was 140kg/cm2 till the specimens failed. This load at failure divided by the specimen area gives the compressive strength of concrete. This was done to ensure the relation between the non destructive and destructive testing on concrete samples.

$\sigma = P/A$;P=Maximum load the sample can take(N)

A=Crossection area of cube (mm^2)

σ=Compressive strength(N/mm^2)

Fig.5.3: Sample in Universal Testing Machine

Fig.5.4 (a): Sample before failure **Fig.5.4 (b): Sample after failure**

5.5.2 Microstructure Analysis using Scanning Electron Microscope (SEM)

The **electron** beam is accelerated through a high voltage (e.g.: 20 kV) and pass through a system of apertures and electromagnetic lenses to produce a thin beam of **electrons**., then the beam **scans** the surface of the specimen by means of **scan** coils (like the spot in a cathode-ray tube "old-style" television).

The main components of a typical SEM are electron column, scanning system, detector(s), display, vacuum system and electronics controls (**fig. 5.5**).

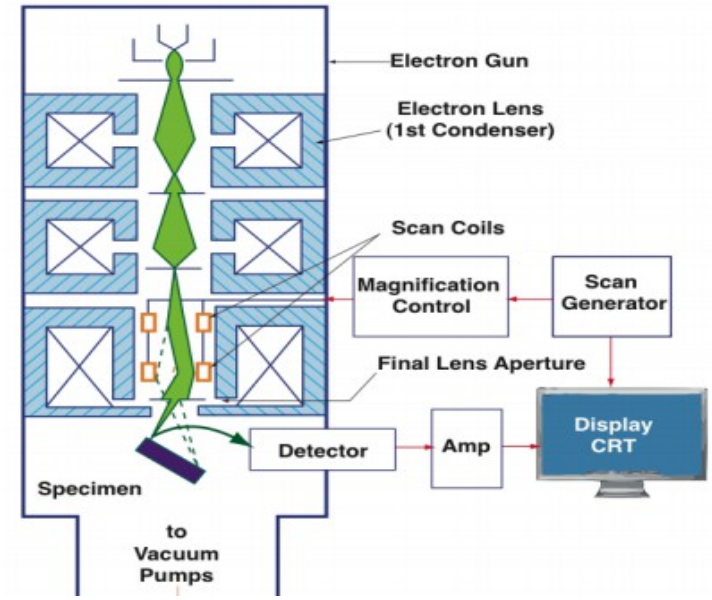

Fig 5.5: Components of SEM (http://www.googleimages.com)

Fig. 5.6: Samples ready for SEM Analysis

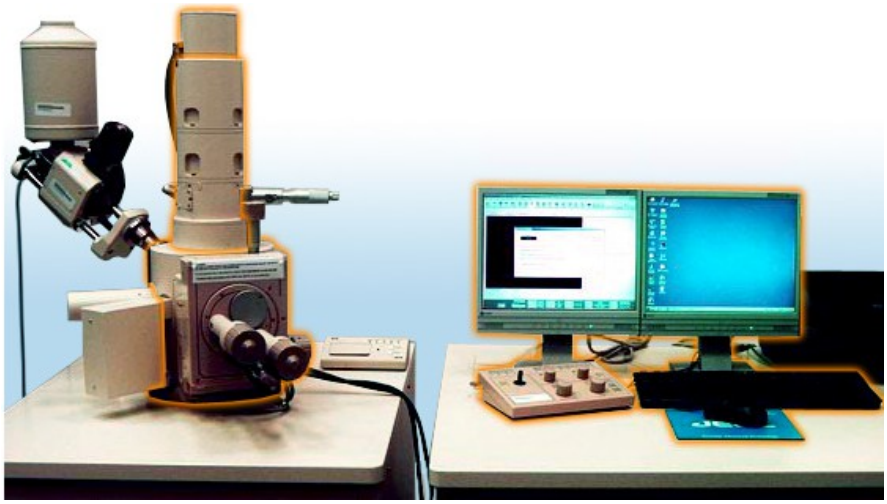

Fig.5.7: Scanning Electron Microscope (http://www.ammrf.org.au)

5.5.3 Ultrasonic Guided waves

Specimen Preparation

Cubes of standard size 150 x 150 x 150 mm size were cast with a mix proportion of 1:1.63:2.53. A slump of 75 mm was observed .A mild steel bar of diameter 25 mm is kept embedded in the cube horizontally in centre of cross section such that 75 mm length of the

bar exposed to the environment from both sides **(Fig 5.8).** This scheme of set-up was used for guided wave monitoring andfor AET monitoring.

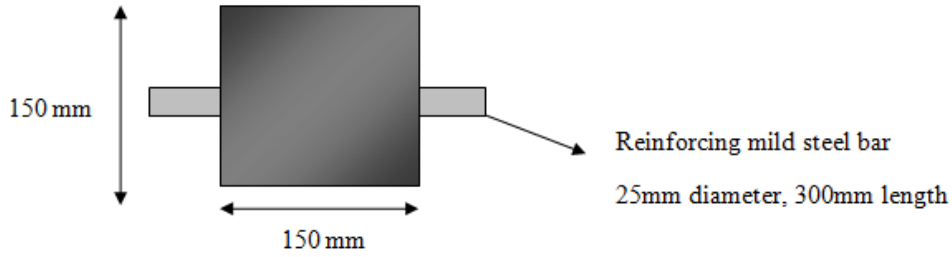

Fig. 5.8 : Ultrasonic Guided Wave specimen

Setup Details

The Ultrasonic Guided Wave setup consists of a DPR 300 pulse receiver which generates an electronic pulse. It is used to excite a piezoelectric transducer which in this case was a cylindrical transducer. The mechanical vibration of the PZT patch emits ultrasonic waves. The transmitter was kept in contact with the solid mild steel bar of 25mm diameter and 300mm length which is embedded in a concrete cube of size 150 mm x 150 mm x 150 mm **(Fig 5.8)** The contact was ensured with the help of a couplant (ultrasonic gel) and a holder assembly. The receiver transducer is arranged on the opposite end of bar. This receiver is connected back to the pulser receiver, which sends the signals to the digitizer card and is displayed on LCD of computer screen **(Fig 5.9)**.

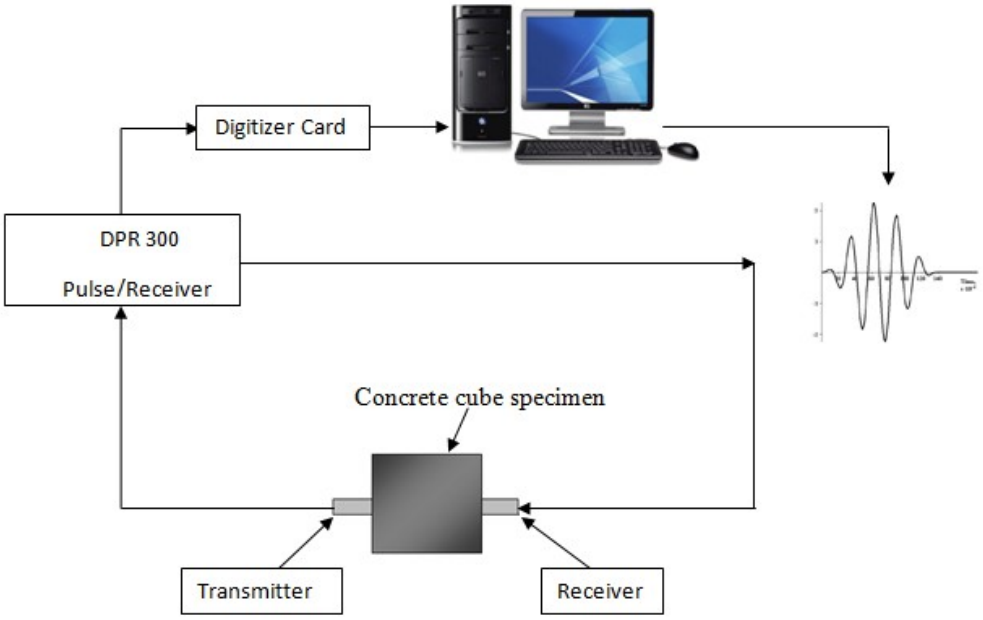

Fig. 5.9: Schematic of Ultrasonic Guided Waves Technique

Driven by the pulser/receiver, the compressional transducer generates ultrasonic pulse that propagates through the steel bar in the form of guided waves. When concrete start setting the surrounding concrete begins making bond with the embedded steel rod which result in attenuation i.e. loss of wave energy occurs into the surrounding concrete. This attenuation is due to material absorption and energy leakage into the surrounding concrete. This attenuation energy is picked up by the receiver transducer and then converted into an electrical signal which has been processed in a computer and digitized for display.

Features of the UGW equipment used are as follows:

(a) Transducer It is a single element longitudinal wave transducer. It can be used in straight beam flaw detection and thickness gauging, detection and sizing of delamination, material characterization and sound velocity measurements, inspection of plates, billets, bars, forgings castings, extrusions, and a wide variety of other metallic and non-metallic components. S 24 HB 0.1S (KARL DEUTSCH) & S 24 HB 0.1 E (KARL DEUTSCH) Standard transducers of 0.1 MHz frequency and 24 mm diameter has been used, as shown in **Fig. 5.10**.

Fig 5.10: Transducers used

(b) JSR Ultrasonics DPR 300 Pulser/ Receiver System JSR Ultrasonics DPR300 pulser shown in **Fig 5.10**produces a high voltage electrical excitation pulse (up to 475 Volt) and applies this pulse to the instruments T/R connector. An ultrasonic transducer connected to the T/R connector via a length of 50 Ω coaxial cable has been then employed to convert the electrical energy of the excitation pulse into an ultrasonic pulse that has been propagated into a test material or medium.DPR 300 can be configured to both pulse-echo and through transmission mode operations as discussed below; ᵒ With the DPR300 configured for pulse-echo mode operation, acoustic echoes reflected from interfaces or defects within the test material are converted by the transducer into electrical signals that are presented to the T/R connector of the DPR300. The low-noise DPR300 receiver amplifies these electrical signals, and the signals then pass through adjustable high pass and low pass filters. The DPR300 receiver gain has been adjustable between -13 dB and 66 dB, and there are six high pass and six low pass filter settings for band-limiting the receiver frequency response. The amplified and filtered signals are available on the instruments Receiver Output connector. The DPR300 may also be used in transmission mode operation wherein a separate receiving transducer has been used to detect acoustic pulses that have propagated through a test material or medium.

5.5.3.1Methodology for UGW monitoring

Pulse-transmission method is used for characterizing the young concrete strength and hardening process. To produce guided waves in the bar of concrete cube two transducers are attached at the two ends of the bar in projected cube. One transducer acting as a transmitter and the other acting as a receiver are attached parallel to the axis at the two ends of bar.

Selection of Excitation Mode and Frequency

The selection of frequencies for testing is done using the software Disperse (Pavalakovic & Cawley,2000). The selection of a suitable test mode and frequency can be made by close examination of the dispersion curves. The modes that are easily distinguishable and have lowest signal attenuation are selected. It is desirable to use a mode at a point of low attenuation, to maximize the inspection range, and to use a mode at a point of maximum energy velocity, to limit the effects of dispersion, and to reduce the risk of other modes complicating the received signal (Beard et al. 2003). Dispersion curves for a 25mm bar embedded in concrete are plotted**.** Only longitudinal modes have been considered in the study as the flexural and torsional modes experience high theoretical attenuation. Guided longitudinal waves are produced in the embedded bars by keeping compressional transducers parallel to the guiding configuration at the two ends of the bars embedded in concrete. The different longitudinal modes are excited by varying the excitation frequencies. The selection of frequencies for testing is done based on the phase velocity dispersion curves .They are validated by experimentally confirming the signal fidelity. In this work where bars are embedded in concrete, which is a layered waveguide system and leakage plays an important role. High frequency low attenuating modes with displacement profiles centered in the middle of bar to minimize leakage are found to be the best for layered systems. Phase velocity dispersion curves show the fundamental L (0,1) mode starting at zero frequency with each higher order mode starting from a higher cut off frequency. Each of the higher modes shows a plateau region around the steel longitudinal bulk velocity line. This mode is selected for ultrasonic investigation being the lowest attenuation and having lower frequency. Another contributing factor to the selection of mode is the relative sensitivity of ultrasonic waves to setting of concrete.. The energy for L(0,7) is concentrated in the central core portion of the bar and has relatively less surface component. Hence, it should be more sensitive to local bar topography or loss of material changes and not the surface profile changes. Another contribution factor to the selection of L(0,1) mode is the mode shape of this mode. This mode has significant surface component would be sensitive to bonding effect of concrete on the bar. This mode shows significant axial displacement at the interface and is a ***surface sensitive mode*** and hence, is chosen to monitor the bond development at 100 kHz.

Transducers having longer wave form duration and a relatively narrow frequency bandwidth with centre frequency of 0.1 MHz (surface seeking mode) has been used because the main

aim of the experiment was to monitor the bonding between the 25mm mild steel rod & the surrounding concrete in the cube.

5.5.4 Acoustic Emission

Specimen

Cube specimen of size 150mm x 150mm x150 mm was used wherein sensors were attached directly on concrete. Another set of reading was taken by attaching steel sensors on mild steel bars. For this, cube specimen of size 150mm x 150mm x150 mm with 12 mm mild steel bars immersed at one of the diagonal as shown in the **Figure 5.11** were used**.**

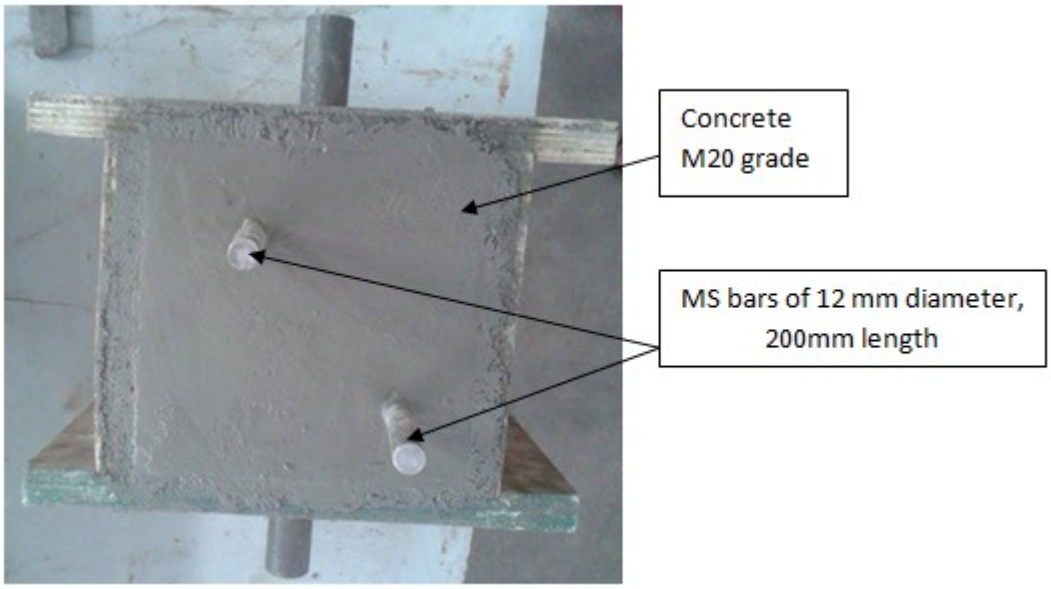

Fig. 5.11: Top view of concrete specimen for Acoustic Emission

The phenomenon of acoustic emission is defined as the propagation of elastic waves due to release of localized internal energy, such as micro-fracture in elastic material. Structural deformation processes such as plastic deformation, crack expansion and other kinds of material degradation are the sources of the AE activity. Detection, amplification, filtering and analysing the signal are some of the important issues in AE technology. AE monitoring system typically consists of sensors, preamplifiers and AE acquisition and analysis system. The schematic representation of AE set up is as shown in the **Fig 5.12.**

Sensors are placed on the surface of the structure to record acoustic emission signals

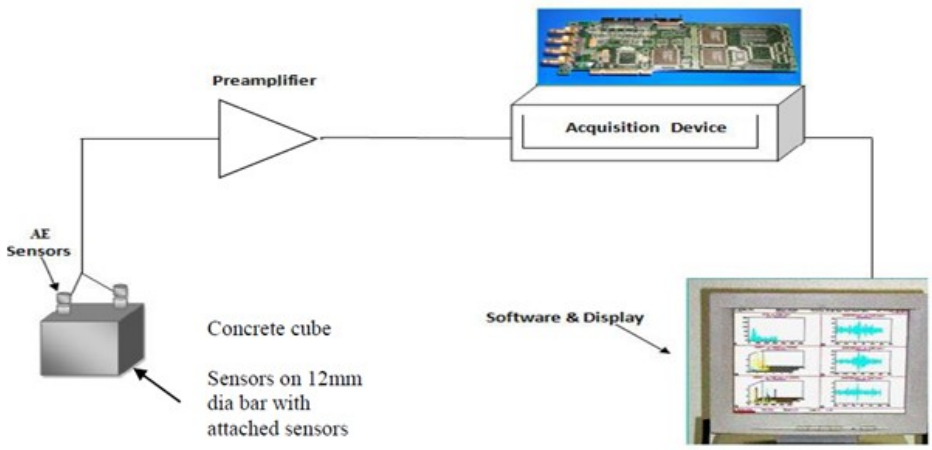

Fig. 5.12: Schematic Representation of AE Monitoring Setup

5.5.4.1 AE Monitoring Methodology

Good coupling of the sensors to the test specimen is necessary for the effective transmission of AE signals. Sensors are attached on the surfaces using magnetic holders, glues, even rubber bands and tapes. A layer of couplant such as vacuum grease, ultrasonic gel, and oil is applied between the two surfaces. Operating frequency range is important during sensor selection. The common frequency range for AE testing in civil infrastructure is 100-300 kHz. In this experimental study, two AE sensors R3α sensors (resonant at 150 KHz) were mounted on the 12 mm diameter steel bars and held tightly with brown tape. The sensors were attached to the steel bars using grease as a coupling agent. Two amplifiers were used with a gain set at 40 db and frequency range of 20-1200 KHz. A band pass filter of 20-400 KHz was set in the software control of the data acquisition system. A threshold value was set at 45 db for experimental purpose. Any acoustic activity occurring in the specimen is detected by the AE sensors mounted on 12mm diameter reinforcing bar. These signals are amplified by the pre-amplifiers before entering the data acquisition system. The data acquisition set (Micro II

Digital AE system) which processes the data and finally displays the data on the monitor screen.

5.5.4.2 Equipment Details

AE Sensors

AE sensors are chosen in accordance with their application. Sensors convert mechanical energy of elastic waves detected into electrical signal, hence they function as transducers. AE testing consists of two types of sensors namely resonance (narrow band) and broadband sensors. Where AE features like time of arrival, amplitude and energy are main parameters of study resonant AE sensors are used. They are sensitive to surface waves and resonant frequency plays important role in deciding which AE sensor is to be applied. Broadband sensors respond to a wide range of wave frequency components and are used if frequency desired is unknown or for modal analysis. For the present study R15α sensors were used when sensors were mounted on steel bars whereas R3α sensors were used when sensors were attached on the concrete surface directly, specifications of which are as follows:

Table 5.10: Specifications of R15 α Sensors Used

S.NO.	R15α
Operating Frequency Range	35-100 KHz
Resonant Frequency	150 KHz
Physical Dimensions	19mm dia x 22.4 mm height
Weight	31 grams
Case Materials	Stainless Steel

Fig. 5.13: R15α sensors used in the study

Table 5.11: Specifications of R3α Sensors Used

S.NO.	R15α
Operating Frequency Range	29-50 KHz
Resonant Frequency	30 KHz

Fig. 5.14: R3α sensors used in the study

Table 5.12 Test matrix for AE Examination

Sample	Sensors used	Monitoring time(hours)
CC	R3α	48
FA5	R3α	48
FA15	R3α	48
FA30	R3α	48
CC(S)	R15α	24
FA30(S)	R15α	24

(b) Preamplifier

The signal produced by sensors is further amplified by preamplifier. Preamplifier by Mistras is used which has gain of 40 , 20 and 60 dB and 20-1200 KHz of frequency range .

Fig. 5.15:Preamplifier used in the study (Mistras)

(c) AE data acquisition system

It consists of Micro II digital AE system provided by PAC (Physical Acoustics Corporation) shown in the **Figure 5.12** .

Fig. 5.16: AE data acquisition system (Micro II , Digital AE system)

5.6 Closing Remarks

This chapter discusses in detail the working, technical information & various components of different testing equipment used in this experimental study. Emphasis is also given on the different concrete mix, Types & number of concrete specimens casted. The next chapter discusses the results obtained under various test conducted in the two different phases.

CHAPTER-6

RESULTS AND DISCUSSIONS

The present chapter discusses the results obtained by carrying out various tests on flyash concrete as well as control concrete. Destructive tests done on fly ash concrete include compressive strength test using UTM (Universal Testing Machine) &SEM (Scanning Electron Microscope) analysis whereas the non-destructive tests include Ultrasonic Guided Waves and Acoustic Emissions techniques.

6.1 Compressive Strength Test

Table 6.1: Compressive Strength Results

Age of concrete(Days)	**Average Compressive Strength (N/mm^2)**					
	CC	**FA5**	**FA10**	**FA15**	**FA20**	**FA30**
3	18.05	17.7	16.76	15.95	11.97	9.41
7	24.57	23.5	19.96	18.43	13.85	11.86
28	28.52	27.65	26.83	26.45	28.2	24.59
56	33	34.6	35.4	36.47	36.6	25.6

.

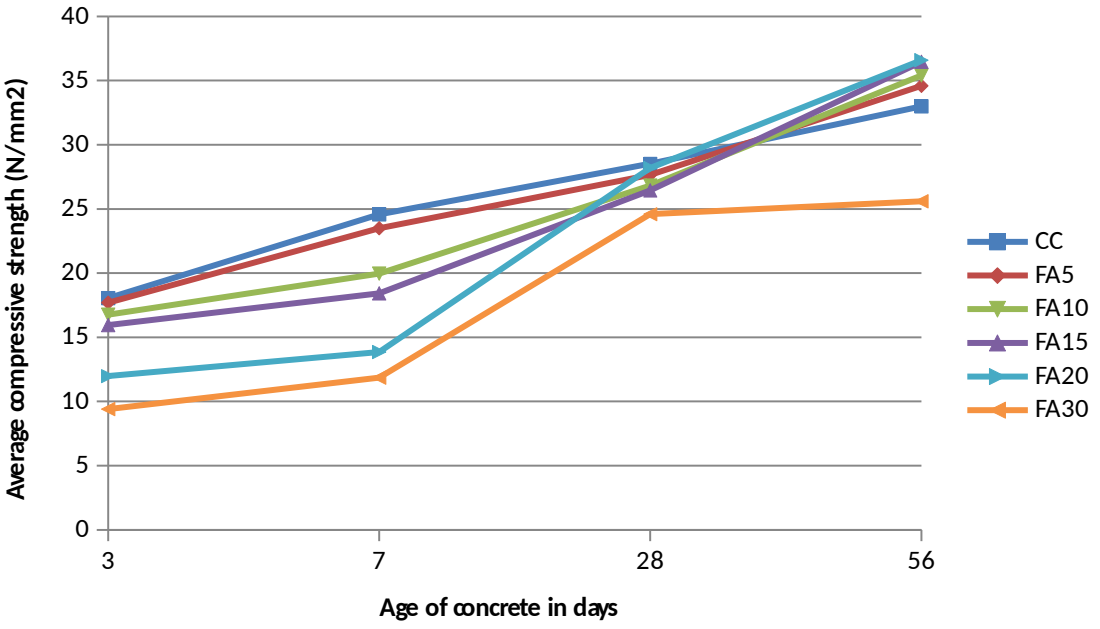

Fig 6.1: Compressive Strength Results

Following observations were made from the compressive strength results:

- From **Table 6.1** and **Fig 6.1** it can be seen that in general, the compressive strength decreases as the percentage replacement of flyash in concrete increases.
- The 3 day compressive strength decreases with increase in flyash content and thus is a maximum for CC at 18.05 N/mm^2 and a minimum for30% flyash replacement at a mere 9.41 N/mm^2.
- Similarly, it can be observed that same trend continues for 7 day compressive strength i.e. maximum compressive strength occurs for CC at 7 day curing at 24.57 N/mm^2 and minimum is for 30 % flyash replacement at 11.86 N/mm^2.
- At 28 days, the compressive strength decreases with increase in flyash replacement percentage but is comparable to control concrete. But for 30%replacement, the strength is lower as compared to other replacement percentages.
- It is evident that beyond 28 days, the strength increased with the addition of fly ash.56 day compressive strength for CC, FA5, FA10, FA15 and FA20 increased with increase in flyash content .However, increase in strength was more prominent at 20% replacement level whereas the strength decreased for 30% flyash replacement sample.
- The decrease in strength during early ages is due to slow hydration process since fly ash is a slow reactive pozzolan. This is so because the strength development contributed by fly ash occurs through chemical combination of reactive fly ash glass

with calcium hydroxide generated by hydration of portland cement which is known as pozzolanic reaction. Hence as the hydration progresses, pozzolanic reaction takes place resulting in increase in strength of flyash concrete.

- For all the concrete mixes, the strength increases as the number of curing days increase i.e. a minimum at 3day curing and maximum at 56 day curing.
- Hence, from above it can be concluded that optimum percentage replacement of flyash in concrete is 20%.

6.2 Microstructure Analysis (using SEM)

SEM images of control concrete and concrete containing 5%,10%,15%,20% and 30% flyash were taken at 3 days and 28 days. **Fig. 6.2** and **Fig. 6.3** show the SEM images of different concrete samples at 3 days and 28 days. For SEM analysis, samples were taken from specimens that had been broken during compression test, polished, and gold coated

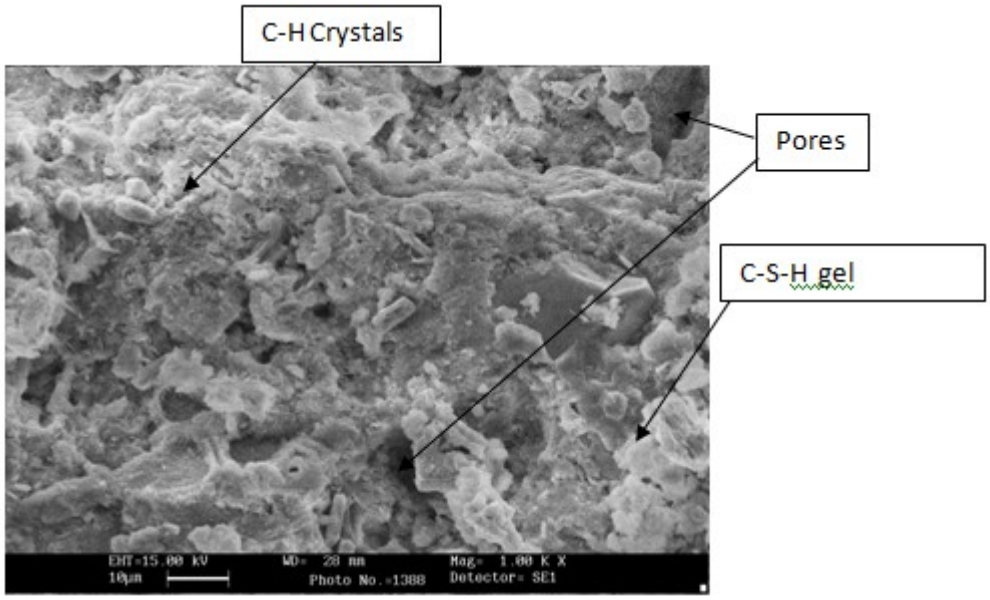

(a)SEM image of CC at 3 days

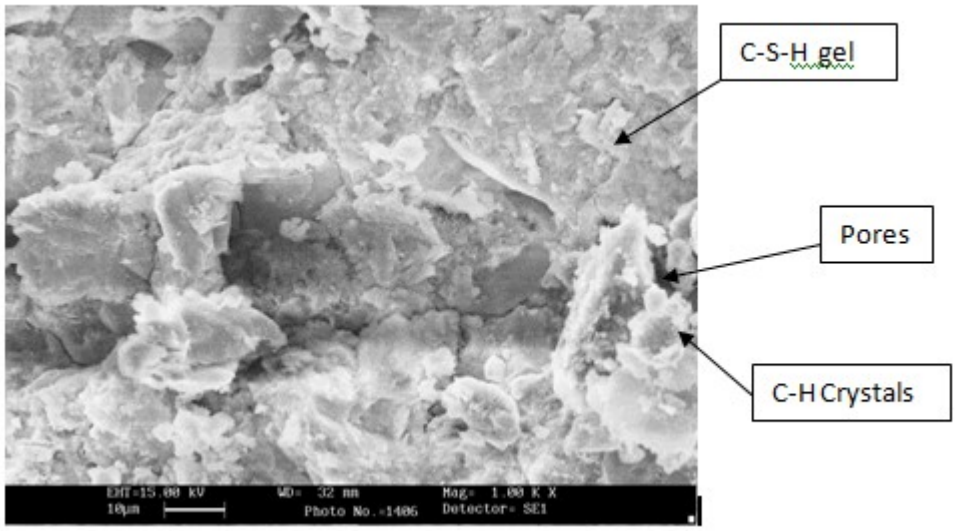

(b) SEM image of CC at 28 days

Fig 6.2 SEM images of Control Concrete

Fig. 6.2(a) shows SEM images between aggregate and paste; the aggregate surface was covered by small amounts of C-S-H gels and were irregularly structured, the matrix is porous and non- uniform with pores clearly visible. Further $Ca(OH)_2$ portlandite crystals (C-H crystals) were seen.

Fig 6.2(b) shows SEM images of CC at 28 days **.**Apart from C-S-H small and large crystals of CH and pores were visible.

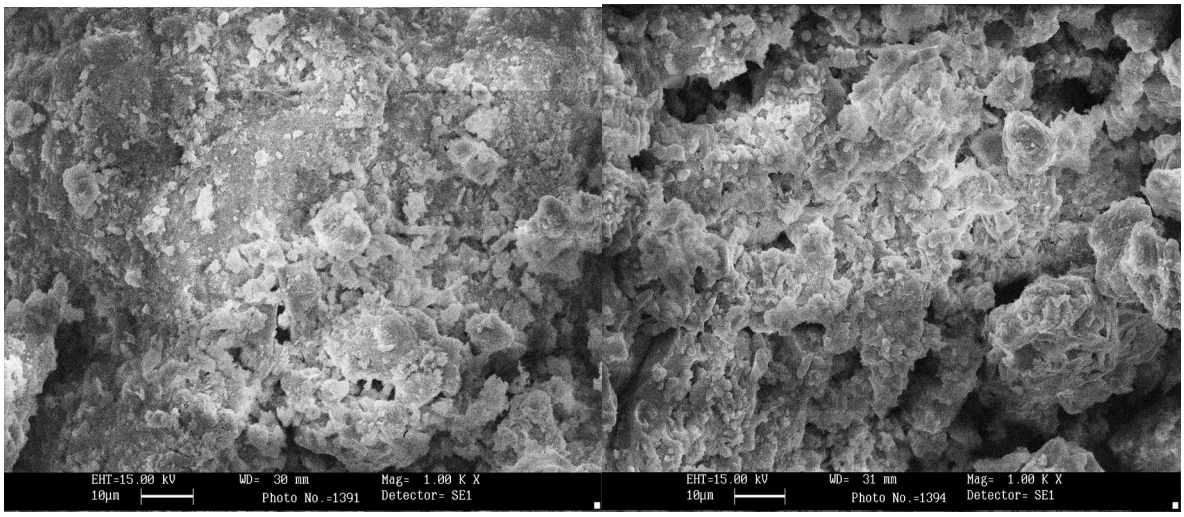

(a) FA5 **(b) FA10**

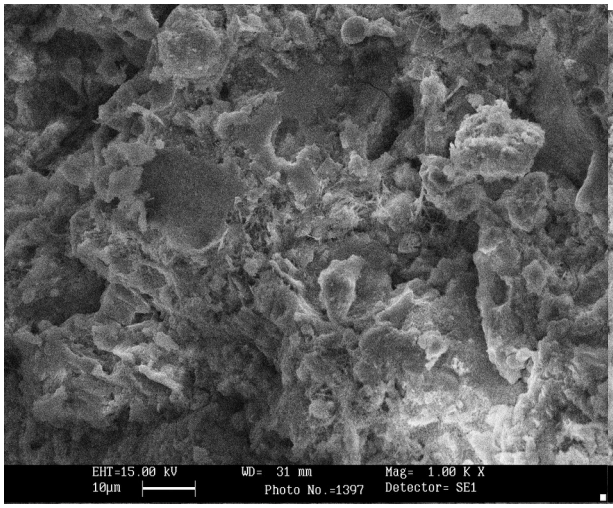

(c)FA15

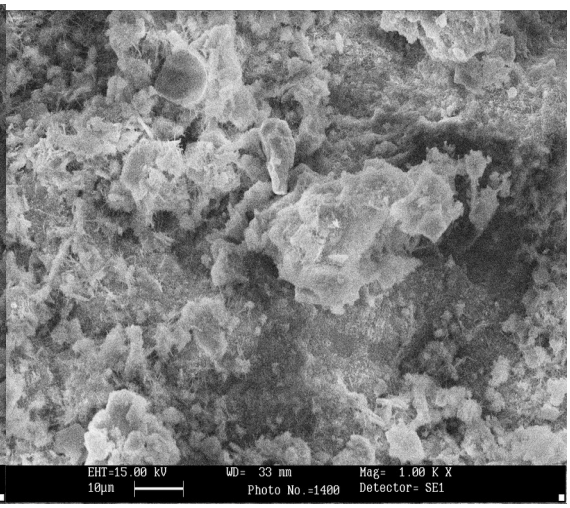

(d)FA20

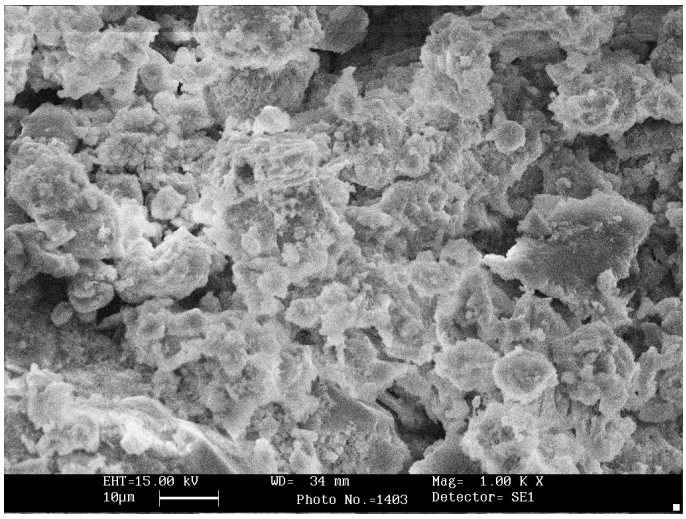

(e) FA30

Fig. 6.3:SEM images of flyash modified concrete at 3 days

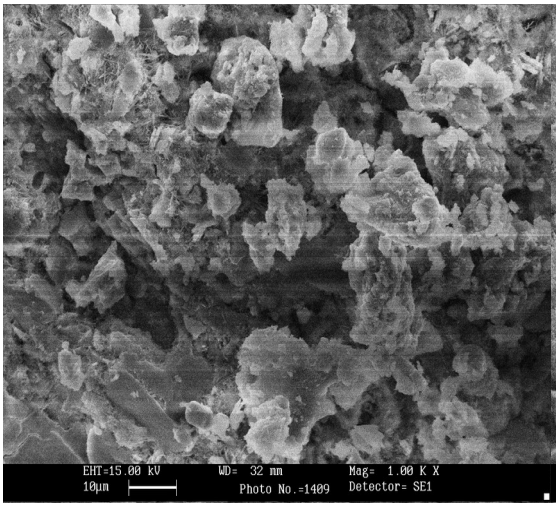

(a)FA5

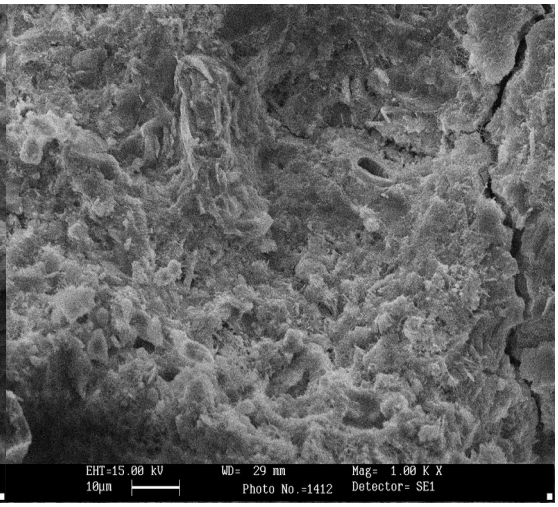

(b)FA10

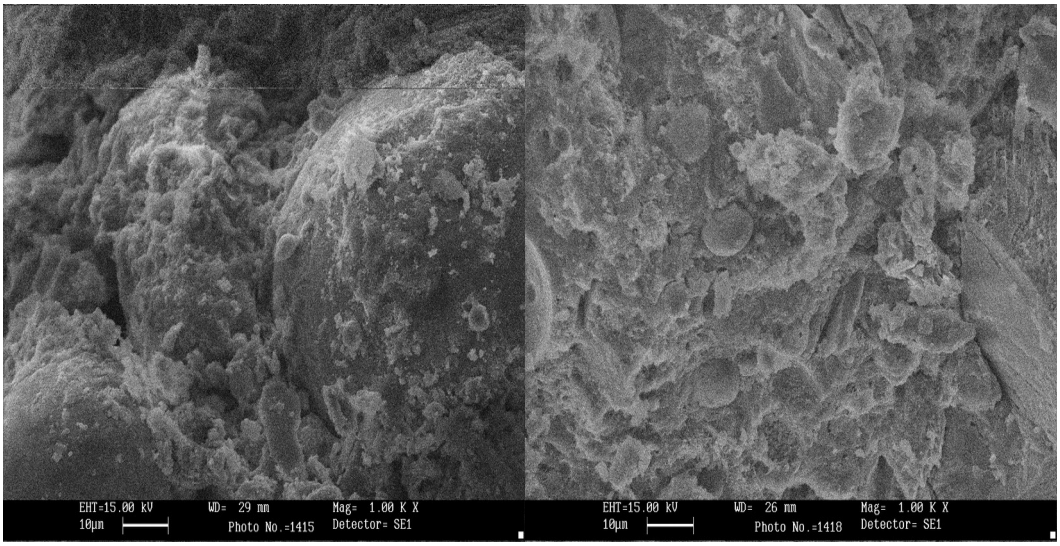

(c)FA15 **(d)FA20**

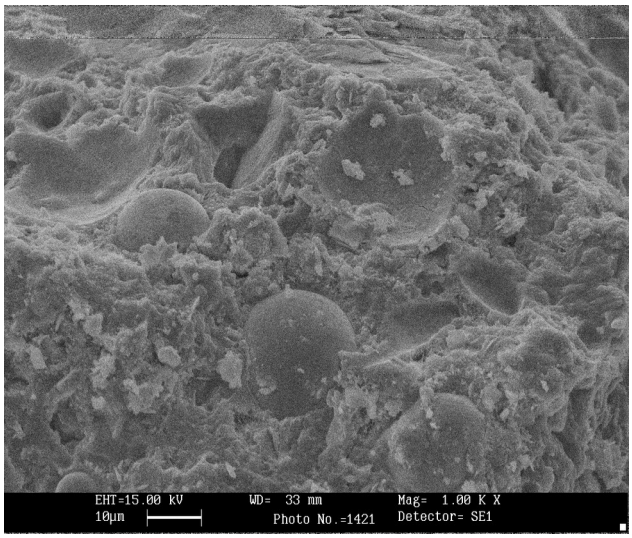

(e)FA30

Fig. 6.4:SEM images of flyash modified concrete at 28 days

Following observations were made

- As the percentage replacement of cement by flyash increases, the microstructure becomes more dense and compact. It is due to the fact that the fly ash particles provide well dispersed and suitable points within the paste for nucleation to occur and this leads to encapsulation of individual ash spheres by the cement hydration products.
- SEM investigations revealed that homogeneity of the interface microstructure is improved to a great extent by the addition of fly ash. This was mainly accredited to the pore filling effects as well as pozzolanic reaction of the fly ash.

- As the hydration occurs about individual spheres, the outward growth leads to mechanical interlocking of the needles and plates. This feature is thought to be fundamental to the strength imparting mechanism.
- An overall impression from the examination of the micrographs and from the study of the strength results is that a dense and strong structure, presumably of C-S-H, can be achieved either by using a high cement content or by replacing part of the cement with fly ash and then relying upon either time or elevated temperature to bring about the desired structure.
- The microstructure analyses of concrete showed that presence of fly ash in concrete mixtures reduces the amount of calcium hydroxide that formed during early stages of hydration process. In general, the rate of pozzolanic reaction increased with fly ash content in concrete.
- Denser and compact structure was observed due to hydration products formation with flyash at 28 days.

6.3 Ultrasonic Guided Wave Investigation and Results

Ultrasonic pulse transmission signals were recorded using both L (0, 1) and L (0, 7) modes at an interval of 2 hours till 48 hours until the pulse transmission vanished after 48 hours. The sample consists of a 150m x 150mm x 150mm cube with 25mm diameter, 300 mm length mild steel bar embedded into it. A pulse transmission signature i.e. Voltage–Time signals were captured immediately after preparing concrete mould and at regular two hours interval upto 48 hours.

Figures 6.6 and 6.7 show the pulse transmission signatures at different intervals using L(0,7) at 0.1MHz and L(0,1) at 0.1MHz respectively for CC sample. Peak to peak voltage amplitudes (pk –pk) of the signals were calculated from the signatures obtained and further normalized which are reported as pk-pk voltage ratio (R). A plot of pk-pk voltage ratio Vs age of concrete at different durations of setting of concrete is plotted for both the selected modes . It was observed that using L(0,1) at 0.1MHz**(Figure 6.7)**a continuous drop in pk-pk voltage amplitude of the signals with increasing age of concrete occurred.

This is due to the bond between embedded rebar and surrounding concrete improves as the concrete sets thus leading to increase in leakage of energy into surrounding concrete, causing fall in signal strength. But with 1 MHz (**Figure 6.6)** frequency it was seen that no drastic change in voltage amplitude occurred throughout the 48 hours of pouring concrete. This difference in detection of setting process due the two modes can be explained by their energy

distribution profiles .In case of L(0,7) mode it has negligible surface component, radial distribution of displacement and strain energy density is concentrated in the core area of bar, therefore signal is sensitive to deteriorations and irregularities inside the bar rather than its surface. Whereas L (0,1) is referred as surface seeking mode as it has significant surface component and is sensitive to interface changes such as bond development between rebar and concrete due to setting of concrete. Hence on the basis of **Figure 6.6 and 6.7**the L(0,1) at 0.1MHz was selected further for monitoring early age setting of flyash concrete.

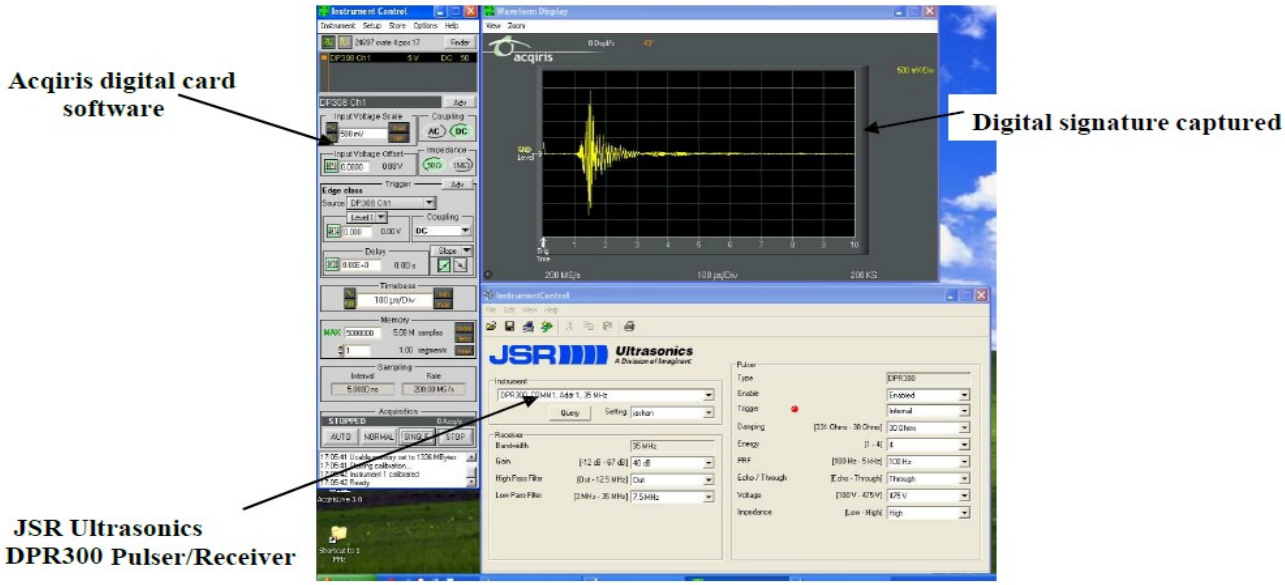

Fig. 6.5: JSR and Acqiris Software

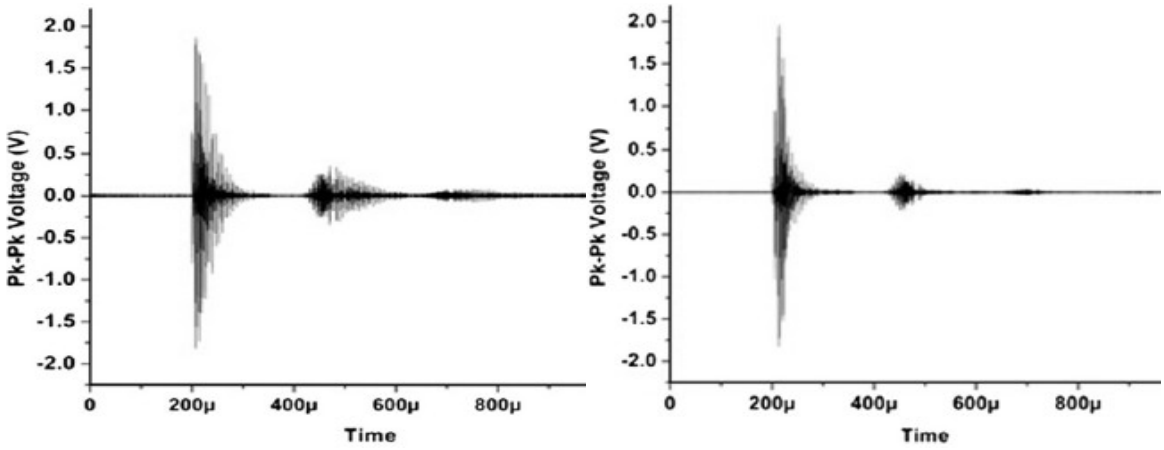

(a) Immediately after pouring **(b) 6 hours**

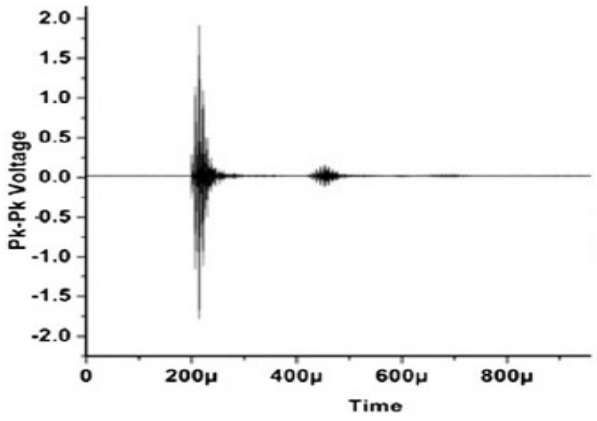

(b) 12 hours

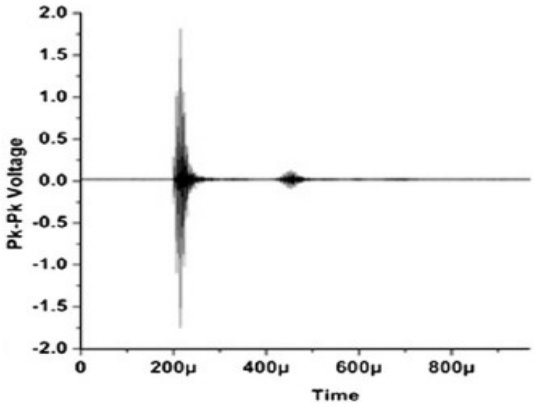

(c) 24 hours

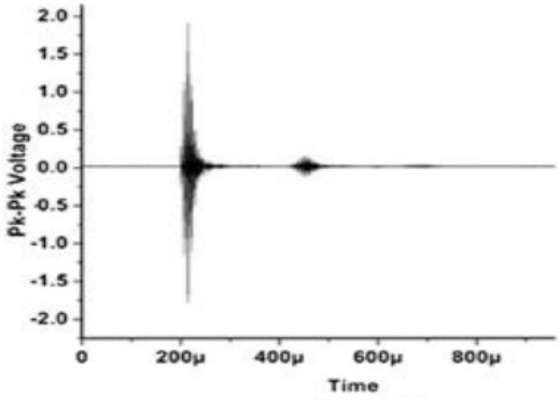

(d)36 hours

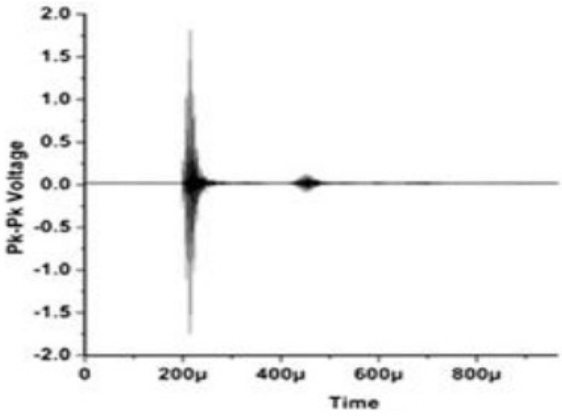

(e)48 hours

Fig. 6.6 :Waveforms for L(0,7) at 1MHz for CC

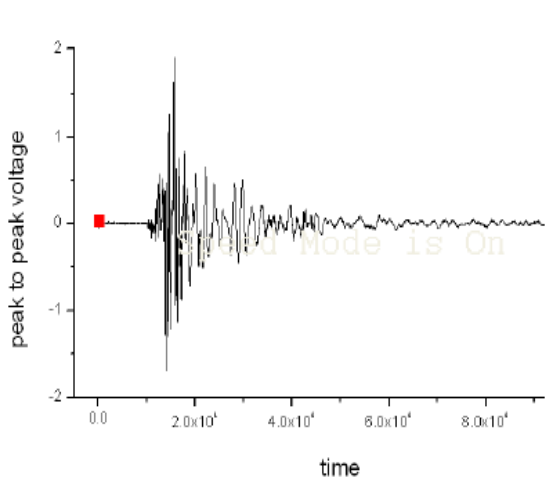

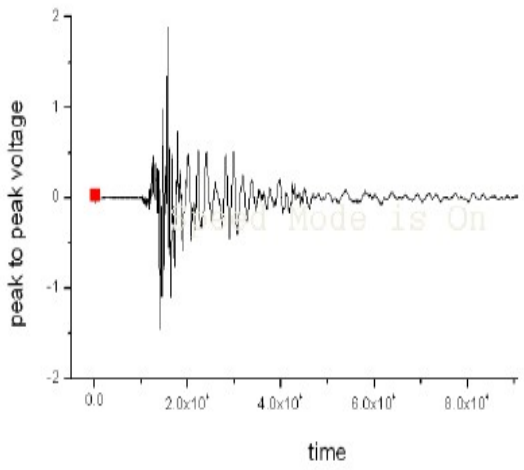

(a) Immediately after pouring **(b) 6 hours**

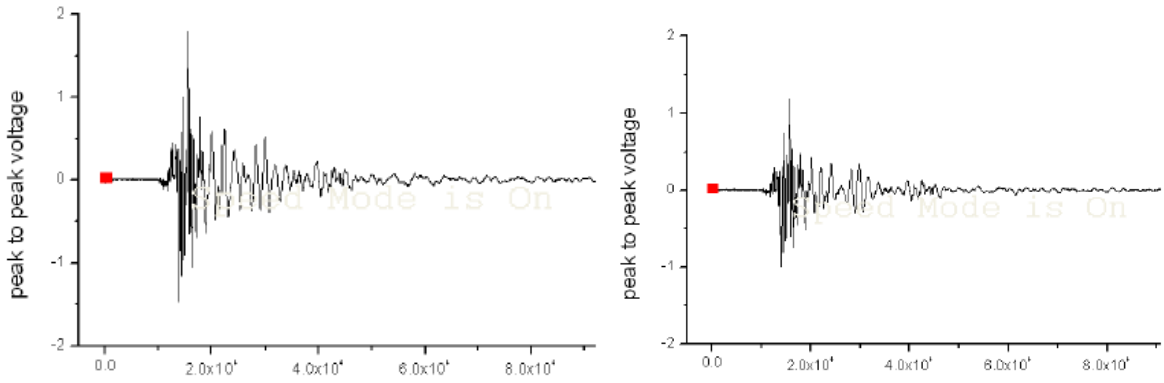

(b) 12 hours **(c) 24 hours**

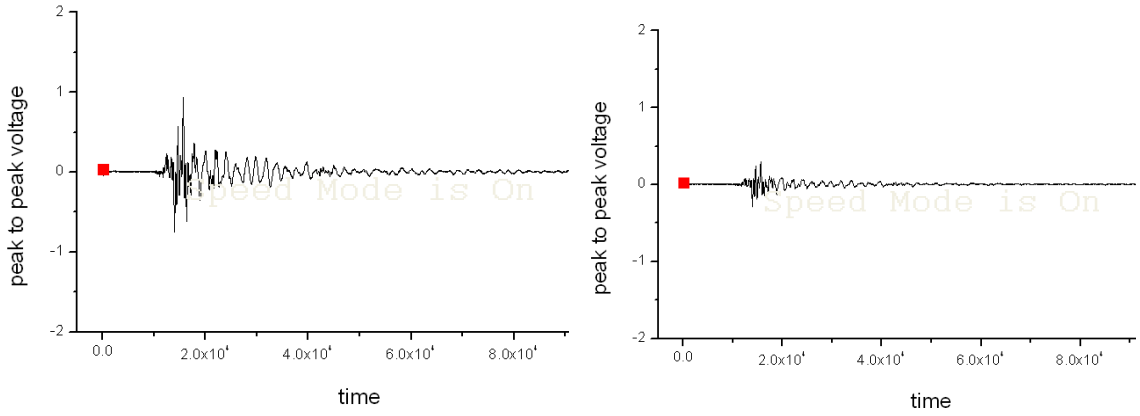

(c) 36 hours **(d) 48 hours**

Fig 6.7: Waveforms L(0,1) at 0.1 MHz for CC

6.3.1 CC Results

- It was observed that using L(0,1) at 0.1MHz**(Figure 6.7)** a continuous drop in pk-pk voltage amplitude of the signals with increasing age of concrete occurred. But with 1 MHz (**Figure 6.6)** frequency it was seen that no drastic change in voltage amplitude occurred throughout the 48 hours of pouring concrete. Hence on the basis of **Figure 6.6 and 6.7**the L(0,1) at 0.1MHz was selected further for monitoring early age setting of concrete.

- It is clear after seeing the UGW result graph that concrete setting involves two phases as discussed below:

Fluid Phase. It is marked by very small peak-peak voltage of transmitted signal. Thus indicating there is not significant setting or bonding between the mild steel bar and the surrounding concrete**.**

Semi sold phase: The maximum fall in peak-peak voltage is observed in this phase indicating maximum bond development between steel bar and surrounding concrete. Towards the end, concrete undergoes a change of phase from semi- solid to solid state or in other words concrete is starting to set or making bond with the embedded mild steel bar and there is again marginal fall in peak-peak voltage of the signal, indicating the concrete has become almost solid and no leakage takes place in surrounding concrete.

- The fall in transmitted signal strength was observed with time which was attributed to improvement in the development of bond , as concrete solidifies its acoustic impedance goes closer to that of steel thus increase in leakage of energy from bar to concrete hence fall in signal strength .

As discussed above, L(0,1) at 0.1MHz was selected for monitoring early age setting of control concrete. This was further extended to monitoring the early age setting and hardening of flyash modified concrete and the waveforms for FA30 compared with those of CC are as given in the figure below.

FA30	**CC**

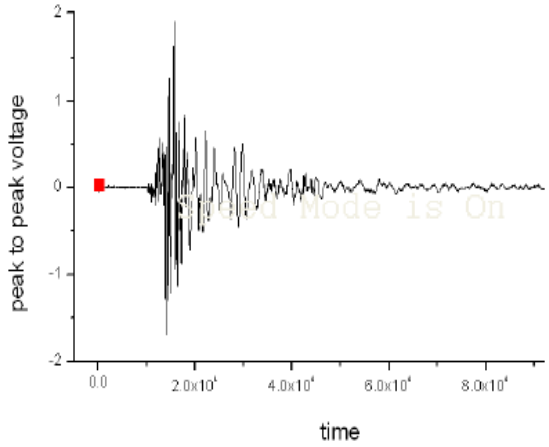

Immediately after pouring

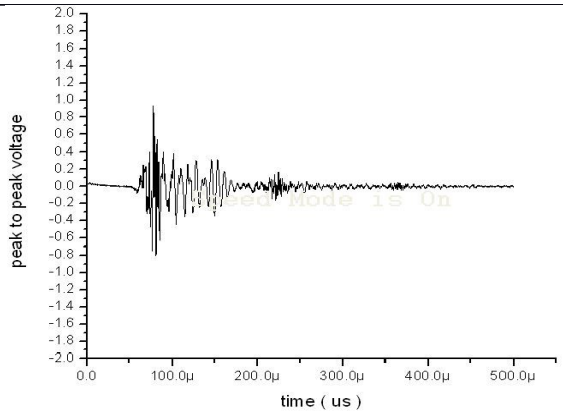

Immediately after pouring

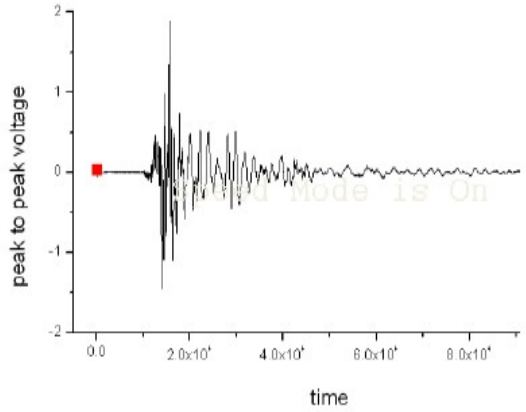

6 hours

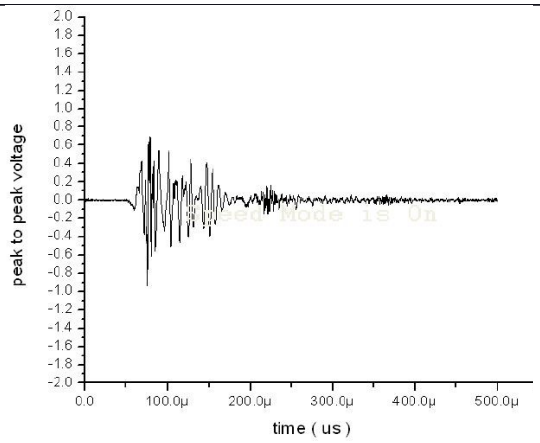

6 hours

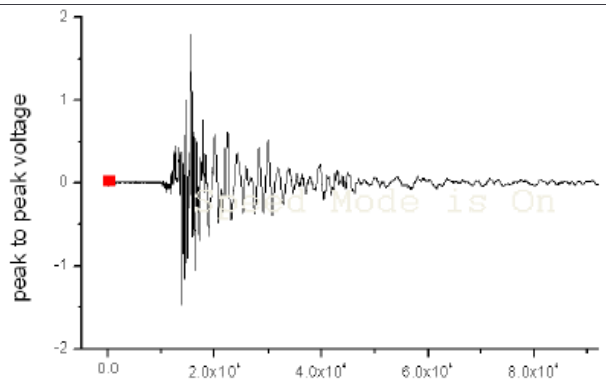

12 hours

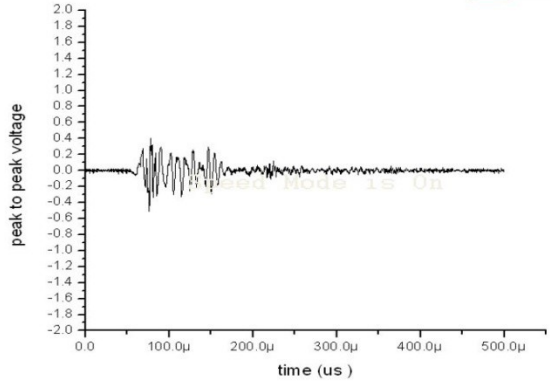

12 hours

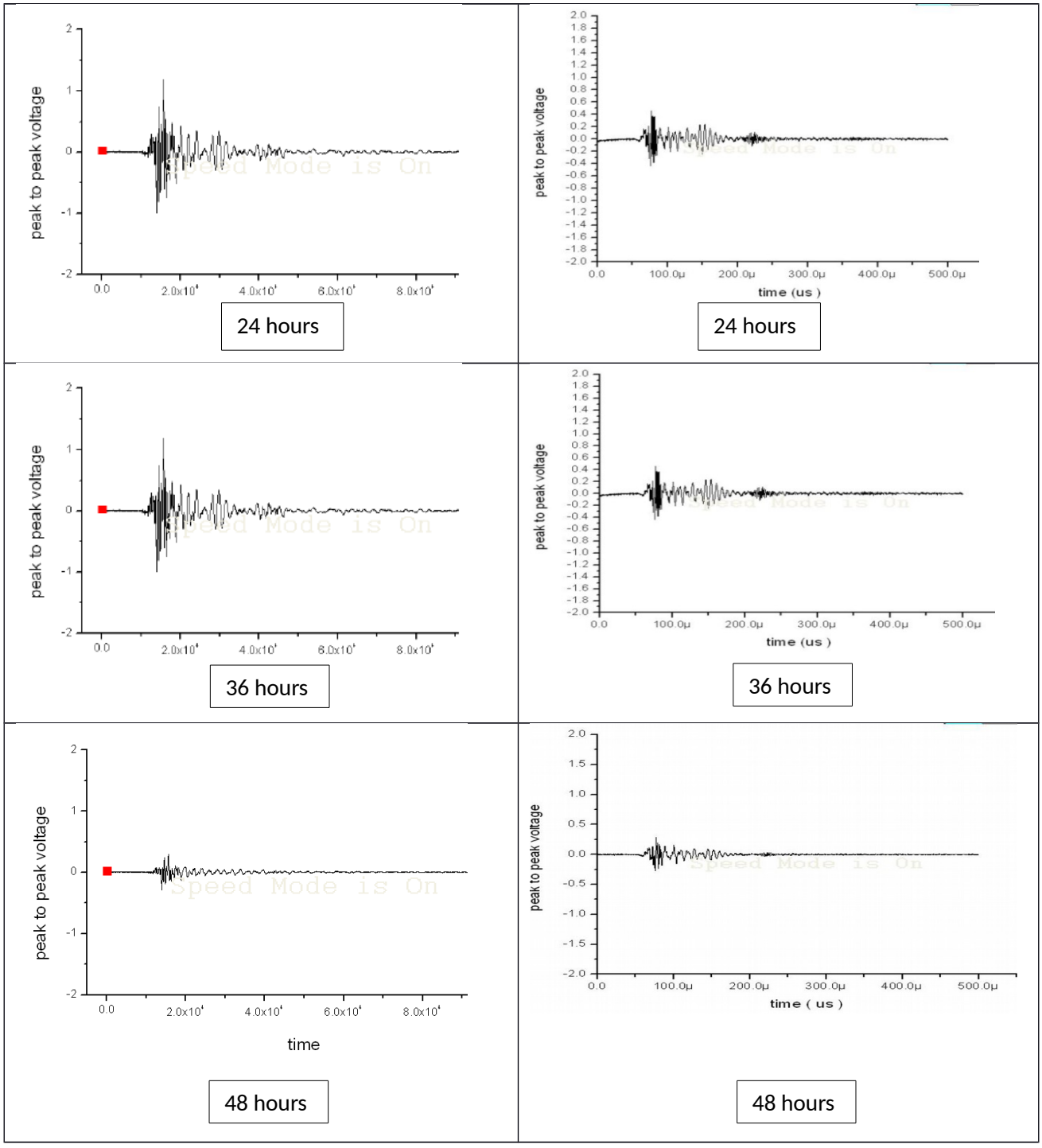

Fig. 6.8: Waveforms of FA30 and CC

Similar tests were conducted on other flyash modified concrete samples namely FA5,FA15 along with FA 30 and CC samples as mentioned above and waveforms for same were obtained. The trend lines for various flyash modified concrete samples are given in figures below.

Fig. 6.9: Comparison of CC and FA5 UGW Results

Fig. 6.10: Comparison of CC and FA15 UGW Results

Fig. 6.11: Comparison of CC and FA30 UGW Results

6.3.2 Comparison of CC Results with Flyash modified concrete Results

- From **Fig. 6.9, Fig. 6.10 and Fig. 6.11** it was observed that FA30 and FA15 concrete sets slowly than CC and FA5. The pattern was well validated by compressive strength test results as discussed previously.
- The initial fluid phase lasts for about 24 hours in control concrete whereas it is gradually delayed as percentage replacement of flyash increases due to slow setting of flyash concrete
- The semi-solid phase starts after 24 hours in control concrete whereas it is gradually delayed as the percentage replacement increases indicating slow setting of flyash replaced concrete
- The fall in transmitted signal strength was observed in all the samples (control as well as samples with replacement) which was attributed to improvement in the development of bond , as concrete solidifies its acoustic impedance goes closer to that of steel thus increase in leakage of energy from bar to concrete hence fall in signal strength .
- Another observation from **Fig. 6.8** is that in case of CC sample, signal falls more rapidly due to early setting whereas in flyash concrete, the signal falls slowly indicating slower setting.

6.4 Acoustic Emission Study:

AE signals are picked up using the AE sensors and recorded using AE win software and are displayed in the form of various parameters like AE hits, Amplitude, Counts, and Energy etc. AE monitoring was conducted in two ways. Firstly, the AE sensors were mounted on the surface of concrete directly and monitoring was done for 48 hours. Secondly, AE sensors were mounted on the steel bars embedded partially in concrete. The monitoring in this case was done for first 24 hours. The nomenclature is given in the **Table: 5.11**

Two parameters of AE signals i.e. the AE hits and AE amplitude as a function of time have been used to analyse the whole process of setting and hardening of concrete.

6.4.1 CC using Concrete Sensors

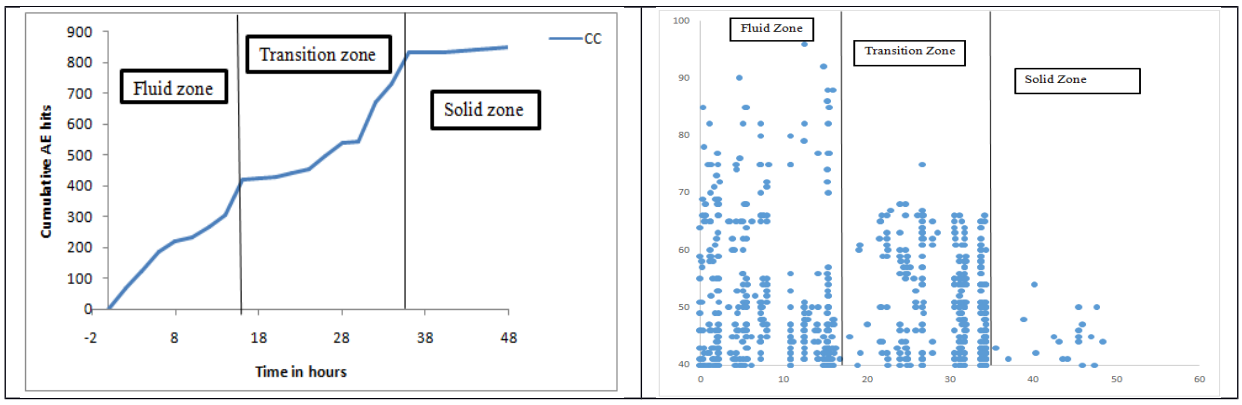

Fig. 6.12 (a) AE Hits Vs time for CC **(b) AE Amplitude Vs time for CC**

Fig.6.12 shows the graph of AE hits and AE amplitude plotted as a function of time for the CC, monitored for a period of 48 hours.The following observations were made:

- It can be clearly seen that there is a great increase in the number of AE hits during the early hours of setting of concrete. From the AE hit graph and AE amplitude graph**,** following observations can be made:
- In the fluid zone, i.e. from 0-16 hours, the rate of rise of cumulative AE hits is very steep. This is attributed to the higher rate of hydration in this duration and is equivalent to the semi-solid or the fluid zone. UGW indicates the slow development of bond between steel and concrete by slow fall in the voltages but steep rise in the AE cumulative AE hits indicates the first rate of hydration in this phase. This is also reinforced by plot of amplitude and time, that in the first phase, the values of amplitude range between 40-100. This represents major changes taking place inside concrete and hence the fluid zone.

- In the transition zone i.e., 18- 36 hours, the rate of change of cumulative AE hits is not as high as it is in the case of Fluid zone. Since the change is in the slope is gradual and not very steep i.e. less number of hits are recorded during this period, it is known as a transition phase. This phase corresponds to the fact that the rate of hydration process is reduced during this period and is equivalent to the transition phase. During this phase, the value of amplitude limits itself between 40-70 and does not increase. This represents the gradual shift of macro-minor changes from Fluid zone to transition zone. Although hits are recorded but that could be due to the decrease in attenuation due to solidification of concrete. However, lower values of amplitude indicate less intensity of AE activity.
- Time period from 36-48 hours can be termed as "Solid Zone", for there is hardly any increase in the number of AE hits suggesting that the very less signal or no signal has been recorded by the instrument. Therefore, it can be implied that the hydration process has slowed down to a great extent and can also be termed as a calm phase. The values of AE amplitudes that are recorded during this period is much too less than the previous two phases. This further represents that AE activity has almost stopped and therefore signifies the solidification of the concrete specimen.
- The slope of the cumulative number of AE hits during the various time intervals can be very well related with the process of hardening of concrete with time. The initial steep slope i.e., the time interval immediately after when the concrete is in fluid zone may be attributed to the fact that there is a lot of heat of hydration which is released with the setting of concrete. The greater the loss of heat of hydration, greater will be the molecular changes amongst the stress planes inside the concrete and hence greater the no. of acoustic emission recorded. With the progression of time, loss of heat of hydration reduces, therefore, explaining the gradual slope of cumulative AE hits during the transition phase. And after 36 hours of pouring of concrete, most of the heat of hydration has been lost and concrete is set.

6.4.2 Flyash modified concrete using concrete sensors

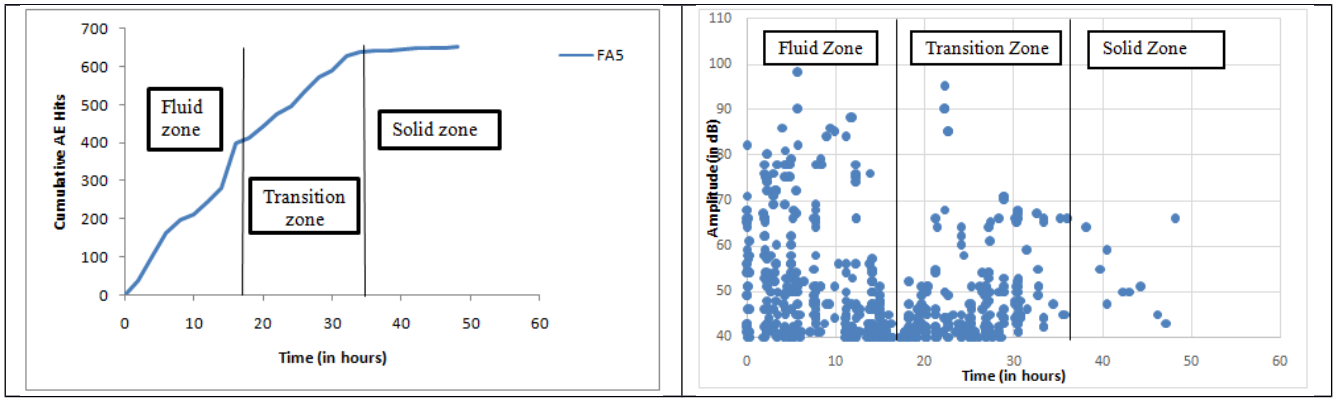

Fig.6.13 (a): AE Hits Vs time for FA5 sample (b) AE Amplitude Vs time for FA5 sample

Fig. 6.13 (a&b) shows the graph of Cumulative AE hits and AE amplitude plotted as function of time for FA5, monitored for a period of 48 hours and the following observations were made:

- It can be clearly seen that the variation in the AE hit plot for this sample, is not much different from that of control sample. The duration of the fluid zone is same and the rate of increase of AE hits is similar. This further implies that with the addition of 5% fly ash in concrete, very small changes in the process of setting and hardening of concrete exist.
- The values of amplitude remain somewhat similar to that of the control specimen and therefore, not much change is observed from that of the control sample. This suggests that adding 5 % of fly-ash brings no significant change in the setting and hardening characteristics of concrete.

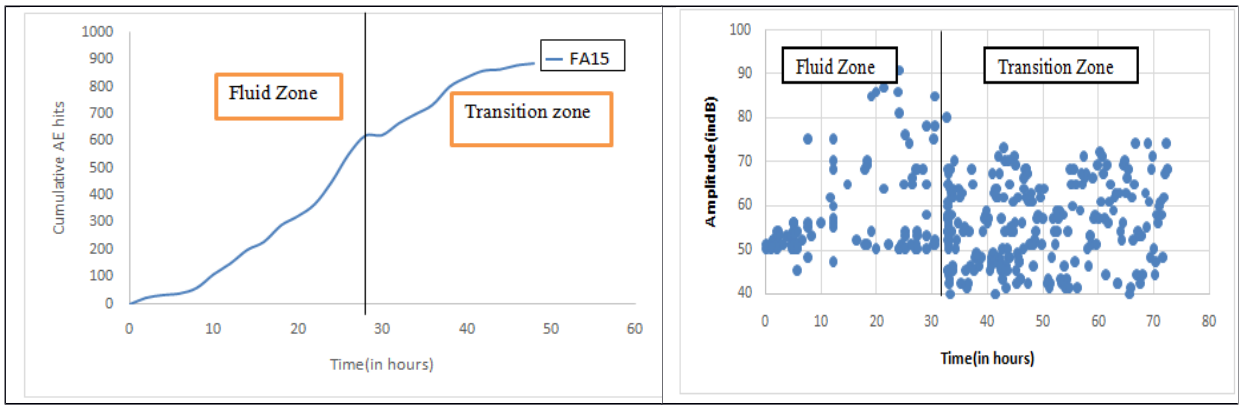

Fig. 6.14 (a) AE Hits Vs Time FA15 sample (b) AE Amplitude Vs time FA15 sample

Fig. 6.14 (a & b) shows the Cumulative AE hits and AE amplitude, plotted as function of time for FA 15, monitored for a period of 48 hours. The following observations were made:

- In this case, the increase in rate of AE hits is very small in the first few hours implying that the process of setting of concrete has been delayed. It is only after a period of 10 hours that there is significant increase in the AE hit activity as was observed during the 0-18 hours of the control sample. This signifies that the rate of increase in AE hits and the corresponding setting of concrete been delayed by 10 hours approximately.
- For this specimen, only two zones:1) Fluid zone 2) Transition Zone can be observed. Here in this case, very small values of amplitudes are recorded for the first 10-12 hours of AE monitoring. But afterwards, the trend is almost similar to that of control sample in the fluid zone. This could imply that the adding 15 % of fly ash in concrete has delayed onset of fluid zone and therefore the setting of concrete by 10 hours. In this case, fluid is identified by higher values of amplitude and the transition zone is succeeding fall in the values of amplitude.

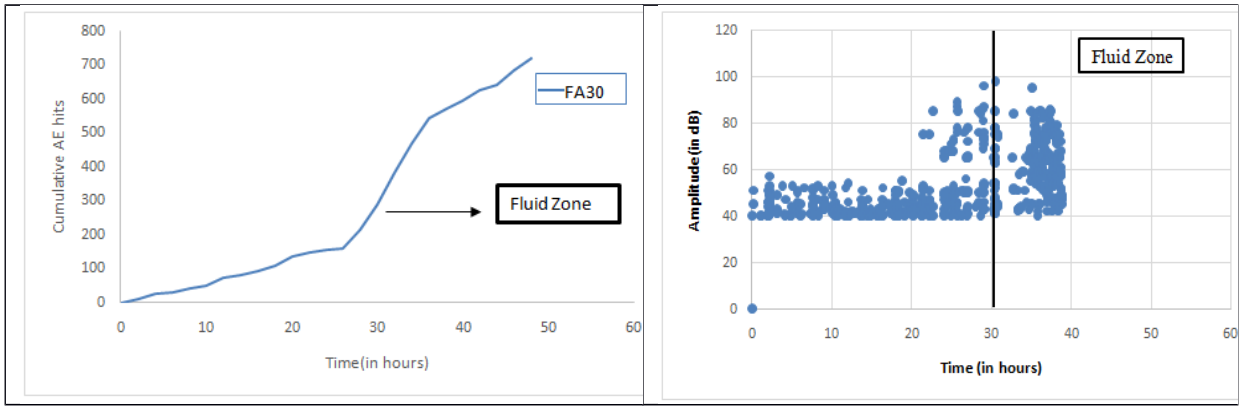

Fig.6.15 (a):AE Hits Vs time FA 30 sample (b)AE Amplitude Vs time FA 30 sample

Fig. 6.15 (a & b) shows the graph of Cumulative AE hits and AE amplitude, plotted as a function of time for FA30 sample monitored for a period of 48 hours. The following observations were made:

- The plot clearly identifies the presence of fluid zone. For first 25 hours, the rate of increase of AE hits has been very slow in comparison with those recorded for control sample. And the significant increase in AE hits start after 26 hours of pouring of concrete. This further implies that the addition of 30 % of Fly ash in concrete significantly delays the process of setting and hardening.
- The plot of amplitude with time, gives a very clear picture of the effect of Fly ash on the setting and hardening characteristics of concrete. For the first 30 hours, the rage of Amplitudes recorded has been between 45-55 and after 30 hours of pouring of

concrete, it jumps up to 98 dB value of amplitude even. This implies that, adding 30 % of fly-ash in concrete brings about significant variations in the setting and hardening characteristics of concrete.

6.4.3 CC and FA30 using Steel Sensors

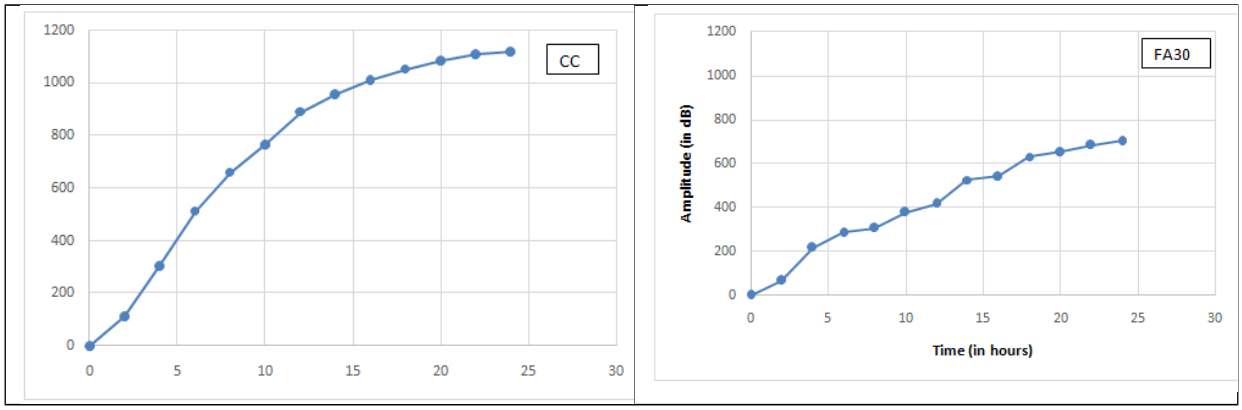

(a) (b)

Fig. 6.16: AE monitoring with R15α sensors. (a) CC sample (b) FA30 sample

Another study was conducted with the same purpose of finding the change in the hardening and setting characteristics of concrete using AET. But in this case, instead of mounting sensors directly on the surface of concrete, two steel bars of 12mm dia were embedded partially in the concrete. The sensors (R15α) were mounted on the top of the steel bar. A control sample and a sample with 30 % fly ash were monitored for a period of 24 hours and the following observations were made

- **Fig.6.16 (a) and (b)** shows the AE hit plot as a function of time for both the CC and FA 30. It can be clearly seen that the no. of hits recorded in this case are far more than those recorded from the sensors mounted on the concrete surface directly. In case of FA30, the calm period initially due to delay in the setting, is also indicated by large no. of recorded hits.
- From both the studies, it can be observed that the AE monitoring done with AE sensors mounted on steel bars gives far clearer picture about the setting and hardening characteristics of concrete.

6.5 Closing Remarks

This chapter shows the results obtained by ultrasonic guided waves , acoustic emission , ultrasonic pulse velocity under non – destructive techniques and compressive strength with

SEM/EDS analysis for destructive techniques for control concrete and concrete containing various different percentages of flyash.For destructive testing a minimum of 3-7 days period is required and it indicates the strength of concrete whereas NDT parameters give an indication of quality of concrete within few hours of casting. So if the mixture is not good, it can be redesigned.

CHAPTER-7

CONCLUSIONS

7.1 General

Destructive and non destructive test were carried out on concrete samples in this research. The concrete samples included control concrete and flyash concrete samples with flyash content varying as 5%, 10%, 15%, 20% and 30% respectively. The non destructive techniques carried out include acoustic emissions and ultrasonic guided waves to monitor setting and hardening of concrete samples. Further destructive testing was carried out to validate the above results. The destructive tests carried out were compressive strength tests and SEM (Scanning Electron Microscope) analysis. The main conclusions drawn from the study are as follows:

7.2 Ultrasonic Guided Waves Investigations

- Ultrasonic guided wave technique using L(0,1) mode at 0.1 MHz has proven to be very effective in monitoring the hydration and setting of control concrete and also of concrete with varying flyash replacements.
- The L(0,7) mode at 1 MHZ showed no major change in voltage amplitude throughout the testing duration of 48 hours.
- Change of slopes in curves show two stages , namely the fluid and the semi solid phase.
- Due to slower reaction of flyash, the fluid zone extends over a larger period (26-40 hours) as against control concrete (24 hours).
- A fall in the transmitted signal strength was observed in all the samples. In initial phase called the fluid phase , the fall of peak to peak voltage is nominal indicating there is not significant setting or bonding between the mild steel bar and the surrounding concrete. During the semi-solid phase, fall in transmitted pulse voltage is observed as concrete undergoes a change of phase from fluid to semi-solid.
- It is thus observed that rate of pozzolanic reaction is slower for flyash concrete samples as compared to control concrete and hence flyash concrete solidifies slowly.

7.3 Acoustic Emission Technique Investigation

- Acoustic commission monitoring successfully identified various stages of concrete setting after pouring of concrete in the mould. The parameters studied under concrete commission included cumulative AE hits and Amplitude.

- All the above mentioned parameters increased with age of concrete portraying the setting & hardening process of concrete.
- It can be clearly seen that there is a great increase in the number of AE hits during the early hours of setting of concrete
- Also gentler slopes and lower values of various parameters were obtained in 20% and 30% concrete samples which is due to low flyash reactivity
- It was seen that adding 15 % and 30 % fly ash in concrete delayed the onset of fluid zone and therefore the setting of concrete. In these cases, fluid is identified by higher values of amplitude and the transition zone is succeeding fall in the values of amplitude.
- Decrease in the rate of increase of AE parameters is due to the formation of hydration products also due to water absorption by capillary pores and porosity.
- It was observed that the no. of hits recorded while making use of steel sensors are far more than those recorded from the sensors mounted on the concrete surface directly. It was observed that the AE monitoring done with AE sensors mounted on steel bars gives far clearer picture about the setting and hardening characteristics of concrete.

REFERENCES

- Abeele, K. V. D., Desadeleer, W., Schutter, G. D., Wevers, M. (2009) "Active and passive monitoring of the early hydration process in concrete using linear and nonlinear acoustics". (39) pg 426- 432.
- Achenbach, J.D. (1975) ,Wave Propagation in Elastic Solids. Elsevier, New York.

- Beard, M. D., Lowe, M. J. S. and Cawley, P. (2003), Ultrasonic Guided Waves for inspection of grouted tendons and bolts. Journal of Materials in Civil Engineering.
- Bindal, V.N. (1999), "Transducers for Ultrasonic Flaw Detection". Narosa Publishing house.
- Carette, J.and Staquet, S. (2016), Monitoring the setting process of eco-binders by ultrasonic P-wave and S-wave transmission velocity measurement: Mortar Vs concrete, Construction and Building Materials, 110, 32–41.
- Carino, N. (2001) The Impact-Echo Method: An Overview. Structures 2001: pp. 1-18.
- Cawley Peter., (2002). "Practical Long Range Guided Wave Inspection – Applications to Pipes and Rail". Department of Mechanical Engineering, Imperial College, London SW7 2BX, UK.
- Che-Way Chang and Hung-Sheng Lien (2008), "Nondestructive Measurement of Concrete Strength at Early Ages". Department of Civil Engineering and Engineering Informatics, Chung-Hua University. No.707, Sec. 2, Wufu Rd., Hsinchu City 300, Taiwan (R.O.C.)
- Chotard, T. J., Smith, A., Codet, N., De Baillencourt, M., Fargeot, D. and Gault, C. (2002), New applications of acoustic emission technique for real-time monitoring of material processes, Journal of Materials Science Letters, 21(16), 1261–1266.
- Darquennes. Aveline, Stéphanie Staquet, Bernard Espion, Olivier Germain and Christian Pierre(2009), "Comparison between different techniques for monitoring setting and hardening of concrete". NDTCE"09, Non-Destructive Testing in Civil Engineering Nantes, France, June 30th– July 3rd, 2009.
- Demma, A., (2003), A Thesis report "The interaction of guided waves with discontinues in the structure". Imperial College of science, technology and medicine. University of London.
- Ervin. Benjamin Land Reis.Henrique.,(2008)."Longitudinal guided waves for monitoring corrosion in reinforced mortar".www.stacks.iop.org/MST/19/055702.
- Ervin, B. L., Kuchma, D.A., Bernhard, J.T.,and Reis, H.,(2009)."Monitoring corrosion of rebar embedded in mortar using high frequency guided ultrasonic waves." J.Engrg.Mech. Volume 135, Issue 1, pp.9-19.
- Ervin, L. B., Kuchma ,A.D., Bernhard, T.J. and Reis,H. (2009), Monitoring Corrosion of Rebar Embedded in Mortar Using High-Frequency Guided Ultrasonic Waves . Journal of Engineering Mechanics, 135(1) , 9-19.
- Haneef, T. K., Kumari, K., Mukhopadhyay, C. K., Rao, B. P. and Jayakumar, T. (2013), Influence of fly ash and curing on cracking behavior of concrete by acoustic emission technique,Construction and Building Materials, 44, 342–350.

- Harison A., Srivastava V. and Herbent A., (2014), Effect of Fly-ash on Compressive Strength of Portland Pozzolona Cement Concrete, Journal of Academia and Industrial Research, Vol. 2, ISSN:2278-5213.
- Idrissi, H., Limam, A., (2003). "Study and characterization by acoustic emission and electrochemical measurements of concrete deterioration caused by reinforcement steel corrosion". NDT&E International 36 (2003) 563–569
- Jatale A., Tiwari K., Khandelwal S.(2013) ,Effects on Compressive Strength When Cement is Partially Replaced by Fly Ash, IOSR Journal of Mechanical and Civil Engineering, e-ISSN 2278-1684, Vol. 5, pp 34-43.
- Jinying Zhu & Seong-Hoon Kee (2010), "Monitoring early age microstructure development of cement paste using bender elements" Department of Civil, Architectural and Environmental Engineering, University of Texas at Austin, TX USA 79712.
- Kamada, T., Uchida, S. and Rokugo, K. (2005) , Nondestructive Evaluation of Setting and Hardening of Cement Paste Based on Ultrasonic Propagation Characteristics, Journal of Advanced Concrete Technology, 3(3), 343–353.
- Kim, S., Kwun, H. and Light, G.(2001), Long-range guided wave inspection of structures using the magnetostrictive sensor,Journal of Korean Society, *NDT*, *21*(4), 383–390
- Kundu T.(2007), Advanced Ultrasonic Methods for Material and Structure Inspection , ISTE Ltd.
- Kundu, T., Ehsani, M. R., Na, W. B.,(2002 a) "Ultrasonic Guided Waves for steel bar concrete interface testing". Material Evaluation.
- Kundu, T., Ehsani, M. R., Na, W. B., (2002 b)."A comparison of steel/concrete and glass fiber reinforced polymers/concrete interface testing by guided waves". Material Evaluation.
- Kundu, T., Ehsani, M. R., Na, W. B., (2003)."Lamb Waves for Detecting Delamination between Steel Bars and Concrete"., Computer-Aided Civil and Infrastructure Engineering., Published by Blackwell Publishing, 350 Main Street, Malden,MA02148, USA,and 108 Cowley Road, Oxford OX4 1JF, UK..
- Lee .H.K., K.M. Lee, Y.H. Kim, H. Yim & D.B. Bae (2004), "Ultrasonic in-situ monitoring of setting process of high-performance concrete" Cement and Concrete Research 34 (2004) 631–640.
- Mukherjee, S., Mandal, S. and Adhikari, U.B. (2013),Comparative study on physical and mechanical properties of high Slump and zero slump high volume fly ash concrete (HVFAC). *Global NEST J.* 20(10): 1-7.

- Naik, T.R. and Singh, S.S. (1997), Use of High-Calcium Fly Ash in Cement-Based Construction Materials, ACI Special Publication No. SP-150, 1994, pp. 39-51.
- Nicolas, R. and Nele D.B. (2009), Monitoring the setting of concrete by measuring the change in ultrasonic p-wave energy, NDTCE, Nantes, France, June 30th-July 3rd, 2009.
- Patil S.L, Kale J.N., Suman S., (2012), Fly ash concrete: A technical analysis for compressive strength, International Journal Of Advanced Engineering Research and Studies, ISSN 2249 – 8974, Issue 1, Volume II, pp 128-129.
- Pavalakovic, B.N., and Cawley, P.,(2000). Disperse User's Manual Version 20.11.2000. Imperial college, University of London.
- Randhawa , J. (2011),Monitoring early age strength and hardening of concrete using ultrasonic guided waves, M.E. Thesis , Thapar University .
- Reinhardt, H. W. and Grosse, C. U. (2003), Continuous monitoring of setting and hardening of mortar and concrete, Construction and Building Materials, 18(3), 145–154.
- Robeyst, N., Gruyaert, E. & De Belie N. (2007), "Ultrasonic monitoring of setting and hardening behaviour of concrete and mortar with blast-furnace slag cement" Proceedings 12th International Congress on the Chemistry of Cement, Montréal, 2007, T2-03.2 on CDROM.
- Rose Joseph, L. (2004), Ultrasonic Guided Waves in Structural Health Monitoring, Department of Engineering Science and Mechanics, Penn State University, 212 Earth-Engineering Science Building, University Park, PA 16802, USA.
- Reis, H., Ervin, B.L., Kuchma, D.A., and Bernhard, J.T., (2005). "Estimation of Corrosion Damage in Steel Reinforced Mortar Using Guided Waves" Journal of Pressure Vessel Technology;August 2005, Vol. 127 / 255-261.
- Rizzo Piervincenzo, Elisa Sorrivi, Francesco Lanza di Scalea and Erasmo Viola., (2007). "Wavelet-based outlier analysis for guided wave structural monitoring: Application to multi-wire strands", Journal of Sound and Vibration 307 (2007) 52–68.
- Sachu Naveen., (2010). "Monitoring of damage in prestressing tendons using ultrasonic guided waves".(M.E Thesis, Thapar University, Patiala).
- Sang-Young Kim, Hegeon Kwun & Glenn M. Light. (2001), "Long-Range Guided Wave Inspection of Structures Using the Magnetostrictive Sensor" Applied Physics Division, Department of NDE Science and Technology, Southwest Research Institute, San Antonio, Texas, U.S.A.
- Shahidan, S. (2014), Damage Classification in Reinforced Concrete Beam By, 45, 78–86.

- Sharma, S. and Mukherjee, A. (2010), Longitudinal Guided Waves for Monitoring Chloride Corrosion in Reinforcing Bars in Concrete, Structural Health Monitoring. 6(9) .
- Sharma, S.and Mukherjee, A. (2011) , Monitoring Corrosion in Oxide and Chloride Environments Using Ultrasonic Guided Waves, ASCEJournal of Materials In Civil Engineering , 2(23).
- Sharma, S.and Mukherjee (2012),Non-Destructive Evaluation Of Corrosion In Varying Environments Using Guided Waves , Research in non-destructive evaluation, 1-40.
- Sharma, S. and Mukherjee, A.(2014), Ultrasonic guided waves for monitoring the setting process of concretes with varying workabilities,Construction and Building Materials ,72 ,358–366.
- Sharma, S.and Mukherjee, A. (2015), Monitoring freshly poured concrete using ultrasonic waves guided through reinforcing bars,Cement & Concrete Composites , 55 , 337–347.
- Siddique, R. (2003), Performance characteristics of high-volume Class F fly ash concrete, Cement and Concrete Research, 34 (2004) 487–493.
- Siddique, R. (2010), Wear Resistance of High-Volume Fly Ash Concrete, Leonardo Journal of Sciences, Issue 17, July-December 2010 p. 21-36
- Skal's'kyi, V. R., Koval', P. M., Serhienko, O. M. and Lotots'kyi, Y. L. (2004), Investigation of the solidification of concrete according to the signals of acoustic emission, Materials Science, 40(5), 698–701.
- Sleiman, H., Perrot, A. and Amziane,S. (2010), A new look at the measurement of cementitious paste setting by Vicat Test, Cement and Concrete Research , 40, 681-686.
- Trtnik, G. and Gams, M. (2015), Ultrasonic assessment of initial compressive strength gain of cement based materials. Cement and Concrete Research, 67, 148–155.
- Upadhyaya, S.(2014), Effects of flyash on compressive strength of M20 mix design concrete, International Journal of Advancements in Research & Technology, Volume 3, Issue 9, September -2014.
- Vermani Garima., (2008)."Damage detection in reinforcing steel bars using ultrasonic wave propagation", (M.E Thesis, Thapar University, Patiala).
- Web References :
  http://www.ndt-ed.org
  http://www.uomisan.edu.iq
  http://civilengineeringmaterials2012.blogspot.in
  http://controls-group.com
  http://researchgate.net
  http://googleimages.com

http://www.fhwa.dot.gov
http://ntpc.co.in
http://en.m.wikipedia.org/wiki.Fly_ash
http://www.ammrf.org.au

- Zhu, J., Kee, S.-H., Han, D. and Tsai, Y.-T. (2011), Effects of air voids on ultrasonic wave propagation in early age cement pastes, Cement and Concrete Research, 41(8), 872–881.